SUPPLEMENT TO

LC GC north america

solutions for separation scientists

THE APPLICATION NOTEBOOK

February 2014

www.chromatographyonline.com





THE APPLICATION NOTEBOOK

A SUPPLEMENT TO LCGC NORTH AMERICA

ADVANSTAR SCIENCE

FEBRUARY 2014

Is the foundation of your molecular characterization based on measurements without SEC-MALS?

Scientists shouldn't have to guess the molecular weights of their samples. But that's pretty much what they do when they don't use Wyatt's SEC-MALS solutions to calculate molecular weights. Only Wyatt's industry-leading DAWN® multi-angle light scattering (MALS) instruments make absolute molar mass determinations—without column calibration *or* reference standards. When you connect a DAWN to your SEC/GPC system, you'll determine *absolute* molar masses completely *independent* of elution times.

Since 1982, we've been committed to solving the toughest macromolecular characterization problems for our customers. Every day, thousands of leading scientists throughout the world depend on our instruments. And more than 9,300 peer-review articles have been published, all of which attest to the versatility and superiority of our unique MALS technology.

Free training and PhD-level customer support come with your purchase, as well as a remarkable, three-day, all-expenses-paid Light Scattering University® (LSU) training course in Santa Barbara (US customers only). Our personalized, friendly and accessible customer support staff includes 18^{+} PhD scientists dedicated to sharing their expertise in chromatography, polymer chemistry, protein science, biochemistry and, of course, light scattering.

There's no mystery in determining absolute molecular weights—just a superior solution. And by choosing Wyatt Technology you'll get measurements that are solidly grounded in science, not based on a house of cards.

WYATT TECHNOLOGY
www.wyatt.com

DAWN® HELEOS® Multi-angle light scattering for characterizing macromolecular mass, size and conformation. No other MALS detector comes close in range or sensitivity.

Optilab® T-rEX™ Differential refractometer for on-line concentrations. Unparalleled measurement and temperature ranges.

Mobius® Electrophoretic mobility from proteins to nanoparticles. Uniquely sensitive and versatile for all types of solvents.

Eclipse™ Column-free, field-flow fractionation of macromolecules and nanoparticles in solution. One system covers all your separation needs.

DynaPro® Plate Reader Automated dynamic light scattering for proteins and nanoparticles, *in-situ* in standard micro-well plates. Now with a camera!

THE APPLICATION NOTEBOOK

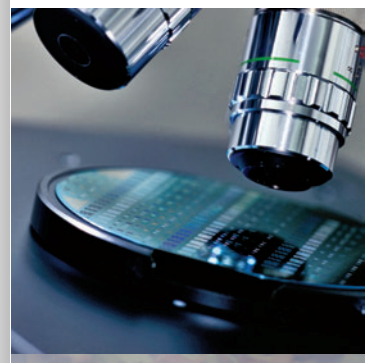

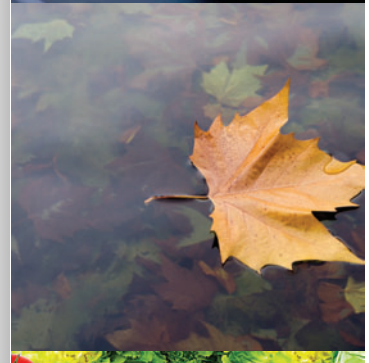

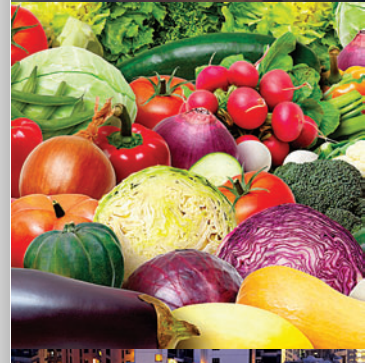

Medical/Biological

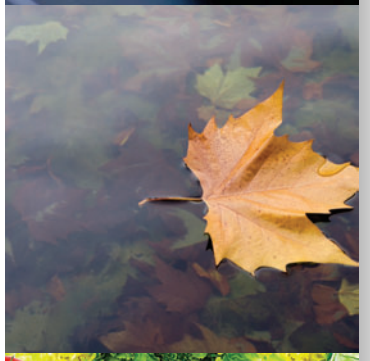

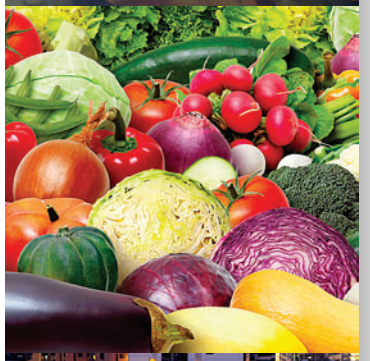

Environmental

Food and Beverage

Pharmaceutical/Drug Discovery

General

Articles

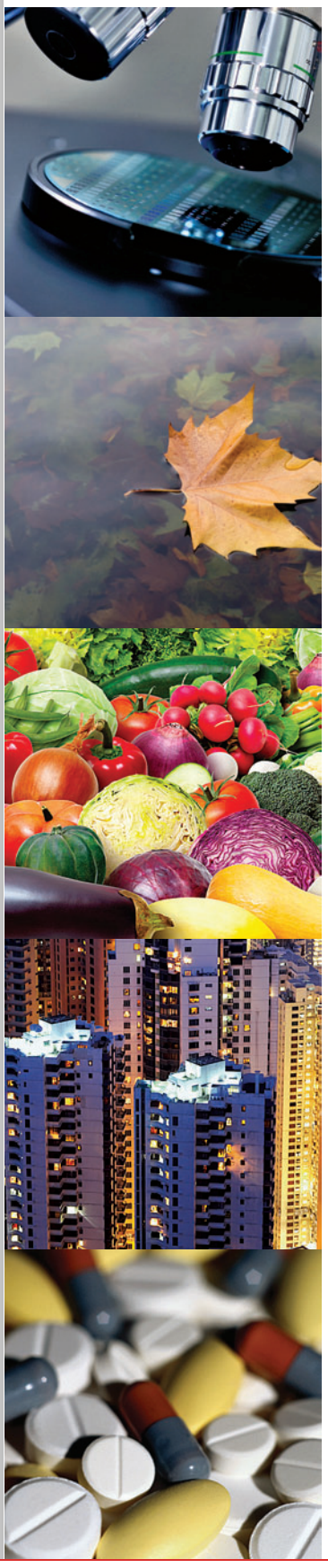

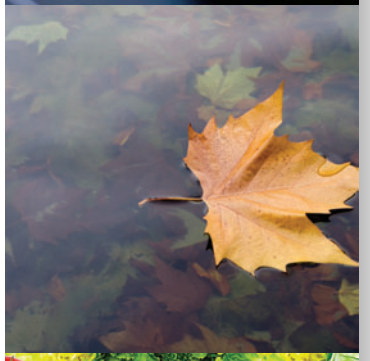

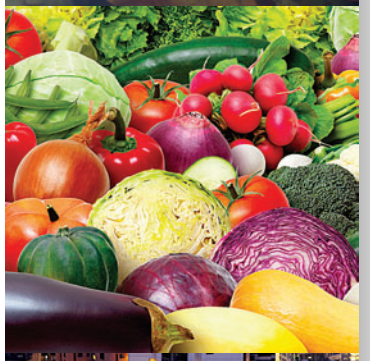

Departments

Cover Photography: Getty Images

LCGC® north america

MANUSCRIPTS: For manuscript preparation guidelines, see chromatographyonline.com/AuthorInfo, or call The Editor, (732) 596-0276. *LCGC* welcomes unsolicited articles, manuscripts, photographs, illustrations, and other materials but cannot be held responsible for their safekeeping or return. Every precaution is taken to ensure accuracy, but *LCGC* cannot accept responsibility for the accuracy of information supplied herein or for any opinion expressed.

SUBSCRIPTIONS: For subscription and circulation information: *LCGC*, P.O. Box 6168, Duluth, MN 55806-6168, or call (888) 527-7008 (7:00 a.m.–6:00 p.m. central time). International customers should call +1-218-740-6477. Delivery of *LCGC* outside the United States is 14 days after printing. For single and back issues, call (800) 598-6008 or (218) 740-6480. (*LCGC Europe* and *LCGC Asia Pacific* are available free of charge to users and specifiers of chromatographic equipment in Western Europe and Asia and Australia, respectively.)

CHANGE OF ADDRESS: Send change of address to *LCGC*, P.O. Box 6168, Duluth, MN 55806-6168; alternately, send change via e-mail to magazines@superfill.com or go to the following URLs:
• Print: https://advanstar.replycentral.com/Default.aspx?PID=469
• Digital: https://advanstar.replycentral.com/?PID=469&V=DIGI
Allow four to six weeks for change. PUBLICATIONS MAIL AGREEMENT No. 40612608. Return all undeliverable Canadian addresses to: IMEX Global Solutions, P.O. Box 25542, London, ON, N6C 6B2, CANADA. Canadian GST number: R-124213133RT001.

DIRECT MAIL LIST RENTAL: Contact Tamara Phillips, tel. (440) 891-2773, e-mail TPhillips@advanstar.com.

REPRINTS: Reprints of all articles in this issue and past issues of this publication are available (500 minimum). Call 877-652-5295 ext. 121, or email bkolb@wrightsmedia.com. Outside US, UK, direct dial: 281-419-5725. Ext. 121.

MARKETING DEVELOPMENT/CLASSIFIED: Contact Tod McCloskey, tel. (440) 891-2739, fax (440) 826-2865.

RECRUITMENT: Contact Tod McCloskey, tel. (440) 891-2739, fax (440) 826-2865.

INTERNATIONAL LICENSING: Contact Maureen Cannon, tel. (440) 891-2742, fax (440) 891-2650, or e-mail mcannon@advanstar.com.

Advanstar Communications Inc. (www.advanstar.com) is a leading worldwide media company providing integrated marketing solutions for the Fashion, Life Sciences and Powersports industries. Advanstar serves business professionals and consumers in these industries with its portfolio of 91 events, 67 publications and directories, 150 electronic publications and Web sites, as well as educational and direct marketing products and services. Market leading brands and a commitment to delivering innovative, quality products and services enables Advanstar to "Connect Our Customers With Theirs." Advanstar has approximately 1000 employees and currently operates from multiple offices in North America and Europe.

Ultra-High Throughput Amino Acid Analysis in Less Than One Minute

Robert Puryear and Itaru Yazawa, Imtakt USA

High throughput analysis of amino acids has been a goal for both column and instrument manufacturers for many years. Current technologies have resulted in HPLC runtimes as low as 8 min, which is considered to be quite fast. However, when you also add the time it takes for the necessary derivatization steps, the total analysis time can be more than 15 min per sample. The solution presented here reduces this time to less than 1 min which can be achieved in a two-step process. First, use of the new Intrada Amino Acid column enables the separation of amino acids by LC–MS, without pre- or post-LC derivatization. This eliminates the need for costly reagent kits and can significantly reduce the analysis time per sample. Second, by using the available 10 mm length column, runtimes under 1 min are reliably produced.

Experimental

All data were generated using a semi-micro HPLC system equipped with ESI MS detection in positive ion mode. High throughput separations of carnitine-related compounds (Figure 1) were accomplished using an Intrada Amino Acid 10 × 2 mm column. Separation of 19 amino acids in less than 1 min was accomplished using an Intrada Amino Acid 10 × 3 mm column (Figure 2). Identical mobile phases A and B were used in both experiments, ACN:Formic Acid, and 100 mM ammonium formate, respectively. Amino acids were detected using a Shimadzu LCMS-8040 in positive ion mode.

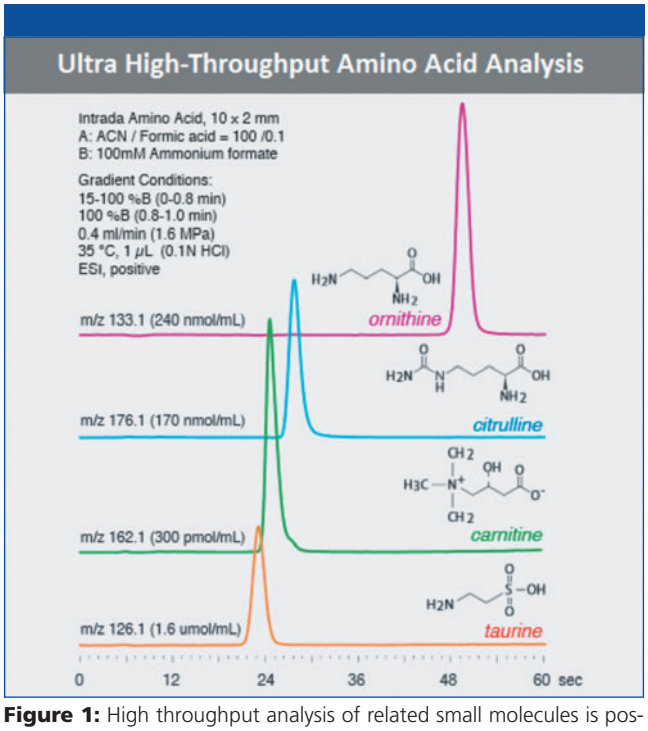

Figure 1: High throughput analysis of related small molecules is possible using Intrada Amino Acid and detection via single quadrupole mass spectrometry.

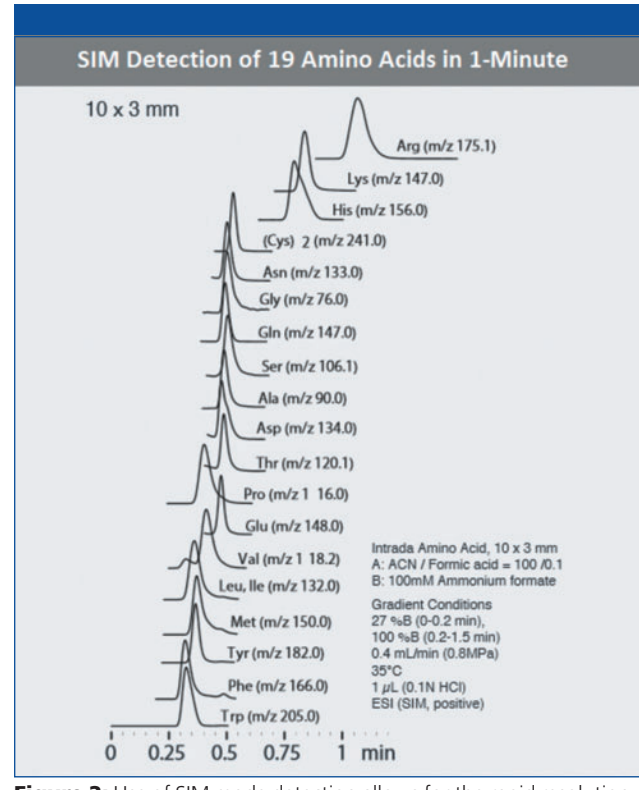

Figure 2: Use of SIM mode detection allows for the rapid resolution of these 19 amino acids in under one min.

Discussion

Current amino acid analysis techniques take more than 15 min per sample. With the development of this unique, proprietary ligand the additional derivatization step is no longer necessary, which can potentially provide a significant cost and time savings. As seen in Figures 1 and 2, by using 10 mm length columns, further dramatic increases in time savings can be accomplished. There are some limitations with this technology particularly if chromatographic separation is necessary, as in the case of isobaric amino acids. In this case, a 50 mm column length is adequate for chromatographic resolution. If isobaric compounds are not present, there is an opportunity with the Intrada Amino Acid column for the development of ultra-high throughput amino acid analyses.

Imtakt USA
1104 NW Overton St., Portland, OR 97209
tel. (888) 456-HPLC, (215) 775-8902, fax (501) 646-3497
Website: www.imtaktusa.com

Analysis of Choline, Acetylcholine, and Monoamine Neurotransmitters by Polymer-Based Ion Chromatography and Mass Spectrometry

Melissa Turcotte* and Junji Sasuga†, *Showa Denko America and †Showa Denko K.K.

Monoamine neurotransmitters (adrenaline, dopamine, noradrenaline, and acetylcholine) are released from the brain and peripheral nervous system in minute amounts. These neurotransmitters play a role in arousal, emotion, and cognition. The detection of an increase or decrease of these neurotransmitters through physiological changes or the use of drugs can be of importance for treating psychiatric disorders, mood, and thought processes.

Shodex IC YS-50, a polymer based ion chromatography column for cation analysis with non-suppressor methods, has demonstrated the separation of these compounds at low concentration levels by MS with SIM (selected ion monitoring) mode.

Experimental Conditions

Separation was carried out by Shodex IC YS-50 (4.6 mm i.d. × 125 mm L). Column temperature was set at 30 °C and flow rate used was 1.0 mL/min. The following isocratic eluent conditions were applied: 4 mM HNO_3 (aq.)/ CH_3CN = 70/30. Sample contained 0.01–1.0 µM of each neurotransmitter. Injection volume of 20 µL was used for the experiments. HPLC system was coupled with an ESI-MS and SIM mode was used for detection.

Results

Choline, acetylcholine, and monoamine neurotransmitters were analyzed successfully by the HPLC–MS method (Figure 1). Of note, the method achieved baseline separations of choline and acetylcholine which previously required a post-column immobilized enzyme reactor with addition of an ion-pair reagent to the eluent. The calibration curves for each of the neurotransmitters and choline were shown to be highly linear for all species (Figure 2).

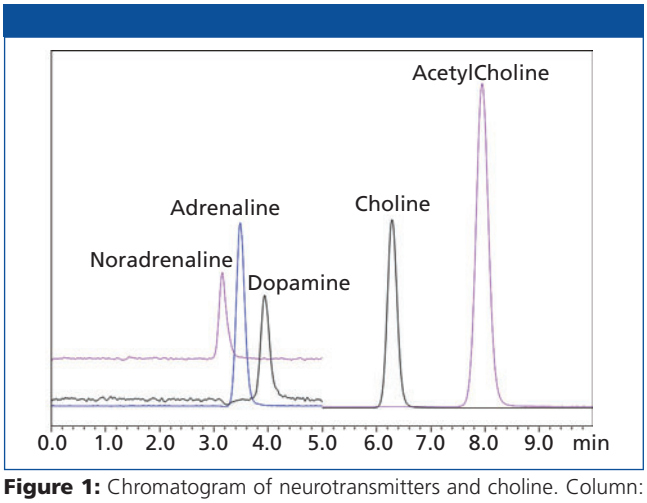

Figure 1: Chromatogram of neurotransmitters and choline. Column: Shodex IC YS-50; column temperature: 30 °C; injection volume: 20 µL; eluent: 4 mM HNO_3 (aq)/CH_3CN=70/30; flow rate: 1.0 mL/min; detector: ESI-MS (SIM).

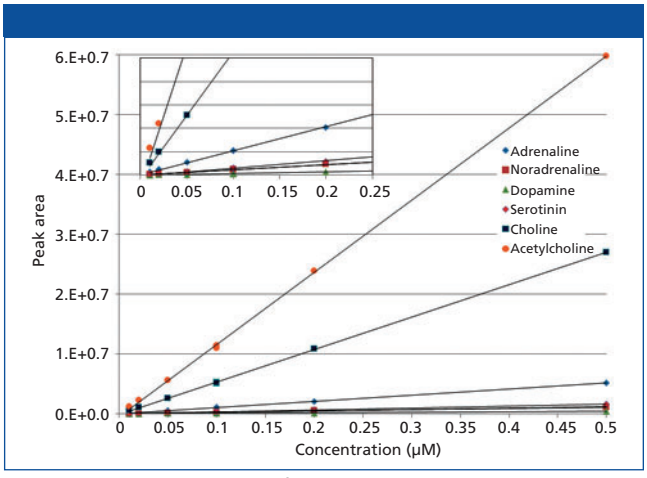

Figure 2: Calibration curves for neurotransmitters and choline. Column: Shodex IC YS-50; column temperature: 30 °C; injection volume: 20 µL; eluent: 4 mM HNO_3 (aq)/CH_3CN=70/30; flow rate: 1.0 mL/min; detector: ESI-MS (SIM).

Conclusions

Shodex IC YS-50, a polymer-based ion chromatography column coupled with ESI-MS is feasible for the analysis of choline, acetylcholine, and monoamine neurotransmitters at low levels of concentration. The presented method using the YS-50 column provides a simple and rapid analysis of neurotransmitters, and the eluent conditions used for ion chromatography are desirable for ESI-MS measurements.

Shodex™/Showa Denko America, Inc.
420 Lexington Avenue Suite 2335A, New York, NY, 10170
tel. (212) 370-0033 x109, fax (212) 370-4566
Website: www.shodex.net

UHPLC Separations Using HPLC Methods and TSKgel® Columns

Tosoh Bioscience LLC

The use of UHPLC systems for small molecule analysis has gained widespread acceptance among researchers in recent years. A UHPLC system is a HPLC system optimized with regards to dead volume, injection performance, and detector sampling rate and is able to tolerate application pressures exceeding 1000 bar. It is therefore advantageous to use UHPLC instrumentation for methods developed on conventional HPLC systems with HPLC columns. The use of HPLC columns with UHPLC systems offers the advantages of cost and time savings over having to purchase and develop new methods with UHPLC columns. This application note demonstrates the excellent performance of conventional TSKgel HPLC columns on a UHPLC system.

Experimental Conditions

Column:	TSKgel SP-STAT, 7 µm, 4.6 mm i.d. × 10 cm
Systems:	Dionex UltiMate® 3000 HPLC System (equipped with Dionex UVD 170S Detector) Dionex UltiMate 3000RS UHPLC System
Mobile phase:	A: 10 mmol/L sodium phosphate, pH 7.0 B: 10 mmol/L sodium phosphate, pH 7.0, + 1 mol/L sodium chloride
Gradient:	0–50% B in 25 min
Flow rate:	1.0 mL/min
Detection:	UV @ 280 nm
Injection vol.:	5 µL
Sample:	monoclonal IgG, 1 mg/mL

Column:	TSKgel G2000SW$_{XL}$, 5 µm, 7.8 mm i.d. × 30 cm
Systems:	Dionex UltiMate 3000 HPLC System (equipped with Dionex UVD 170S Detector) Dionex UltiMate 3000RS UHPLC System
Mobile phase:	0.1 mol/L sodium phosphate, pH 6.7 + 0.1 mol/L sodium sulfate
Flow rate:	1.0 mL/min
Detection:	UV @ 280 nm
Injection vol.:	20 µL
Samples:	para-aminobenzoic acid, thyroglobulin, γ-globulin, ovalbumin, ribonuclease A, 2 mg/mL each

Results and Discussion

Figure 1 shows the analysis of a monoclonal IgG using a TSKgel SP-STAT cation exchange column. The same column, sample, and method were used to verify the column-system compatibility on both the HPLC (blue chromatogram) and UHPLC (red chromatogram) systems. The column performs better in the UHPLC system than it does when connected to the HPLC system. The number of theoretical plates is 6% higher for the UHPLC setup.

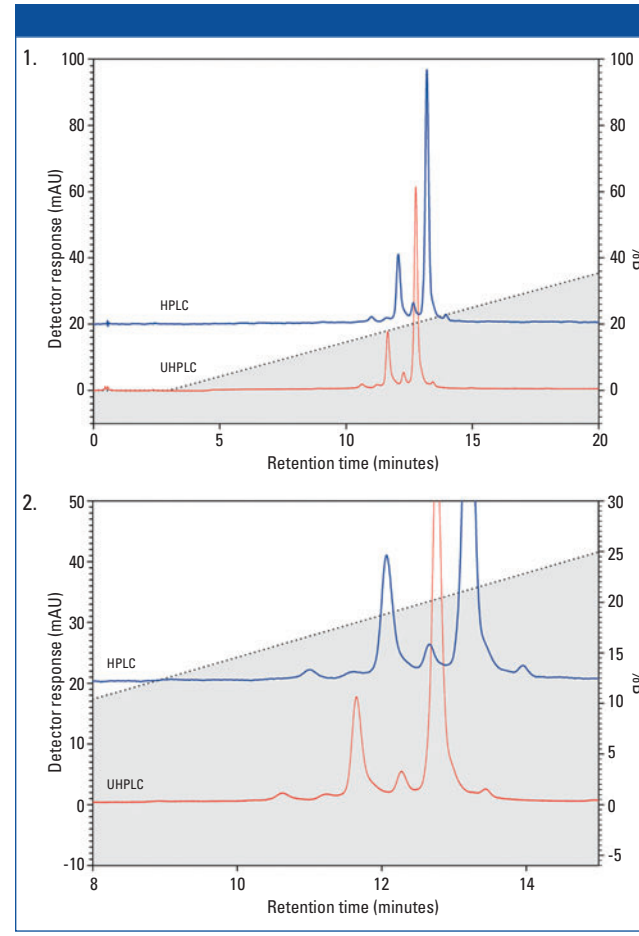

Figures 1 and 2: Analysis of a monoclonal IgG using a TSKgel SP-STAT column and a Zoomed Elution Profile of the mAb charge variants on the TSKgel SP-STAT column.

Figure 2 shows a zoomed elution profile of the mAb charge variants on the TSKgel SP-STAT column, which provides better insight into what extent the elution profile benefits from using a UHPLC system. The peak width is smaller for the UHPLC chromatogram. The decreased system dead volume resulted in the peak elution to occur earlier than it did on the HPLC system.

Figure 3 shows a standard protein mixture analyzed using a TSKgel G2000SW$_{XL}$ size exclusion column. The number of theoretical plates exceeds 32,000 for para-aminobenzoic acid when connected to the UHPLC system (blue chromatogram), while the column connected to the HPLC system (red chromatogram) only

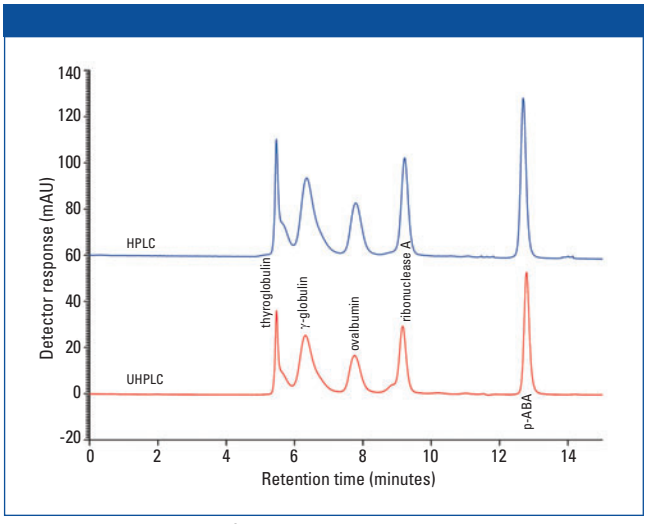

Figure 3: Separation of a standard protein mixture using a TSKgel G2000SW$_{XL}$ column.

reaches 29,000 for the same component.

Of course, resolution is an important factor when considering chromatographic performance. The HPLC data shows a resolution of 2.1 for the separation of γ-globulin and ovalbumin, and 10.2 for ribonuclease A and para-aminobenzoic acid. For the UHPLC data, the resolution factors increase to 2.2 and 10.9 for the respective peak pairs.

Conclusions

The results of both analyses using a TSKgel SP-STAT ion exchange column and a TSKgel G2000SW$_{XL}$ size exclusion column indicate excellent separation with high resolution when used on a UHPLC system. As a UHPLC system is simply an optimized HPLC system, bioseparation method transfer from HPLC to UHPLC is hardly more complicated than from one HPLC instrument to another. The applied pressure in these applications was far from exceeding the limit of a conventional HPLC system. This is the case in most bioseparation applications, since many biological sample molecules themselves cannot withstand very high pressure. Transferring established HPLC methods using HPLC columns to a UHPLC system is an economical and time-saving way to take advantage of this latest wave of development in HPLC technology.

TOSOH BIOSCIENCE

TOSOH

Tosoh Bioscience LLC
3604 Horizon Drive, Suite 100, King of Prussia, PA 19406
tel. (484) 805-1219, fax (610) 272-3028
Website: www.tosohbioscience.com

Improved SEC Separations Using TSKgel® Columns on a UHPLC System

Tosoh Bioscience LLC

Ultra high performance liquid chromatography (UHPLC) continues to grow in popularity due to highly efficient columns and fast run times, which result in excellent resolution and high throughput. UHPLC instrumentation is an optimized HPLC with low dead volume and has the ability to maintain constant flow rate against the higher back pressure generated by columns packed with small particles.

Recently introduced by Tosoh Bioscience, the TSKgel SuperSW mAb HTP column is able to be used with a UHPLC system, taking advantage of this column's smaller particle size and optimized dimensions. The end result is fast run times with a traditional HPLC column on a UHPLC system.

This note details the rapid analysis of an aggregated monoclonal antibody.

Experimental Conditions

Column:	TSKgel SuperSW mAb HTP, 4 µm, 4.6 mm i.d. × 15 cm
System:	Dionex UltiMate® 3000RS UHPLC System
Mobile phase:	0.1 mol/L sodium phosphate, pH 6.7 + 0.1 mol/L sodium sulfate
Flow rate:	0.35 mL/min 0.5 mL/min 0.7 mL/min
Detection:	UV @ 280 nm
Injection vol.:	5 µL
Sample:	aggregated monoclonal antibody

Results and Discussion

Figure 1 shows what is possible with a short gel filtration column made of HPLC column hardware packed with 4 µm particles when used on a UHPLC system. The new TSKgel SuperSW mAb HTP (4.6 mm i.d. × 15 cm) is optimized for high throughput applications and is compatible on UHPLC systems because of its ability to withstand high flow rates and low pressure drops.

It is possible to shorten analysis time of antibody aggregates from 15 min, using a conventional 30 cm column with 5 µm particles, down to 4 min when using a 15 cm column with 4 µm silica particles. The particle size is still large enough to keep the pressure in a moderate range, avoiding frictional heating inside the column, which might cause further aggregation or fragmentation during the analysis. These kinds of artifacts can be misinterpreted as an indication of a higher degree of impurity than actually exists within the sample vial.

Conclusions

The results of the analysis of a monoclonal antibody using the new TSKgel SuperSW mAb size exclusion column show a fast and high resolution separation using a UHPLC system. The TSKgel SuperSW mAb HTP column can withstand high flow rates and low pressure drops.

The use of HPLC columns with UHPLC systems offers the advantages of cost and time savings over having to purchase and develop new methods with UHPLC columns. Whether you are working with a UHPLC system or a conventional system, TSKgel columns are the first choice for bioseparations.

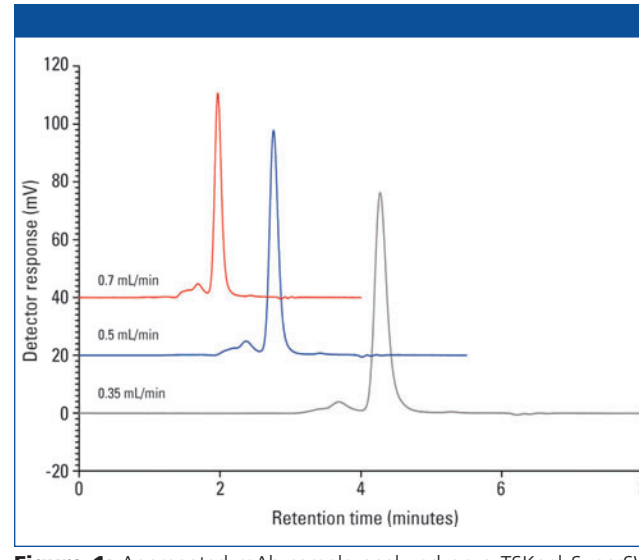

Figure 1: Aggregated mAb sample analyzed on a TSKgel SuperSW mAb HTP column.

TOSOH BIOSCIENCE

TOSOH

Tosoh Bioscience LLC
3604 Horizon Drive, Suite 100, King of Prussia, PA 19406
tel. (484) 805-1219, fax (610) 272-3028
Website: www.tosohbioscience.com

Molecular Weight Determination of Unfractionated Heparin

Wyatt Technology Corporation

Heparin is a polydisperse, heterogeneous polysaccharide derived from animal tissue. Heparin has been used as an anticoagulant for over 60 years and one of the fundamental parameters for characterizing unfractionated heparin (UFH) is its molecular weight (MW) and MW distribution. The molecular weight of heparin ranges from 3 to 50 kDa, but, typically falls within the 10 to 20 kDa range for unfractionated heparins used in medical applications. In light of heparin contamination issues in 2008, USP has proposed to include heparin molecular weight determination for the stage 3 heparin monograph revisions.

Many high-performance size-exclusion chromatography (SEC) systems have been developed and represent the most commonly used method in the MW determination of UFH. At Scientific Protein Laboratories (SPL) we have developed an SEC system coupled with multi-angle light scattering (MALS) for the determination of absolute MW and MW distribution of UFH and heparin derivatives. MALS eliminates the need for well-characterized molecular weight standards derived from heparin, and our procedure represents an improvement over the column calibration techniques used in other, relative MW determination methods.

For this application note, this method uses an Agilent LC-1200 series HPLC, 0.1 M ammonium acetate mobile phase, Shodex SB-804HQ analytical column (8.0 × 300 mm) with Shodex SB-G guard column, miniDAWN TREOS light scattering detector, and Optilab rEX refractive index detector. In addition to UFH, the method is capable of analyzing dermatan sulfate and over-sulfated chondroitin sulfate (OSCS) and can distinguish among the three (Figures 1 and 2). The specific refractive index increment (*dn/dc*) and second virial coefficient (A_2) measurements can also be determined using the Wyatt Optilab rEX and Wyatt miniDAWN TREOS detectors, respectively.

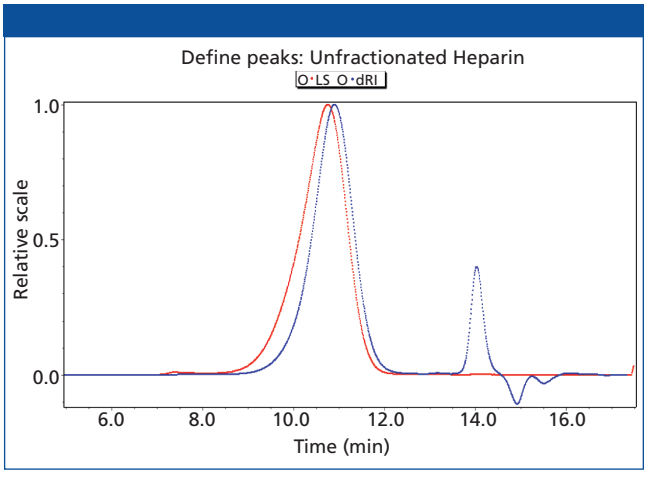

Figure 1: Examples of light scattering and RI traces for heparin.

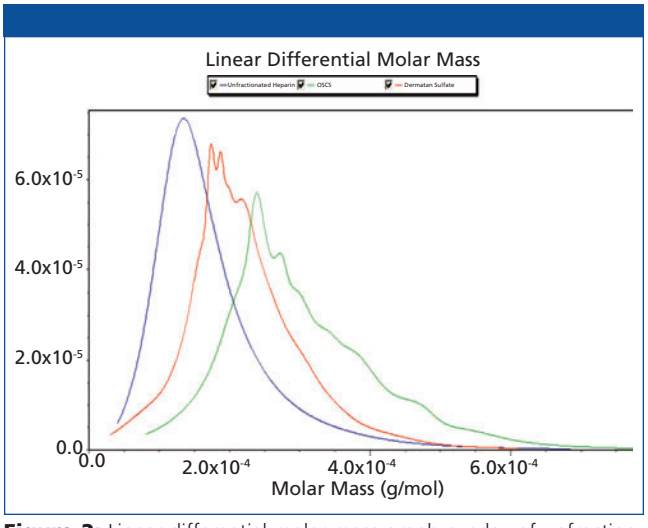

Figure 2: Linear differential molar mass graph overlay of unfractionated heparin, dermatan sulfate, and over-sulfated chondroitin sulfate (OSCS). The structural heterogeneity of glycosaminoglycans is demonstrated by the overlapping molecular weight distributions of the three samples.

This note graciously submitted by Lin Rao and John Beirne, Scientific Protein Laboratories, LLC.

Wyatt Technology Corporation
6300 Hollister Avenue, Santa Barbara, CA 93117
tel. (805) 681-9009, fax (805) 681-0123
Website: www.wyatt.com

Polycarbonate-Urethane Molar Mass Distributions

Wyatt Technology Corporation

Analysis of polycarbonate urethanes (PCUs) are a class of biocompatible polyurethanes that show great promise for use in orthopedic implants, such as artificial hips.

Traditional implant wear surfaces made from ultrahigh molecular weight polyethylene (UHMWPE) generate wear debris that induce osteolysis, causing the implant to loosen and ultimately require surgical replacement. PCU has been found to have lower friction properties than UHMWPE and has a modulus of elasticity similar to cartilage, resulting in PCU having superior wear behavior compared to UHMWPE (1). The molar mass distribution of PCU is of critical importance for its performance in medical device applications.

The molar mass distribution of a PCU resin was characterized using size exclusion chromatography (SEC) in N,N-dimethylacetamide (DMAc) containing 0.1-M lithium bromide. The SEC separation employed a pair of Tosoh Bioscience TSK-Gel Alpha-M columns, followed by Wyatt miniDAWN TREOS and Optilab rEX detectors connected in series. The molar mass distributions of PCU samples were measured using SEC-MALS, and also using conventional column calibration with a series of narrow polystyrene standards.

The PCU molar mass calculated using MALS is plotted versus retention volume in Figure 1. The column calibration plot using polystyrene standards is shown in Figure 1 for comparison. The differential molar mass distribution plots from light scattering and column calibration are compared in Figure 2. The molar mass was greatly overestimated using column calibration with polystyrene standards, due to the significant difference in the size in solution of a polystyrene molecule compared to a PCU molecule of the same molar mass. The M_w value of the PCU resin as measured by column calibration was 134,600 g/mol, compared to the actual value of 60,800 g/mol measured by SEC-MALS.

References

(1) R.W. Treharne and A.H. Greene, "The Case for the Use of Polycarbonate-Urethane in Orthopedic Implants," Med-Tech Precision (2008).

This note graciously submitted by Jason Todd, Polymer SolutionsIncorporated, Blacksburg, VA.

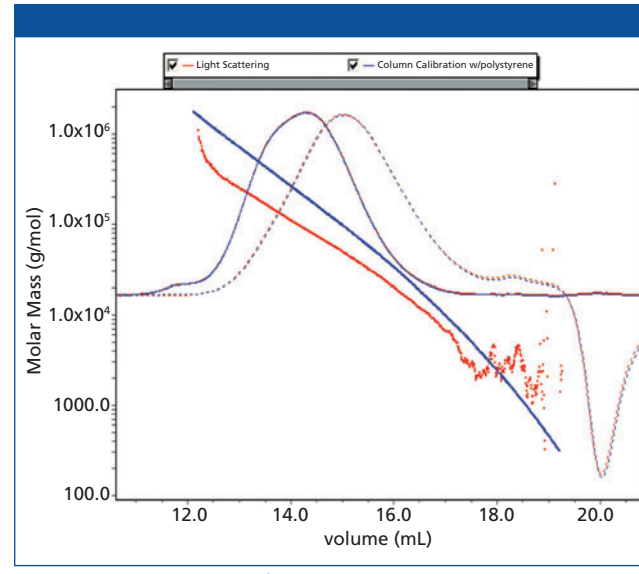

Figure 1: Comparison of polycarbonate-urethane absolute molar mass measured using SEC-MALS, versus apparent molar mass relative to polystyrene standards. The 90° light scattering (solid line) and refractive index (dashed line) chromatograms are overlaid.

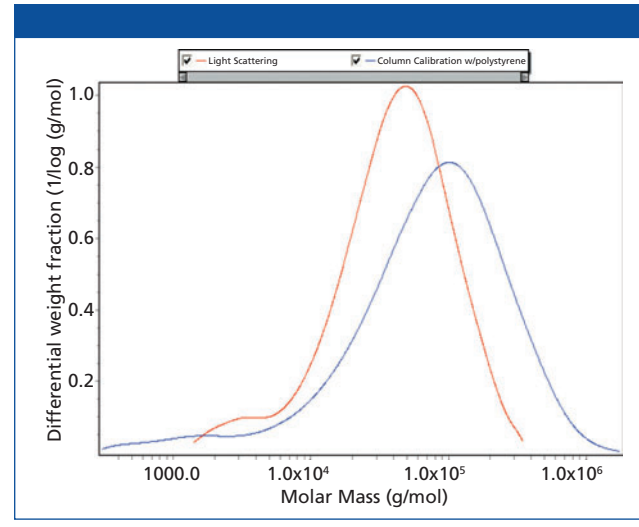

Figure 2: Comparison of the differential molar mass distribution plots obtained for a polycarbonate-urethane resin using SEC-MALS versus column calibration with polystyrene standards.

Wyatt Technology Corporation
6300 Hollister Avenue, Santa Barbara, CA 93117
tel. (805) 681-9009, fax (805) 681-0123
Website: www.wyatt.com

Hexavalent Chromium Determination Hamilton PRP-X100 Anion Exchange HPLC Column

Derek Jensen and Mark Carrier, Hamilton Company

Chromium (Cr) is a metal with an interesting relationship to the environment. Whereas trivalent chromium (Cr(III)) is an essential nutrient, hexavalent chromium (Cr(VI)) is a poison to humans and aquatic life and poses serious environmental and ecological threats. Recent studies of various ground and drinking water sources have detected toxic levels of Cr(VI). This dangerous trend has gained the attention of national and worldwide health organizations, such as the United States Environmental Protection Agency (EPA) and the US Food and Drug Administration (FDA), who seek to understand how widespread the problem is. The California Department of Public Health included Cr(VI) as an unregulated chemical requiring monitoring in 2001. Based on recent data, 3107 of 6565 public wells in Los Angeles, San Bernardino, and Fresno counties had Cr(VI) concentrations above 1 µg/L. A Public Health Goal of 0.02 µg/L was published in July 2011.

Analysis of chromium species is made challenging due to the nature of the element and diverse sample matrices. Because chromium exists in two oxidation states, it is important to differentiate between the nutrient, Cr(III), and the poison, Cr(VI) in samples. An HPLC-ICP-MS method using the Hamilton PRP-X100 has been developed in order to determine relative abundance of Cr(III) and Cr(VI) in diverse sample matrices.

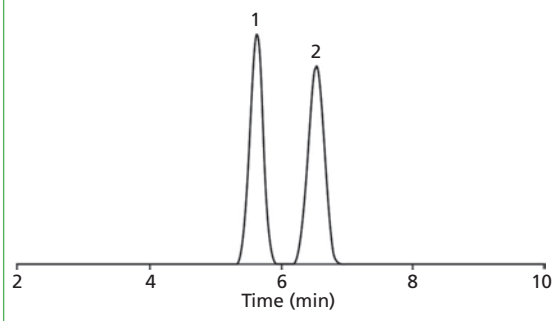

1) Cr(VI) and 2) Cr(III) EDTA separation on Hamilton PRP-X100

Experimental Conditions
Column: Hamilton PRP-X100, 5µm, 4.6 x 250 mm
Part Number: 79181
Flow Rate: 1.0 mL/min
Mobile phase: 2mM $(NH_4)_2CO_3$ for 0–3 min
40mM $(NH_4)_2CO_3$ for 3–14 min
2 mM $(NH_4)_2CO_3$ for 13–17 min
Injection volume: 50 µL, 100µg/L of each standard
Detection: ICP-MS

Trivalent chromium (Cr(III)) is stabilized as a chelation complex by incubating the sample at 70 °C in 0.2 mM EDTA. The Cr(III)-EDTA complex is suitable for binding to an anion exchange resin. Resolution of the two species then becomes a straightforward isocratic separation. Although UV and conductivity are suitable for detecting chromium species, inductively coupled plasma-mass spectrometry (ICP-MS) is the method of choice for trace analysis.

PRP-X100 HPLC Column Ordering Information

Column Type	Hardware Size (mm)	Particle Size		
		5 µm	10 µm	12 – 20 µm
PRP-X100	2.1 x 150 PEEK	79852		
PRP-X100	4.6 x 150 PEEK	79174	79354	
PRP-X100	4.6 x 250 PEEK	79181	79455	
PRP-X100	Bulk Resin (1 Gram)	79584	79585	79586

PRP-X100 HPLC Guard Column Ordering Information

Part Number	Description
79383	Analytical Guard Column Starter Kit (1 holder, 2 cartridges), PEEK
79385	Analytical Guard Column Replacement Cartridges (5/pk), PEEK

Hamilton Company
4970 Energy Way, Reno, NV 89502
tel. (775) 858-3000, (800) 648-5950
Website: www.hamiltoncompany.com

The Automated Extraction of Aqueous Samples by Method EPA 8270D Using the TurboTrace® ABN SPE System

FMS, Inc.

EPA 8270D calls for the extraction for analysis of semi-volatile analytes in various matrices. Target analytes mentioned in the method cover a wide range of compound classes resulting in reporting lists that often approach 100 compounds. In aqueous samples, the combination of compound groups such as phenols, analines, PAHs, phthalates, explosives, pesticides, n-nitrosoamines, and others results in a tedious process of multiple liquid-liquid extractions (LLE) with multiple pH adjustments to extract all the analytes. Large elution volumes (>360 mL of methylene chloride) combined with highly volatile analytes, usually result in low recoveries of target compounds and poor analytical precision.

The use of solid phase extraction (SPE) to automate the extraction process can drastically reduce many of the challenges traditional 8270 extractions pose. By automating the process with the FMS ABN SPE system, extraction chemists, normally confined to a hood shaking separatory funnels, can be freed up to perform additional tasks.

Instrumentation and Consumables Instrumentation

- FMS, Inc. TurboTrace™ ABN SPE system
- FMS, Inc. SuperVap™ Concentrator
- FMS, Inc. 200 mL concentrator tubes

Consumables

- Fisher Pesticide Optima* Methylene Chloride
- Fisher Anhydrous Sodium Sulfate
- Fisher Optima* Methanol
- Fisher HPLC Grade Water
- FMS 1 gram DVB Cartridges
- Fisher Concentrated Sulfuric Acid
- Fisher Sodium Hydroxide
- Restek Resprep 2 gram coconut charcoal cartridges (Cat# 26032)
- Restek 8270 matrix spike (Cat# 33073)
- Restek SV Internal Standard Mix (Cat# 31006)
- Restek B/N Surrogate (Cat# 31024)
- Restek Acid Surrogate (Cat# 31025)
- Restek Benzidines mix (Cat# 31834)

Procedure

Prepare 1 L samples of DI water
Adjust pH of samples to <2 by adding H2SO4 drop wise.
Spike samples with 8270 matrix spike, B/N surrogate, and acid surrogate spiking solutions
Load samples onto FMS TurboTrace ABN SPE system.
Affix collection bottle to retain post extraction aqueous sample.
Affix coconut charcoal and DVB with pre-filter cartridges to TurboTrace ABN system.

Figure 1: FMS TurboTrace SPE system with the SuperVap concentrator.

SPE

1. Cartridges pre-wet with DCM
2. Cartridges conditioned with MeOH
3. Cartridges conditioned with H_2O
4. Samples passed across DVB cartridges at ~20 mL/min via vacuum
5. Cartridges partially dried with N_2 at 15 PSI
6. Sample bottles sprayed with DCM
7. DCM bottle spray loaded across cartridge and collected through-in-line $NaSO_4$
8. Cartridges eluted with additional 10 mL DCM
9. Cartridges purged with N_2 eluting n-Hexane directly to FMS SuperVap concentrator
10. Remove aqueous collection bottle and add NaOH solution to sample mixing thoroughly till pH is >12
11. Attached sample bottle to system for second pass
12. DVB Cartridge re-conditioned with MeOH
13. DVB Cartridge re-conditioned with H_2O
14. Sample passed across both cartridges at ~10 mL/min
15. Cartridges dried with N_2 for 1 min each
16. Sample bottle sprayed with DCM
17. DCM bottle spray loaded across DVB cartridge and collected through in-line $NaSO_4$
18. DVB Cartridge eluted with additional 5 mL DCM
19. Coconut charcoal eluted with 20 mL DCM
20. Cartridges independently purged of residual solvent via N_2 stream

SuperVap Concentrator

1. Preheat temp.: 10 min at 40 °C
2. Evap mode: 40 °C
3. Nitrogen Pressure: 10 PSI
4. Evaporate extracts 1 mL*

Table I: Results from six 1 L LCS samples (50 µg/L concentration)

Analyte	Mean	Analyte	Mean
Pyridine	71.63	Acenaphthene	95.77
NDMA	54.44	2,4-dinitrophenol	83.84
2-Fluorophenol (Surr)	85.84	4-Nitrophenol	99.19
Phenol-d5 (Surr)	78.32	dibenzofuran	94.81
Pheno	74.6	2,4-dinitrotoluene	96.66
Analine	84.06	2,3,5,6-Tetrachlorophenol	89.25
bis(2-chloroethyl) ether	93.3	2,3,4,6-Tetrachlorophenol	87.3
2-Chlorophenol	85.99	diethyl phthalate	107.46
1,3-Dichlorobenzene	84.86	Fluorene	100.96
1,4-Dichlorobenzene	86.29	4-chlorophenyl phenyl ether	90.49
1,2-Dichlorobenzene	90.67	4-Nitroanaline	112.58
benzyl alcohol	90.12	2-Methyl-4,6-dinitrophenol	102.85
2-methylphenol	91.32	NDA-NDPA	89
bis(2-chloroisopropyl) ether	94.6	Azobenzene	101.4
N-nitrosodi-n-propylamine	103.54	2,4,6-Tribromophenol (Surr)	86.58
4-methylphenol/3-methylphenol	93.3	4-bromophenyl phenyl ether	90.94
Hexachloroethane	89.79	Hexachlorobenzene	92.84
Nitrobenzene-d5 (Surr)	96.27	pentachlorophenol	96.05
nitrobenzene	111.68	Phenanthrene	99.97
isophorone	94.42	Anthracene	100.15
2-Nitrophenol	84.56	Carbazole	108.6
2,4-dimethylphenol	99.46	butyl benzyl phthalate	117.76
bis(2-chloroethoxy)methane	100.55	Pyrene	105.37
2,4-Dichlorophenol	89.01	Fluoranthene	98.53
1,2,4-trichlorobenzene	85.24	Terphenyl-d14 (Surr)	102.05
Naphthalene	87.54	di-n-butyl phthalate	109.91
4-Chloroanaline	80.43	benzo[a]anthracene	106.3
hexachlorobutadiene	81.3	Chrysene	102.82
4-Chloro-3-methylphenol	89.26	bis(2-ethylhexyl)phthalate	124.46
2-methlynaphthalene	103.61	di-n-octyl_phthalate	118.02
1-methlynaphthalene	103.95	benzo[b]fluoranthene	102.23
hexachlorocyclopentadiene	52.78	benzo[k]fluoranthene	114.84
2,4,6-Trichlorophenol	78.76	benzo[a]pyrene	99.25
2,4,5-Trichlorophenol	79.44	indeno[1,2,3-cd]pyrene	96.23
Acenaphthylene	89.58	dibenzo[a,h]anthracene	94.5
1,2-dinitrobenzene	96.45	benzo[g,h,i]perylene	95.43
3-Nitroanaline	100.57	Benzidine	88.21
2,6-dinitrotoluene	101.41	3,3-dichlorobenzidine	94.6

*Evaporator tubes manually rinsed with DCM to ensure no target analytes adhere to evaporator tube walls. Internal standard solution added to extract postevaporation for GC–MS analysis.

Conclusions

Evaluation of the performance spikes on the FMS TurboTrace ABN extraction system resulted in average recoveries for nearly all analytes between 70–130%. Combined with the analysis of blank replicates which yielded background concentrations of less than 1 µg/mL for all analytes, the data, when compared to the performance tables within EPA 8270D, shows that automated solid phase extraction is not only equivalent, but in some cases superior to traditional LLE extractions.

Repeatability data gave percent deviations between replicates of less than ±10% for most compounds, and ±20% for all. Fully automated sample loading and eluting of both cartridges independently, and in sequence, eliminates the need to have an extraction chemist separate the cartridges at different stages of the operation. The reduction of human interaction saves time, reduces human error, and produces consistent reproducible results.

When paired with the FMS SuperVap concentrator, the TurboTrace™ ABN SPE system provides complete, automated sample preparation for aqueous samples by EPA 8270D.

FMS, Inc.
580 Pleasant Street, Watertown, MA 02472
tel. (617) 393-2396, fax (617) 393-0194
Website: www.fms-inc.com; Email: onlineinfo@fms-inc.com

Leveraging Mass Defect Plots for Compound Identification in Complex Matrices by GC-HRT

Jonathan Byer, David E. Alonso, Jeff Patrick, and Joe Binkley, Life Science and Chemical Analysis Centre, LECO Corporation

Gas chromatography coupled to high resolution time-of-flight mass spectrometry (GC–HRT) was used to identify halogenated organic compounds based on their mass defects in fish tissue extracts.

The expression "a needle in a haystack" applies fittingly to modern mass spectrometry users when attempting to identify unknown compounds in complex matrices. Mass defect plots may be thought of as a magnet used for extracting needles from the haystack. Mass defect is defined as the difference between a compound's nominal mass and its exact mass. Every compound characterized by its chemical formula has a unique mass defect resulting from the combination of its elements. This characteristic can be used to simplify the search for unique and novel compounds. Until recently, FT-ICR-MS was the only technique that properly leveraged mass defect. With modern advances in TOF technology, it is now possible to comprehensively achieve sufficient resolution on LECO's Pegasus GC-HRT platform to perform precise mass defect measurements.

Experimental

The IUPAC convention for calculating exact mass stipulates that C = 12.0000. However, the scale can be redefined according to the following equations:

*Scaled Mass Defect (X)= Accurate Mass (IUPAC)*Mass Scale (X)*

Mass Scale (X) = Nominal Mass (X)/Exact Mass (X)

where X is the reference formula, that is, C = IUPAC, CH2 = Kendrick. The advantage of plotting scaled mass defect versus nominal (or accurate) mass is the horizontal alignment of compounds related to the reference formula (such as homologs). A whole fish homogenate was analyzed using the Pegasus GC-HRT in EI mode to identify halogenated persistent organic pollutants by their hydrogen substituted for chlorine (Cl-H) scaled mass defect. The scaling factor was 34/33.96102, for the ratio between the nominal and exact mass of Cl-H.

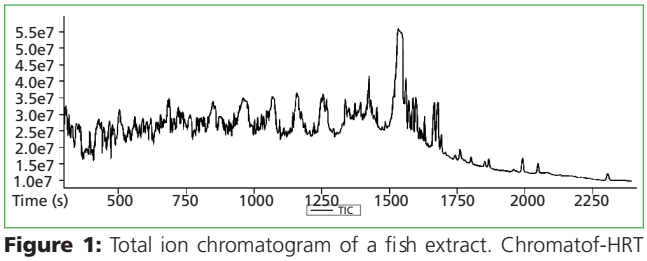

Figure 1: Total ion chromatogram of a fish extract. Chromatof-HRT software identified >2000 unique peaks.

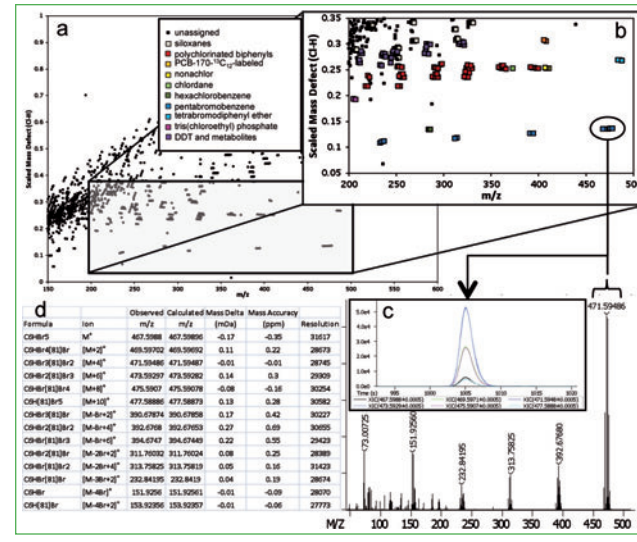

Figure 2: (a) Scaled mass defect plot (Cl-H) highlighting several masses corresponding to halogenated compounds; (b) XICs of the isotope cluster; (c) calculated chemical formula for the selected *m/z* values.

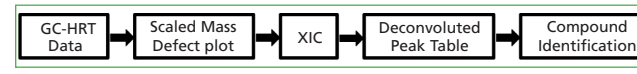

Figure 3: Compound identification workflow that utilizes mass defect as a form of data sorting.

Results and Discussion

Fish extracts are very complex matrices containing many natural and anthropogenic compounds as demonstrated by the chromatogram in Figure 1. The Cl-H scaled mass defect plot (Figure 2a), generated by summing the mass spectra over the entire chromatographic run, showed a region dominated by halogenated compounds that were not apparent in the total ion chromatogram (Figure 2b). From the mass defect plot, accurate masses (+/- 0.5 mDa) were selected for display as extracted ion chromatograms (XIC) (Figure 2c). Data processing the sample using peak find in Chromatof-HRT software, enabled identification of the chromatographic peaks in the XIC by library database searching. Alternatively, if no library hits were found, the accurate mass data were utilized further to calculate chemical formulae, which were then searched against online chemical databases. The mass spectrum in Figure 2c was not found in the NIST library; however, the composite accurate mass data (Figure 2d) enabled it to be identified as pentabromobenzene. This workflow is demonstrated schematically in Figure 3.

Determination of Explosives in Water Using a Novel Polymeric DVB Sorbent

Xiaoyan Wang, UCT, LLC

US EPA method 529 is the procedure to determine explosives and related compounds in finished drinking water. The method is applicable for a variety of explosives that can be partitioned from aqueous samples onto a polymeric solid phase extraction (SPE) sorbent, and with sufficient volatility and thermal stability for GC–MS analysis. Recently, UCT developed a novel polymeric DVB sorbent for EPA method 529. One liter of water sample is passed through an SPE cartridge packed with 500 mg of the sorbent using a large sample delivery tube. The retained explosives are then eluted with ethyl acetate (EtOAc). A drying cartridge packed with anhydrous sodium sulfate is attached to the end of the SPE cartridge in the elution step, eliminating the need for a separate drying step.

SPE Materials	
ECHLD156	500 mg HL DVB in 6 mL cartridge
AD0000AS	Cartridge adaptor
ECSS15M6	5 g anhydrous sodium sulfate in 6 mL cartridge

SPE Procedure

a) Preserve samples as stated in the EPA method 529.
b) Spike with appropriate amounts of surrogates, and target analytes for fortified samples.
c) Connect the large sample delivery tubes to the top of the SPE cartridges (ECHLD156), and attach the cartridges to a SPE manifold.
d) Wash the SPE cartridges with three aliquots of 5 mL EtOAc, condition with three aliquots of 5 mL methanol, and equilibrate with two aliquots of 10 mL DI water.
e) Insert the stainless steel ends of the sample delivery tubes into the sample bottles, and draw the entire sample through the SPE cartridge at a fast drop-wise fashion (about 15 mL/min).
f) Remove the sample delivery tubes from the SPE cartridges and dry the cartridges under full vacuum for 10 min.
g) Attach drying cartridges (ECSS15M6) to the end of SPE cartridges with cartridge adaptors (AD0000AS). Insert collection vials into the manifold.
h) Wash the sample bottles with 5 mL EtOAc, and pass the rinsate through the SPE cartridges slowly and collect. Add a second aliquot of 5 mL EtOAc to the top of the cartridge and elute the solvent slowly into the collection vial.
i) Concentrate the eluate to about 0.9 mL under a gentle stream of nitrogen at 40 °C.
j) Add internal standard and adjust the final volume to 1 mL with EtOAc.
k) The samples are ready for GC–MS analysis.

Instrumental

GC–MS: Agilent 6890N GC with 5975C MSD Injector: 1 µL on-column injection
GC column: Restek Rxi®-5sil MS 30 m*0.25 mm*0.25 µm with 10-m guard column
Carrier gas: Helium at a constant flow of 1.2 mL/min
Oven: Initial temperature at 50 °C, hold for 1 min; ramp at 8 °C/min to 210 °C; ramp at 20 °C/min to 250 °C, hold for 2 min.
Tune: bfb.u
Full Scan: 45–250 amu

Results

Table I: Accuracy and precision data

Analyte	Single-lot		Multiple-lots (5)	
	Avg. Rec%	RSD% (n = 5)	Avg. Rec%	RSD% (n = 25)
Nitrobenzene d5 - Surrogate	92.4	3.5	88.9	4.3
Nitrobenzene	86.8	2.7	88.8	4.6
2-Nitrotoluene	87.6	3.6	89.1	4.7
3-Nitrotoluene	86.6	3.6	87.7	4.6
4-Nitrotoluene	84.4	3.3	87.2	4.9
1,3-Dinitrobenzene	102.4	5.3	99.7	4.2
2,6-Dinitrotoluene	98.2	5.7	97.3	4.8
2,4-Dinitrotoluene	91.2	5.3	92.9	4.2
1,3,5-Trinitrobenzene	100.0	9.1	100.4	5.5
2,4,6-Trinitrotoluene	103.0	6.3	100.9	5.3
RDX	107.0	1.7	111.1	5.8
4-Amino-2,6-Dinitrotoluene	100.1	7.5	99.6	5.8
3,5-Dinitroaniline	104.3	5.6	103.6	6.3
2-Amino-4,6-Dinitrotoluene	103.3	5.2	105.7	5.0
Tetryl	102.2	3.7	105.4	4.7
Overall mean	**96.6**	**4.8**	**97.2**	**5.0**

Conclusion

Excellent recoveries with an overall mean of >95% and minimum lot-to-lot variations of <10% were obtained using UCT's novel DVB sorbent for explosives in drinking water. This procedure is also applicable for explosives in wastewater (EPA method 8330) with minor modifications (SPE method available upon request).

UCT, LLC
2731 Bartram Road, Bristol, PA 19007
tel: (800) 385-3153, Email: methods@unitedchem.com
Website: www.unitedchem.com

Streamlining Sample Processing for Semi-Volatile Organics in the Most Challenging Water Samples

David Gallagher, Jim Fenster, and Michael Ebitson, Horizon Technology, Inc.

Laboratories taking in a high volume of aqueous semi-volatile samples know that every sample is different. Samples can contain varying amounts of suspended particulates and/or sediment due to either the source of the water, or the collection technique. Still other samples may form flocculates under elevated pH conditions resulting in emulsions when agitated in techniques such as liquid-liquid extraction (LLE). These types of samples have historically also proven challenging when using solid phase extraction (SPE).

To meet the demands of this challenging type of sample, a new extraction method only requiring the sample to be acidic to extract over 100 routine compounds has been developed. This method uses SPE technology with an economical and effective extended disk holder. The Fast Flow Sediment Disk Holder allows laboratories to use an economical 47-mm SPE disk while still maintaining the use of a 100 mm prefilter. The Atlantic 8270 One Pass Disk contains sorbent that is able to extract the large list of semi-volatile compounds without a second extraction at an elevated pH, eliminating the formation of flocculates.

This work examines the procedure and performance characteristics of this simplified extraction process.

Figure 1 shows the extraction process using the one-pass disk and a carbon cartridge.

Results and Discussion

Six extractions were performed, each extraction took approximately 120 min to complete. Of this time, a maximum of 10 min of analyst time was taken from start to finish interacting with the samples.

Figure 2 shows the results on a large suite of compounds found in the US EPA 8270 list. The results show that, with an average recovery of 80% and an average relative standard deviation of 5.95% over 114 compounds, the automated SPE methodology presented is an excellent alternative for extracting USEPA 8270 semi-volatile compounds from aqueous samples.

The key to this methodology was the Atlantic 8270 One Pass Disk. The disk's unique sorbent was able to extract a large list of semi-volatile compounds without a second pass of the sample at

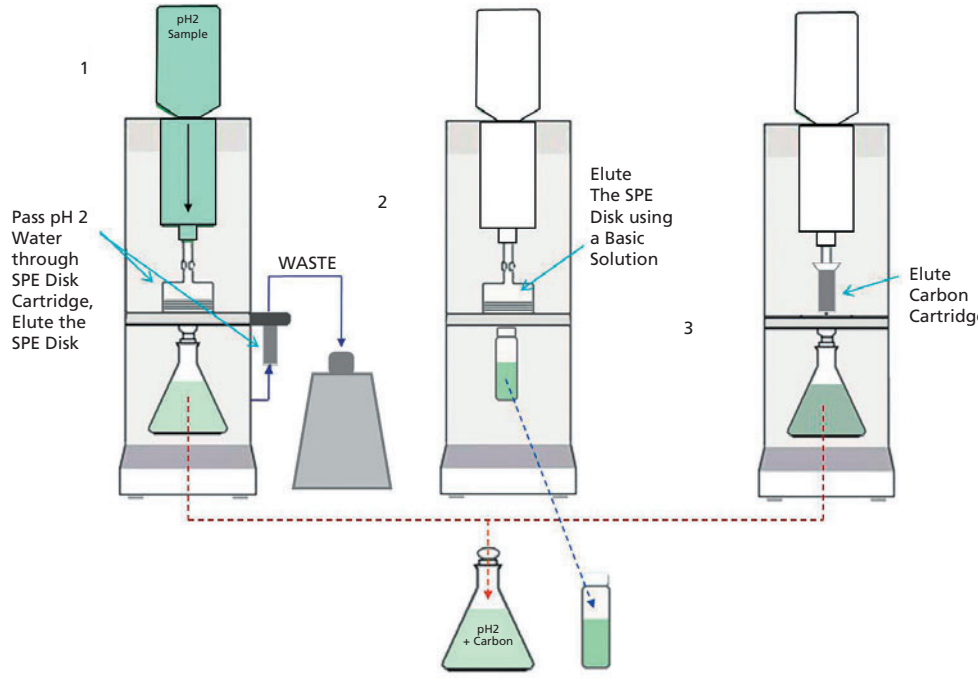

Figure1: SPE extraction scheme.

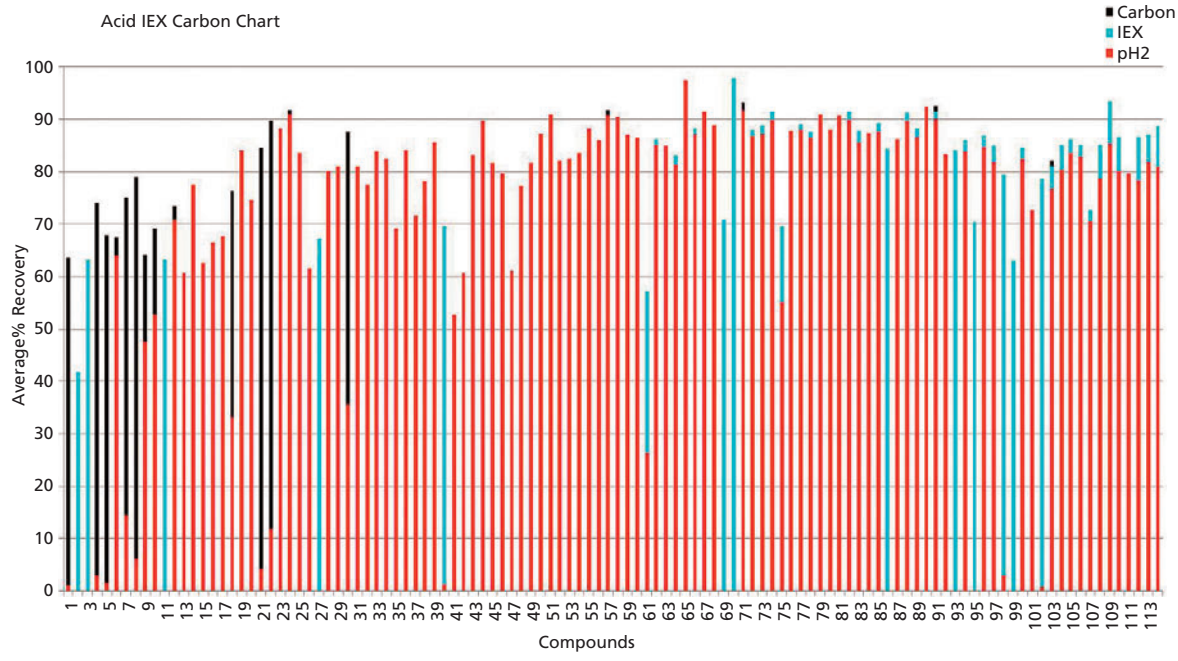

Figure 2: Average recovery of six replicate extractions for a large suite of compounds.

an elevated pH. Each extract was automatically dried and concentrated using the DryVap® System. By concentrating extracts under vacuum it lowered the boiling point ensuring the more volatile semivolatiles were not boiled off and ensures higher recoveries.

Conclusions

The data presented clearly illustrates this automated SPE methodology is capable of successfully extracting over 100 compounds specified by EPA method 8270.

- The single pH extraction eliminates the need to basify the sample, reducing the chance of flocculates and resulting low recoveries.
- This new SPE methodology for semi-volatiles streamlines the extraction process and allows for all types of aqueous samples to be processed at the same high flow rate.
- This automated SPE methodology is a solution that will reduce analyst labor, solvent usage, and turn-around-time while maintaining the high quality results required within today's laboratories.

References

(1) Method 8270D Semi volatile Organic Compounds by Gas Chromatography/Mass Spectrometry (GC/MS). U.S. Environmental Protection Agency, January 1998, Revision 4.

(2) D. Gallagher, J. Fenster, M. Ebitson, and J.McGettrick, "Streamlining Sample Processing for Semi-Volatile Organics Using the Fast Flow Sediment Disk Holder and the Atlantic 8270 One Pass Disk," Application Note 069, Horizon Technology, Inc., 2011.

Horizon technology
PREPARE FOR BETTER RESULTS

Horizon Technology Inc.
16 Northwestern Drive, Salem, NH 03079
tel. (603) 893-3663, fax (603) 893-4994
Website: www.horizontechinc.com.

Analysis of Coffee and Coffee Products by HPLC for the Determination of Natural Components and Harmful Contamination

Edgar Naegele, Agilent Technologies, Inc.

In this application we demonstrate the analysis of coffee and coffee products according to DIN methods. The performance of the analysis is shown for linearity, limit of detection (LOD), limit of quantification (LOQ), retention time, and area precision. The performance is also shown for solvent-saver columns with 2.7 µm superficially porous particles.

The measurement of some compounds inherent in coffee products by means of HPLC with UV absorbance or fluorescence detection is standardized in the DIN ISO methods:

- The determination of caffeine with approximately 80–120 mg per cup is described in DIN 20481. According to the European Commission decaffeinated coffee must contain less than 0.1% caffeine (1).
- The determination of chlorogenic acid, naturally occurring in green coffee beans with about 3.5 g per 100 g is described in DIN 10767. It is the ingredient considered to cause problems for coffee drinkers with a sensitive stomach. To adjust the content of chlorogenic acid in coffee, different roasting procedures are applied (2).
- The determination of methyl cafestol, a diterpene, naturally occurring in green coffee beans up to 0.06% is described in DIN 10779. Biologically, cafestol has an increasing effect on the serum cholesterol level. On the other hand, there are studies showing for example anti-carcinogenic effects (3).
- Ochratoxin A, is a mycotoxin produced by *Apergillus* species and one of the major mycotoxins occurring in coffee. According to European regulations it must not exceed 3.5 µg/kg. Ochratoxin A can cause acute toxicity in kidneys and cancer. It is determined as described in the DIN EN 14132 by HPLC/fluorescence detection after enrichment on an immunoaffinity column (4).

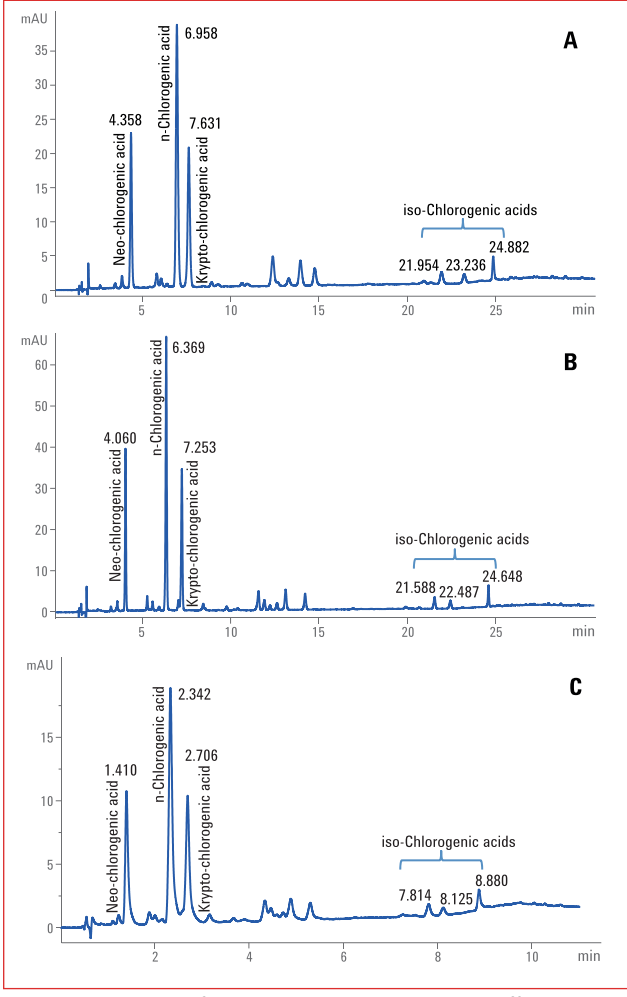

Figure 1: Analysis of isomeric chlorogenic acids on different column dimensions.

Experimental

1) Agilent ZORBAX Eclipse Plus C18, 4.6 × 150 mm, 5 µm. Flow rate 1.0 mL/min.
2) Agilent Poroshell 120 EC-C18, 3.0 × 150 mm, 2.7 µm. Flow rate 0.43 mL/min.
3) Agilent Poroshell 120 EC-C18, 3.0 × 50 mm, 2.7 µm. Flow rate 0.43 mL/min.

Results and Discussion

For all compounds calibration curves were created by means of a UV absorbance detection with the exception of ochratoxin, where a fluorescence detection (FLD) was used. The calibration levels were measured under standard HPLC conditions (column 1) as described in the DIN literature. The dilution series was conducted until the limit of quantification (LOQ) was reached at a signal-to-noise (S/N) ratio of 10 and the limit of detection was calculated for a S/N ratio of 3 (Table I). Typically, the LOQs are in the lower µg/L range, for ochratoxin in the lower ng/L range. From multiple injections, the relative standard deviation (RSD) values of the retention time, below 0.07%, and the area RSD, below 0.2%, were calculated.

Table I: Performance data for different analytes and analysis methods

	Caffeine	Chlorogenic acid	Methyl casfestol	Ochratoxin A
Calibration range	0.125–20.0 mg/L	0.156–20.0 mg/L	0.781–100.0 mg/L	156.25 ng/L–20.0 µg/L
Linearity	0.99999	0.99998	0.99993	1.00000
LOQ (A)	113 µg/L	90 µg/L	580 µg/L	100 ng/L
LOQ (B)	51 µg/L	50 µg/L	380 µg/L	70 ng/L
LOQ (A)	34 µg/L	30 µg/L	170 µg/L	39 ng/L
LOQ (B)	15 µg/L	15 µg/L	120 µg/L	14 ng/L
r.t. RSD (%)	0.06	0.07	0.05	0.27
Area RSD (%)	0.2	0.15	0.15	0.39

As an example, the separation of isomeric chlorogenic acids from a roasted coffee sample under standard HPLC conditions is shown in Figure 1a. The isomers are separated over a run time of 30 min. The experiment was reaped after transferring the method to column 2 with a flow rate of 0.43 mL/min. For the calibration, similar linearity was found but the LOQ and LOD were lower on the 2.7 µm column. This was due to the better separation performance, showing narrower and sharper peaks with improved S/N ratio enabled by the 2.7 µm superficially porous particles (Table I, row B; Figure 1b). In addition, this column saves 57% of solvent. To improve the efficiency, column 3 was used. This decreases the total run time by a factor of three and allows increasing sample throughput by a factor of three (Figure 1c).

Conclusion

The possible improvement of standard DIN methods for the analysis of coffee and coffee products is shown. The throughput could be increased by a factor of three while saving 57% of solvent.

References

(1) E. Naegele, "Determination of Caffeine in Coffee Products According to DIN 20481," Agilent Technologies Application Note, publication number 5991-2851EN (2013).

(2) E. Naegele, "Determination of Chlorogenic Acid in Coffee Products According to DIN 10767," Agilent Technologies Application Note, publication number 5991-2852EN (2013).

(3) E. Naegele, "Determination of Methylcafestol in Roasted Coffee Products According to DIN 10779," Agilent Technologies Application Note, publication number 5991-2853EN (2013).

(4) E. Naegele, "Determination of Ochratoxin A in Roasted Coffee According to DIN EN 14132," Agilent Technologies Application Note, publication number 5991-2854EN (2014).

Agilent Technologies

Agilent Technologies
5301 Stevens Creek Blvd., Santa Clara, CA 95051
Website: www.agilent.com

Analysis of Polyether Antibiotics in Animal Feeds by HPLC with Post-Column Derivatization

Maria Ofitserova and Sareeta Nerkar, Pickering Laboratories, Inc.

Polyether antibiotics are commonly used for preventing coccidiosis and other infections in poultry and for improving feed efficiency for beef cattle and swine. The use of polyether antibiotics is strictly regulated, with only specific ionophores approved for use in feeds intended for different animals.

Analysis of polyether antibiotics by HPLC with post-column derivatization and UV–vis detection has been proven to successfully identify and quantify monensin, narasin, and salinomycin in medicated feeds, supplements, and premixes as well as to determine trace contamination levels in non-medicated feeds (1,2).

Post-column derivatization of polyether antibiotics is done using highly acidic vanillin or DMAB reagents. Pinnacle PCX derivatization system (Pickering Laboratories, Inc.) has an inert flow path and automated system wash capabilities that make it uniquely suitable for handling corrosive reagents. The two-pump system is recommended to extend reagent stability, but the single-pump system for this application is also available.

Adding a fluorescence detector to the instrumentation allows for using the same extraction procedure and HPLC conditions to also determine lasalocid which doesn't require post-column derivatization.

Method

Sample Preparation

To 25 g of finely ground feed sample, add 100 mL of extraction solution (90% methanol–10% water). Shake for 1 h at high speed using mechanical shaker. Let the solids settle and filter an aliquot of the extract for injection. Dilute with extraction solution if needed to fit the calibration curve. Use 2.5 g portion when testing premixes.

Table I: Polyether antibiotics in certified medicated feeds

	Feed Type	Certified Amount	Found in Sample	Recoveries	RSD, $N = 4$
Monensin	Beef feed	267 g/ton	275 g/ton	103%	0.7%
Lasalocid	Milk replacer	72 g/ton	69 g/ton	96%	3.3%

Table II: Spike recoveries for monensin

	Non-Medicated Bird Feed		Non-Medicated Rabbit Feed	
	Monensin A	Monensin B	Monensin A	Monensin B
Spike Level	172 g/ton	8 g/ton	86 g/ton	4 g/ton
Recoveries	100%	100%	101%	102%
RSD, $N = 3$	1.9%	2.1%	1.1%	0.6%
Spike Level	3.44 g/ton	0.16 g/ton	3.44 g/ton	0.16 g/ton
Recoveries	96%	95%	94%	88%
RSD, $N = 3$	0.7%	3.1%	0.9%	1.6%

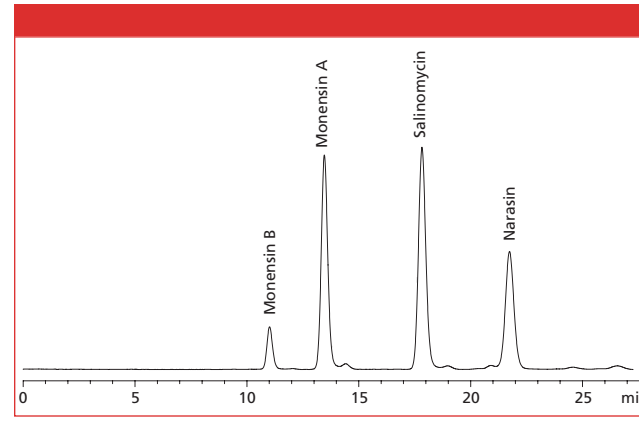

Figure 1: Standard mixture of monensin, salinomycin, and narasin.

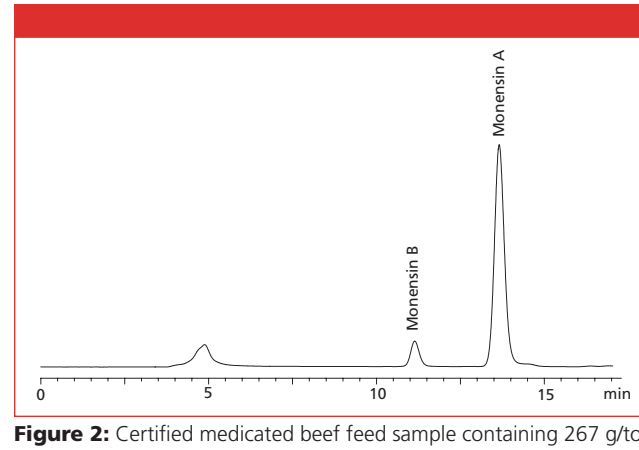

Figure 2: Certified medicated beef feed sample containing 267 g/ton of monensin.

Analytical conditions

Analytical Column: Polyether Column, C18, 4.6 × 250 mm, Catalog No. 2381750
Temperature: 40 °C
Flow rate: 0.7 mL/min
Mobile Phase: 90% methanol, 10% of 5% acetic acid solution in water, isocratic
Injection volume: 20 µL

Post-Column Conditions

Post-column System: Pinnacle PCX
Reactor Volume: 1.4 mL

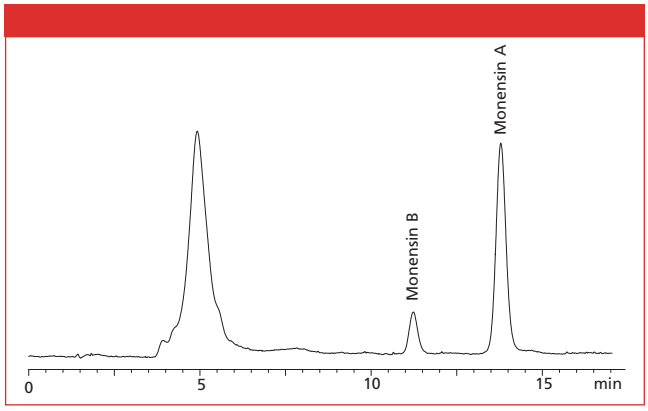

Figure 3: Non-medicated bird feed sample spiked with monensin A (3.44 µg/g) and monensin B (0.16 µg/g).

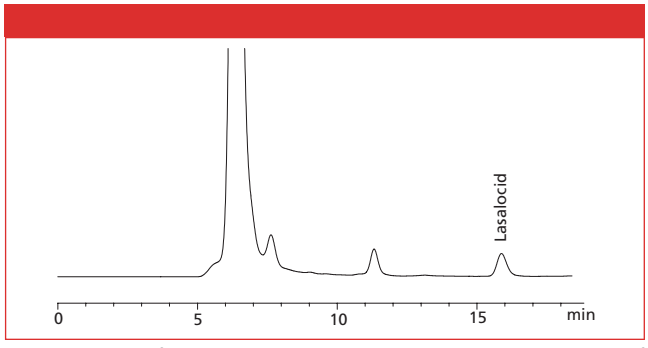

Figure 4: Certified medicated milk replacer containing 72 g/ton of lasalocid.

Reactor Temperature: 90 °C
Reagent 1: Concentrated sulfuric acid/methanol (4:96 v/v)
Reagent 2: 60 g of vanillin in 950 mL of methanol
Reagents Flow Rate: 0.3 mL/min
Detection: UV-vis 520 nm (for Lasalocid – FLD, Ex. 322 nm, Em. 370 nm)

Calibration

Monensin A: 0.1–50 ppm, $R^2 = 0.999$
Monensin B: 0.0035–0.7 ppm, $R^2 = 0.999$
Lasalocid acid: 0.25–50 ppm, $R^2 = 0.999$

Conclusion

Analysis of polyether antibiotics by HPLC with post-column derivatization is a robust and sensitive method that utilizes standard equipment and could easily be adopted by testing laboratories. It allows for testing of different ionophores at wide range of concentrations, including at trace levels. Using Pinnacle PCX post-column derivatization system, factory configured for the analysis, guarantees stable and reproducible results.

References

(1) H. Campbell and G. Nayeri, *J. AOAC Int.* **89**, 1229–1242 (2006).
(2) AOAC Official Method 997.04. Monensin in Premix and Animal Feeds.

PICKERING LABORATORIES

Pickering Laboratories, Inc.
1280 Space Park Way, Mountain View, CA 94043
tel. (800) 654-3330, (650) 694-6700
Website: www.pickeringlabs.com

Alcoholic Beverage Fusel Alcohol Testing with Static Headspace

Roger Bardsley, Teledyne Tekmar

Fusel alcohols, a common byproduct of fermentation, in abnormal quantities or types can indicate alcoholic beverage adulteration. The Alcohol and Tobacco Tax and Trade Bureau of the US Department of the Treasury (TTB) method SSD:TM:200 (1) is a direct injection method which transfers all compounds into the inlet which may requre frequent liner changes. The quality control section of this method suggests changing the liner if the correlation coefficient (r^2) falls below 0.99.

A static headspace method was developed using Teledyne Tekmar automated headspace vial samplers, the HT3 and Versa. Static headspace transfers only volatile compounds to the GC, leaving nonvolatile compounds in the headspace vial.

Experimental-Instrument Conditions

The HT3 was coupled to a GC/FID system equipped with a 624-type column, 30 m × 0.32 mm × 1.8 µm. The Method Optimization Mode (MOM) feature was utilized to determine the best headspace sample temperature for analysis.

Standard/Sample Preparation

The fusel oil stock standard was prepared following the SSD:TM:200 procedure. Working standards were prepared by diluting the stock standard with water. Samples consisted of 10 mL of the working standard or blank water.

Results and Discussion

The TTB QC requires a correlation coefficient (r^2) of greater than 0.99 for all fusel alcohols. The r^2 and the response factor percent relative standard deviation (Rf %RSD) were plotted for each compound at the various platen temperatures.

A sample temperature of 70 °C best meets the TTB requirements of an r^2 value of greater than 0.99 and an Rf %RSD of less than 10%. Table I lists these values for the corresponding compounds.

Table I: Results

Compound	Concentration Range	r2	%RSD
Methanol	0.016% to 0.8% v/v	0.9981	5.05
Ethanol	0.08% to 4% v/v	0.9984	4.02
n-Propanol	8 to 400 mg/L	0.9990	7.70
Ethyl Acetate	16 to 800 mg/L	0.9995	3.50
Isobutanol	16 to 800 mg/L	0.9999	1.01
n-Butanol	0.8 to 40 mg/L	0.9991	6.72
Isoamyl Alcohol	16 to 800 mg/L	0.9996	3.36
Active Amyl Alcohol	16 to 800 mg/L	0.9997	8.50

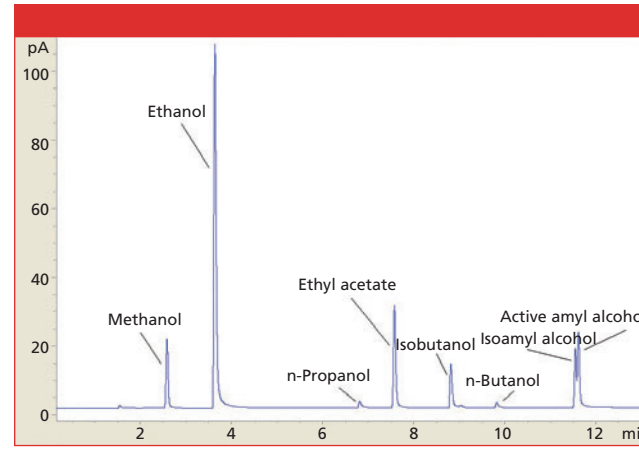

Figure 1: Chromatogram of the 0.2 level standard at 70 °C.

A chromatogram of the lowest level standard is shown in Figure 1.

Conclusions

The current TTB method, SSD:TM:200 was easily converted to a static headspace method with the HT3 utilizing MOM to selecting the best sample temperature. A temperature of 70 °C provided excellent r^2 and Rf %RSD values exceeding the current method r^2 criteria of > 0.99.

The headspace method transfers only the volatile components of the sample while nonvolatile compounds, such as sugars that can quickly contaminate a GC liner and column, remain in the headspace vial. Benefits are two-fold, reducing a lab's budget by minimizing frequent column and inlet liner changes, as well as increasing instrument uptime. The HT3 or Versa automated headspace vial samplers can benefit beverage laboratories by increasing throughput.

References

(1) Capillary GC Analysis of Fusel Oils and Other Components of Interest, US Department of Treasury, Alcohol and Tobacco Tax and Trade Bureau, http://www.ttb.gov/ssd/pdf/tm200.pdf.

To download the full application note, please visit http://info.teledynetekmar.com/LCGCFuselAN

Teledyne Tekmar
4736 Socialville Foster Rd., Mason, OH 45040
tel. (513) 229-7000
Website: www.teledynetekmar.com

Modernizing the USP Monograph for Acetaminophen

Rongjie Fu, Agilent Technologies

In the USP method for acetaminophen (1), the related compound *p*-aminophenol is determined using spectrophotometry while another related compound, *p*-chloroacetanilide, is determined using TLC. We developed a new HPLC method to analyze both compounds in acetaminophen simultaneously using 5-µm columns, including ZORBAX Eclipse XDB-C8 and ZORBAX Eclipse Plus C18. The methods were then transferred to 2.7-µm superficially porous columns, which have efficiencies similar to those of sub-2-µm totally porous particles. This is attributed primarily to a shorter mass-transfer distance and a narrower particle size distribution. Furthermore, the larger particle size results in lower back pressure, allowing these columns to be used on virtually any LC system. The benefits of transferring from larger particle columns include very significant time and cost savings, because superficially porous particles are optimally run at faster flow rates and achieve similar resolution with a much shorter column length. The method was run on several Poroshell 120 phases of different selectivity. The results easily met the requirements of the USP monograph for acetaminophen.

Materials and Methods

The test solution was 20 mg/mL acetaminophen in the mobile phase. The standard solution was 1 µg/mL *p*-aminophenol, acetaminophen, and *p*-chloroacetanilide in the mobile phase, corresponding to 0.005% in 20 mg/mL acetaminophen.

The HPLC analysis was performed with an Agilent 1260 Infinity Binary LC including a G1312B Binary Pump SL, G1376C Automatic Liquid Sampler SL, G1316B Thermostatted Column Compartment SL, and G1316C Diode Array Detector SL.

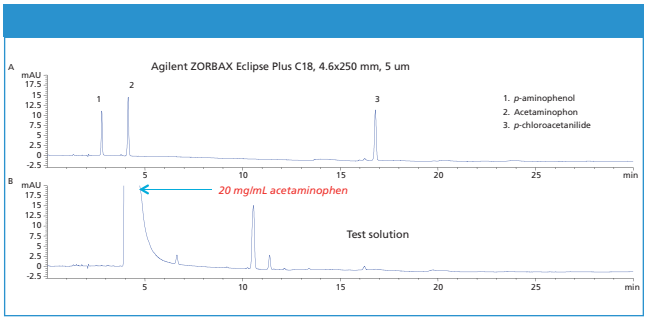

Figure 2: System suitability and test solution for USP acetaminophen analysis using Agilent ZORBAX Eclipse Plus C18. Standards, corresponding to 50 ppm (A), test solution (B).

Results and Discussion

The European Pharmacopoeia (EP) 5.0 includes an HPLC method for determination of related substances in acetaminophen (paracetamol) (2). An isocratic method with an EP-recommended C8 column is used for separation of impurities in acetaminophen. The isocratic method allows a very long analysis time with a broadening peak of *p*-chloroacetanilide, which leads to low sensitivity. A gradient method using phosphate buffer and acetonitrile was developed on 4.6 × 250 mm, 5-µm columns for separating *p*-aminophenol, acetaminophen, and *p*-chloroacetanilide at 1 µg/mL. The three compounds were well separated. The resolution between *p*-aminophenol and acetaminophen was sufficient for limit detection of *p*-aminophenol in a high concentration of acetaminophen. The signal-to-noise of *p*-chloroacetanilide at 1 µg/mL was also sufficient for limit detection. Both columns, the ZORBAX Eclipse

Conditions for Figure 1 and 2:
Columns: Agilent ZORBAX Eclipse XDB-C8, 4.6 x 250 mm, 5 µm (p/n 990967-906); Agilent Eclipse Plus C18, 4.6 x 250 mm, 5 µm (p/n 959990-902)
Mobile phase: A, 20 mM Phosphate buffer, 1.78 g $Na_2HPO_4.2H_2O$ and 1.38 g $NaH_2PO_4.H_2O$; B, acetonitrile
Gradient:

time (min)	B%
0	10
5	15
15	35

Stop time: 30 min
Temperature: 30°C
Flow rate: 1.5 mL/min
Injection volume: 20 µL
Detection: UV, 245
Instrument: Agilent 1260 Infinity Binary LC System

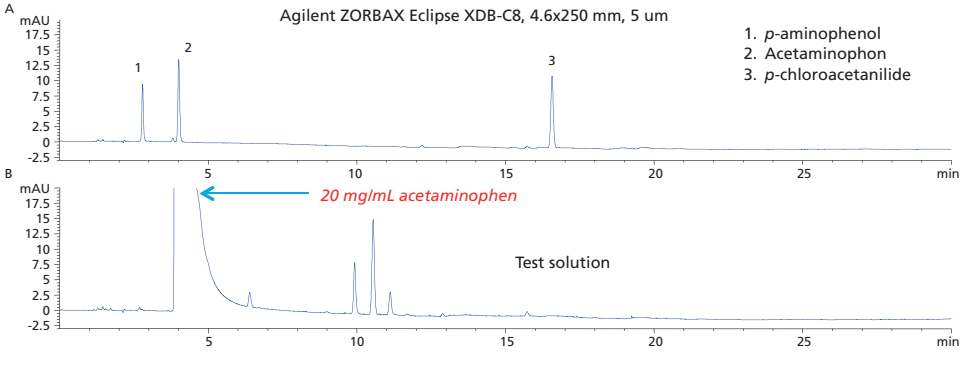

Figure 1: System suitability and test solution for USP acetaminophen analysis using Agilent Eclipse XDB-C8. Standards, corresponding to 50 ppm (A), test solution (B).

Conditions for Figures 3, 4, 5
Columns: Agilent Poroshell 120 EC-C8, 4.6 x75 mm, 2.7 µm (p/n 697975-906), Agilent Poroshell 120 EC-C18, 4.6 x75 mm, 2.7 µm (p/n 697975-902), Agilent Poroshell 120 SB-C18, 4.6 x 75 mm, 2.7 µm (p/n 687975-902)
Mobile phase: A, 20 mM Phosphate buffer, as before; B, acetonitrile

Gradient	time (min)	B%
	0	10
	1.5	15
	4.5	35

Stop time: 8 min
Flow rate: 1.5 mL/min
Column temperature: 30°C
Injection volume: 6 µL
Detector: UV, 245 nm
Instrument: Agilent 1260 Infinity Binary LC System

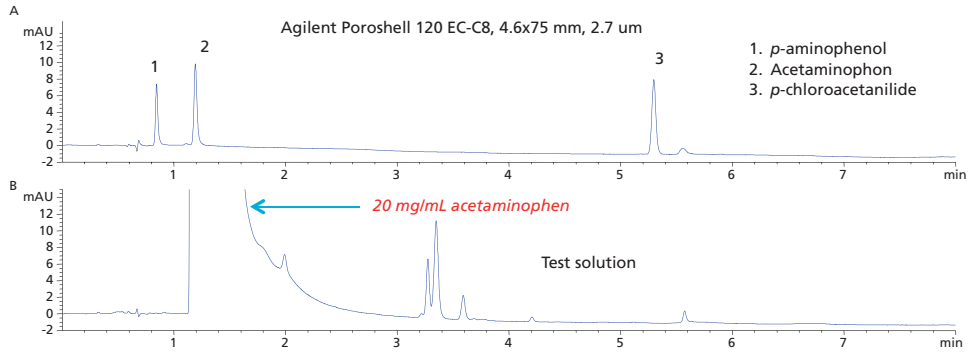

Figure 3: System suitability and test solution for USP acetaminophen analysis using Agilent Poroshell 120 EC-C8. Standards, corresponding to 50 ppm (A), test solution (B).

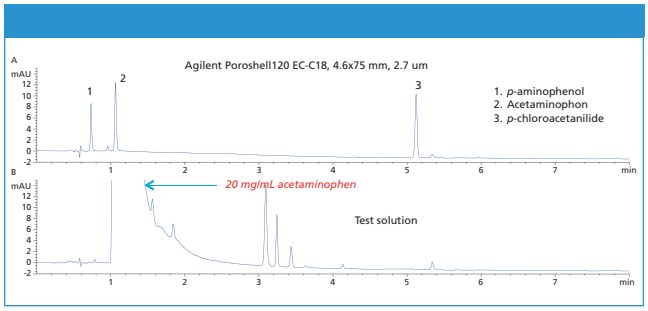

Figure 4: System suitability and test solution for USP acetaminophen analysis using Agilent Poroshell 120 EC-C18. Standards, corresponding to 50 ppm (A), test solution (B).

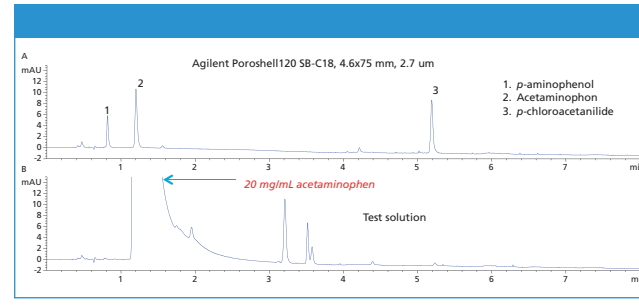

Figure 5: System suitability and test solution for USP acetaminophen analysis using Agilent Poroshell 120 SB-C18. Standards, corresponding to 50 ppm (A), test solution (B).

Table I: Chromatographic system requirements and measured values for related compounds of acetaminophen

System requirements*	ZORBAX Eclipse XDB-C8 (5 µm)	ZORBAX Eclipse Plus C18 (5 µm)	Poroshell 120 EC-C8	Poroshell 120 EC-C18	Poroshell 120 SB-C18	Poroshell 120 Bonus-RP	Poroshell 120 Phenyl-Hexyl
Resolution: minimum 6.0 between the peaks due to impurity K (*p*-aminophenol) and to acetaminophen	12.2	13.1	8.2	9.1	9.8	14.8	5.9
Signal-to-noise ratio: minimum 50 for the peak due to impurity J (*p*-chloroacetanilide)	135.5	250.0	189.3	152.5	99.0	259	150.0
*According to EP 5.0 Paracetamol							

XDB-C8 and Eclipse Plus C18, were appropriate for determination of the two related compounds, but the ZORBAX Eclipse XDB-C8 column resolved more impurities around 10 min, as shown in Figure 1 and Figure 2.

The method was then transferred to 4.6 × 75 mm, 2.7-µm Poroshell 120 EC-C8, Poroshell 120 EC-C18, and Poroshell 120 SB-C18 columns, shown in Figure 3, Figure 4, and Figure 5. The total analysis time was reduced from 30 min to only 8 min, while still meeting the requirements of the method. Of the three phases, the Poroshell 120 EC-C18 column provided the best peak shapes and resolutions between additional impurities that eluted around 3 min.

In addition to these Poroshell 120 phases, the original method was also transferred to other phases, including Poroshell 120 Bonus-RP, a polar embedded amine column that gave unique selectivity, and Poroshell 120 Phenyl-Hexyl, a phenyl-hexyl bonded column that has improved selectivity for aromatic compounds. Results are shown in Figure 6 and Figure 7. Bonus-RP provided good resolution for all the impurities, while the Phenyl-Hexyl column showed several coeluted peaks. Therefore, the Bonus-RP

Conditions for Figures 6 and 7:
Columns: Agilent Poroshell 120 Bonus-RP, 3.0 x100 mm, 2.7 µm (p/n 695968-301), Agilent Poroshell 120 Phenyl-Hexyl, 2.7 µm (p/n 695975-312)
Mobile phase: A, 20 mM Phosphate buffer, as before; B, acetonitrile
Gradient:

time (min)	B%
0	10
2	15
6	35

Stop time: 10 min
Flow rate: 0.638 mL/min
Temperature: 30°C
Injection volume: 3.4 µL
Detector: UV, 245 nm
Instrument: Agilent 1260 Infinity Binary LC System

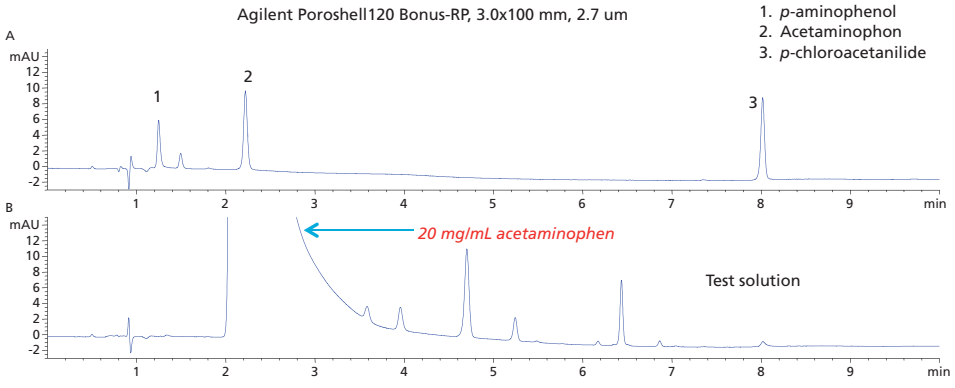

Figure 6: System suitability and test solution for USP acetaminophen analysis using Agilent Poroshell 120 Bonus-RP. Standards, corresponding to 50 ppm (A), test solution (B)

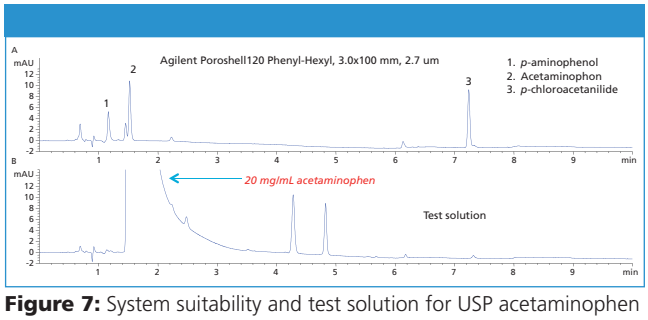

Figure 7: System suitability and test solution for USP acetaminophen analysis using Agilent Poroshell 120 Phenyl-Hexyl. Standards, corresponding to 50 ppm (A), test solution (B).

column could be an alternative to a C18 phase due to its unique selectivity.

According to the EP method for related-substance analysis, the resolution between *p*-aminophenol and acetaminophen, and signal-to-noise ratio for the peak *p*-chloroacetanilide are required for system suitability. Table I lists the resolution and S/N with the new gradient method we developed, which all meet the EP method requirements.

Conclusions

HPLC methods can easily determine *p*-aminophenol and *p*-chloroacetanilide in acetaminophen, replacing current spectrophotometer and TLC methods. Both traditional 5-µm columns and Poroshell 120 columns can be used for the analysis of related compounds. The ZORBAX Eclipse XDB-C8 phase is good for the separation of additional impurities. Poroshell 120 EC-C18 provides the best peak shapes and separation for this analysis, while Poroshell 120 Bonus-RP provides unique selectivity for these impurities. For the full application note with larger images, search for pub number 5991-3679EN at www.agilent.com/chem/library.

References

(1) "Acetaminophen," in *United States Pharmacopeia 30–National Formulary 25* (United States Pharmacopeial Convention, Rockville, MD, USA, 2006).

(2) "Paracetamol" in *European Pharmacopoeia 5.0* (European Directorate for the Quality of Medicines & Healthcare, Council of Europe, Strasbourg, France, 2004).

Agilent Technologies
5301 Stevens Creek Blvd., Santa Clara, CA 95051
tel. (800) 227-9770
Website: www.agilent.com/chem/discoverporoshell

Simultaneous Quantitative and Qualitative Measurements in a Single Workflow to Increase Productivity in Primary Drug Metabolism Investigations

Bruker Daltonics

The ability to simultaneously collect quantitative and qualitative information from a DMPK analysis has the potential to significantly increase productivity in pharmaceutical drug discovery and development. We present a single workflow allowing P450 drug clearance values to be determined as well as metabolites identified, profiled, and their structures elucidated. To be able to do all of this on a high throughput UHPLC chromatographic timescale is essential for the high levels of productivity required for today's DMPK screening laboratories. Haloperidol provides a good example of what can be achieved.

Haloperidol

$C_{21}H_{23}NO_2FCl$ $M+H^+ = 376.1474$

Workflow and Protocol

Microsomal incubations were carried out by Unilabs Bioanalytical Solutions at 1 µM drug concentration and a protein concentration of 0.5 mg/mL. Aliquots were taken and quenched with acetonitrile containing propranolol as an internal standard at eight time points over a period of 60 min.

Chromatography

Column: Fortis, 1.7 µm, H_2O, 2.10 mm × 30 mm
Column temperature: 30 °C
MPA: 0.1% formic acid in 95% H_2O/CH_3CN
MPB: 100% CH_3CN

Gradient:	0.0	0.3	2.0	2.5	2.6	3.0	min
MP %:	95	95	5	5	95	95	%

Flow rate: 300 µL/min
Injection volume: 5 µL

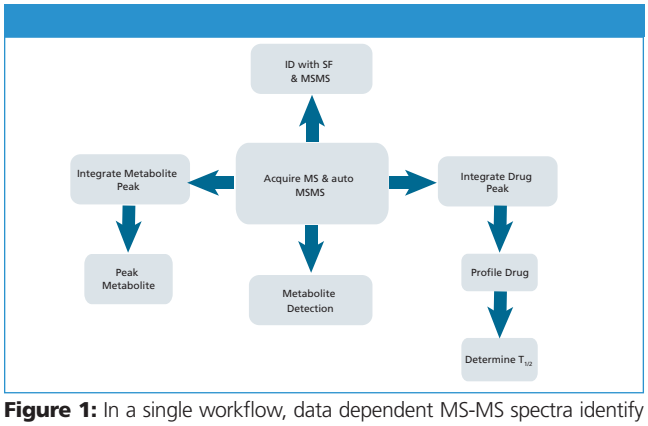

Figure 1: In a single workflow, data dependent MS-MS spectra identify and elucidate metabolite structures and drug clearance is measured.

The high surface area and lipophilic ligand combined with a hydrophilic end cap give this stationary phase a broad selectivity and resolving power for the target drug and the metabolites. The use of small particles allows UHPLC to compress the peak into a tighter and taller peak, therefore enhancing detection of very low level analytes.

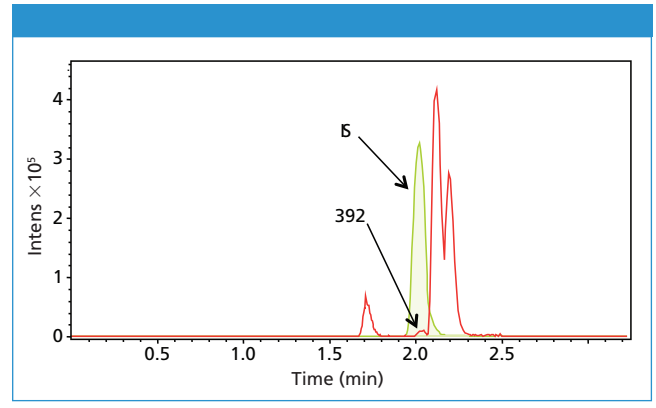

Figure 2: Metabolite detection software compares the data file for the drug (in this case t_{60}) with the corresponding control sample. A base peak chromatogram of the difference is created allowing the metabolites to be easily observed and their mass determined to 4 decimal places.

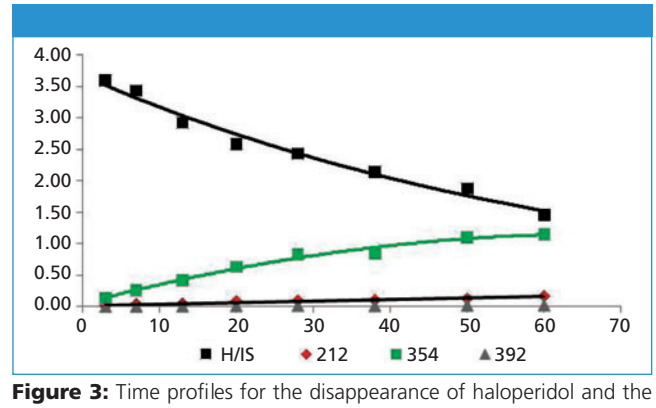

Figure 3: Time profiles for the disappearance of haloperidol and the appearance of three metabolites.

Metabolite Detection

Metabolite detect software compares the data file for the drug (in this case t_{60}) with the corresponding control sample. A base peak chromatogram of the difference is created, allowing metabolites *m/z* 354, 212, and even 392 to be easily observed.

Metabolite detection software is able to detect the *m/z* = 392 metabolite even though it coelutes with the internal standard.

Drug and Metabolite Profiles

Integration is carried out on the XIC for the measured *m/z* of each metabolite +/– 0.005 Da. Plotting the ratio of metabolite to internal standard (M/IS) versus time produces the metabolite profiles. Half-life and clearance values are determined from the natural log (ln) of the drug profile versus time plot.

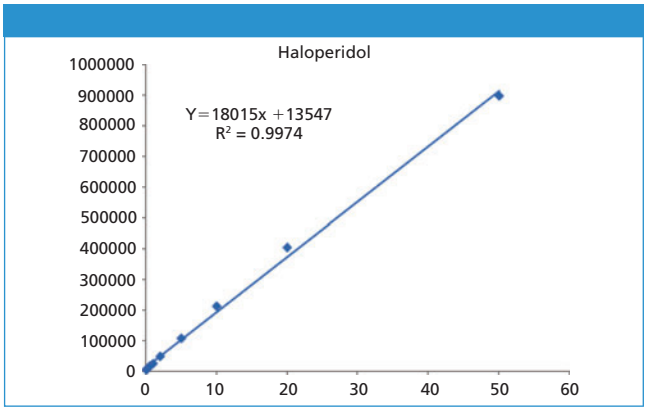

Figure 4: Linear calibration of 50 pg/mL to 50 ng/mL (3 decades) was achieved using the XIC for the measured *m/z* of each metabolite +/- 0.005 Da. R^2= 0.9974.

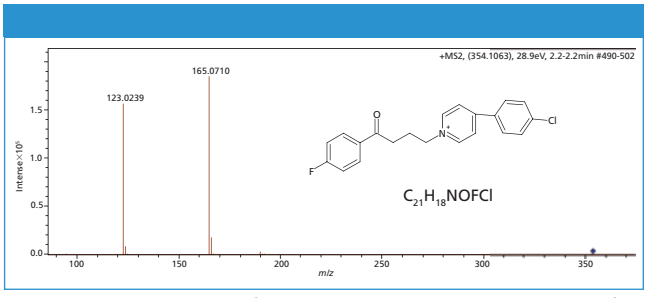

Figure 5: The structure of metabolite *m/z* = 354 is easily identified using SmartFormula 3D to understand the fragmentation pattern.

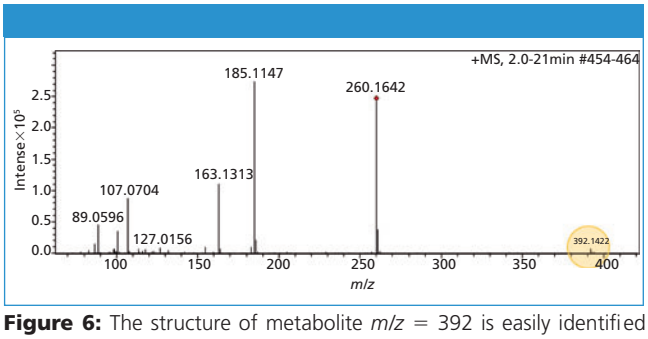

Figure 6: The structure of metabolite *m/z* = 392 is easily identified using SmartFormula 3D to understand the fragmentation pattern.

Linearity

MS–MS data was not available for *m/z* = 392 because of coelution with the internal standard. The high quality data available, even for such a small peak, means SmartFormula is still able to predict the formula and deduce that it is a mono-oxidative metabolite.

m/z = 392.2422 Δm = 0.1 mDa (0.3 ppm)

$C_{21}H_{23}NO_3FCl$ Isotope fit = 23 ms

Comparison with 3Q

Both the AB Sciex API 5000 and Bruker impact QTOF yield equivalent results for the clearance values. This can be clearly seen by comparing the ln [Drug]/[IS] versus time plots.

The linearity and gradients of these plots are nearly identical and result in values for $t_{1/2}$ of 45 and 47 min, respectively.

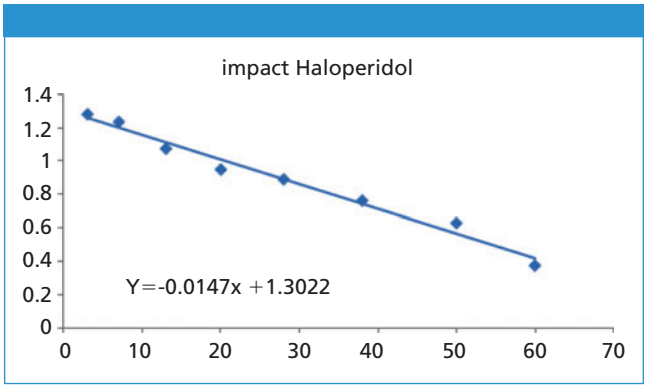

Figure 7: Clearance data from impact.

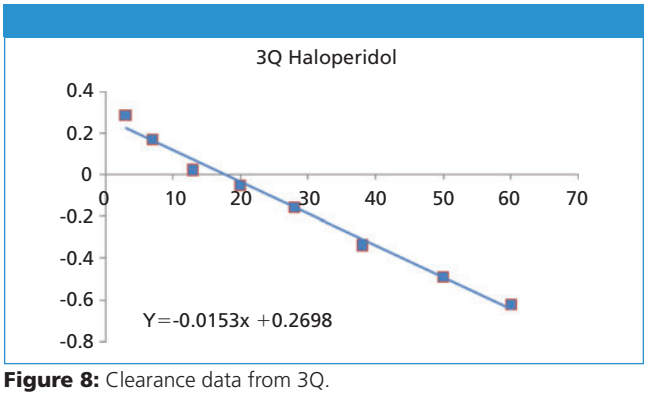

Figure 8: Clearance data from 3Q.

The difference in *y* intercept is a result of a difference in relative response of the internal standard and has no influence on the clearance results.

Conclusions

The quan–qual workflow is effective and robust using a rapid analytical method suitable for high throughput screening at 1 µM drug concentrations.

Metabolite detection software allows metabolites to be rapidly identified and profiled even when compounds coelute.

Bruker Daltonics Inc.
40 Manning Road, Billerica, MA 01821
tel. (978) 663-3660, fax (978) 667-5993
Website: www.bruker.com

Separation of a Mix of Acidic, Basic, and Neutral Compounds at High pH Conditions

Diamond Analytics

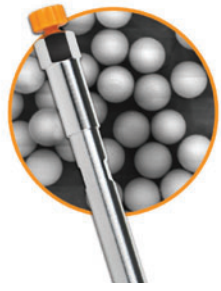

The unique surface chemistry of the Flare diamond core-shell column combines ionic and hydrophobic separation mechanisms to effectively retain a variety of chemical species in a single run.

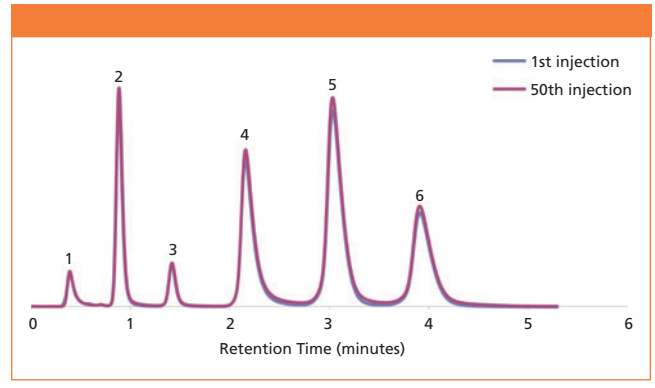

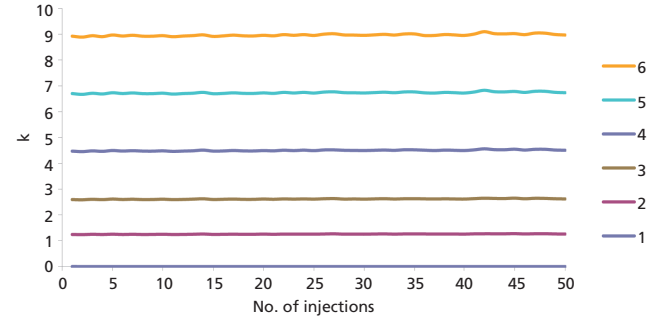

HPLC Conditions

Column Name:	Flare C18 Mixed-Mode Column
Dimensions:	4.6 × 33 mm, 3.6 µm, 180 Å
HPLC System:	Waters® 1525 Binary Pump
Injection Volume:	5 µL
Detection:	UV at 254 nm
Flow Rate:	1.0 mL/min
Separation Mode:	Isocratic
Mobile Phase: A:	10mM phosphate buffer, pH 12; B: acetonitrile
	A/B (70:30)
Temperature:	35°C
	Analytes:

1) 2, 4-D

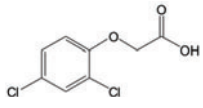

2) Propazine

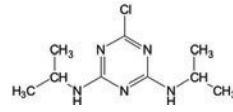

3) Ethylbenzene

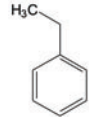

4) Nortriptyline

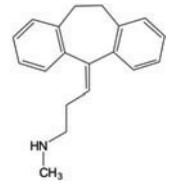

5) Imipramine

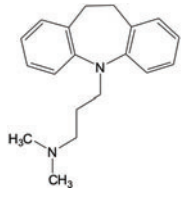

6) Amitriptyline

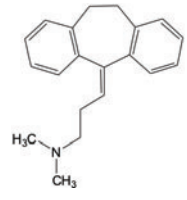

Conclusions

1) Fast separation at high pH
2) Separation possible with 100% aqueous mobile phase
3) Straightforward method transfer to any system

DiamondAnalytics
tools for tomorrows chemistry

Diamond Analytics
11260 S 1600 W. Orem, Utah
tel. (801) 235-9001, fax (801) 235-9141
Website: diamond-analytics.com

Recent Improvements in Time of Flight Mass Spectrometer Detection Technologies

PHOTONIS USA

In mass spectrometry instrumentation, the sensitivity and resolution of the instrument is often limited by the detector. PHOTONIS leads the market with new improvements in detector technologies that have increased resolution and detection efficiencies of several types of time-of-flight (TOF) detectors. The result is that several manufacturers are now able to offer more sensitive TOF-MS instruments with greater resolution using PHOTONIS improved TOF detectors.

PHOTONIS's new Gen2 UltraFast™ TOF detector is designed to address two major areas that affect resolution in time-of-flight mass spectrometry: microchannel plate (MCP) flatness and anode impedance matching. The new Gen2 detector is equipped with PHOTONIS's patented MountingPad™ 2-µm pore microchannel plates with impedance matched anodes, and uses TruFlite™ MCP flatness (+5 µm) technology for a significant reduction in time jitter. These technologies combine to produce a single detector with exceptional levels of detection sensitivity and mass resolution unmatched by standard TOF detectors on the market.

The PHOTONIS Gen2 UltraFast™ TOF detector provides pulse widths of less than 200 picoseconds and a near-symmetric 120 picosecond rise and fall time. It is available with either an 18 mm or 40 mm input area, and can provide gains in excess of 5×10^6. The TOF detector offers built-in beam parallelism to provide uniform ion conversion, and is designed for front flange mount.

For time-of-flight techniques requiring higher mass analysis, PHOTONIS offers a novel high mass detector which improves the detection efficiency of very high mass ions with significantly less complexity when compared to other high mass MALDI-TOF detection solutions. The compact shape and simplified detection system supports many high mass operating modes without the need to manipulate the detector through the ion beam.

The PHOTONIS high mass MALDI-TOF detector features a large 2.54 cm^2 collection area that allows for higher sensitivities without the need for higher post-acceleration voltage. The detector comprises a high-sensitivity 18 mm MCP, a high-speed scintillator, and a photomultiplier that can detect both positive and negative ions with 30 kV isolation.

This innovative solution also features a gridless optic system that provides high sensitivity detection for masses in excess of 100 kDa with fast response time (rise time <1.2 ns) and high dynamic range (>2 V into 50 Ω).

The optical coupling of the signal path allows the high mass detector to operate in multiple modes of operation (high post acceleration, grounded input, etc.) simply by adjusting the detector voltages. The gain values of the three gain stages of the detectors can all be optimized for each application with no physical changes to the detector.

PHOTONIS offers these and other innovative and patented time-of-flight detectors, including BiPolar, Off-Axis, Co-Axial, UltraFast, Low-Profile BiPolar, High Temperature and miniature. PHOTONIS TOF detectors are the fastest on the market, with unmatched levels of temporal resolution, dynamic range, and mass detection sensitivity, and new detectors can be custom-designed to meet specific requirements.

PHOTONIS

PHOTONIS USA Inc.
660 Main St., Sturbridge, MA USA 01566
tel. (508) 347 4000
Website: www.photonis.com

Considerations for Switching from Helium to Hydrogen for Gas Chromatography Carrier Gas

John Speranza, Proton OnSite

As the cost of helium increases and its availability decreases, an increasing number of Gas Chromatography (GC) professionals are considering switching to hydrogen gas for their carrier gas.

Hydrogen is an inexpensive and more efficient alternative carrier gas. It also offers GC practitioners the ability to speed up their processes without sacrificing quality.

Run Time

The carrier gas a GC practitioner chooses can have significant influence on analysis speed. The speed depends on the column pressure drop (p_d). When p_d is compared with the lower outlet pressure (p_o) typically in a shorter column, the optimum average linear velocity (u_{opt}) is proportional to the molecular diffusivity (D) of a solute in the gas (2).

As Table I shows, at a low p_d, helium is 20 percent slower than hydrogen. And, at a high p_d compared to p_o, in a narrow, longer column in which speed is a crucial aspect to the performance of the separation, helium is relatively much slower than hydrogen.

Column Efficiency

Hydrogen carrier gas has the greatest column efficiency. The most efficient columns allow analytes to spend optimal time in the stationary phase at u_{opt}, measured by the height equivalent to a theoretical plate (HETP). HETP specifies the column length necessary when the partitioning of analytes between the carrier gas and the stationary phase is at equilibrium.

Table I: Relative speeds of analysis based on *D* for typical carrier gases at low p_d (run time is inversely proportional to the speed) (1)

Gas	Relative Speed
Hydrogen	1
Helium	0.78
Nitrogen	0.24
Argon	0.21

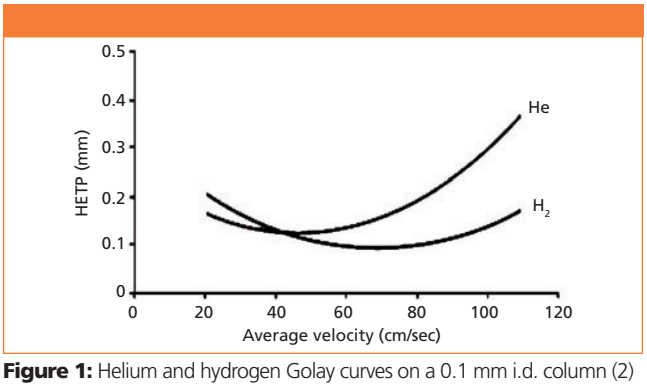

Figure 1: Helium and hydrogen Golay curves on a 0.1 mm i.d. column (2)

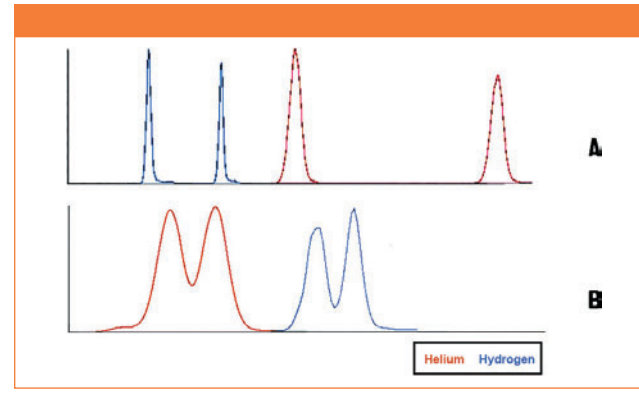

Figure 2: Improved separation of benzo(g&h)flouranthene (A) and improvement of peak shape for Indeno(1,2,3-cd)pyrene and benzo(g,h,i)perylene (B) (3)

Hydrogen has the lowest HETP of any carrier gas. This can be plotted against u_{opt} on a Golay curve (2), where optimal linear velocity is specified at the point where the curve is the lowest. On such a curve, hydrogen produces the flattest curves compared to helium (Figure 1), thus hydrogen can operate at a higher optimal linear velocity than helium, without sacrificing HETP.

Results: Improved Peak Shape and Resolution, in Less Time

Better speed and efficiency means better peak resolution (narrower peak width) and improved peak shapes in less time. This is illustrated when separating polynuclear aromatic hydrocarbons (PNAs) (3). Comparing helium and hydrogen carrier gases in a pair of experiments, hydrogen creates a narrower peak width (Figure 2) and, during the critical separation of a PNA, peak shapes are improved with a hydrogen carrier gas.

References

(1) International Organization of Standardization, Basic Considerations for the Safety of Hydrogen Systems, ISO/TR 15916:2004(E)

(2) E.N. Fuller, P.D. Schettler, and J.C. Giddings, A new method for prediction of binary gas phase diffusion coefficients, *Ind. Eng. Chem.* **58**, 19–27 (1966).

(3) M.J.E. Golay, *Gas Chromatography* (Butterworths, 1958).

(4) J. Butler, N. Semyonov, and P. O'Brien, Fast GC-MS Analysis of Semi-Volatile Organic Compound: Migrating from Helium to Hydrogen as a Carrier Gas in US EPA Method 8270, p 4 (Thermo Scientific, 2013).

Proton OnSite
10 Technology Drive, Wallingford, CT 06492
tel. (203) 949-8697, fax (203) 949-8016
Website: www.protononsite.com

Carbon Nanotubes: Applications in Chromatography and Sample Preparation

Carbon nanotubes (CNTs) are cylindrical allotrope nanostructures of carbon with unique structures and unusual properties. The adsorption capacity of CNTs — along with their thermal and chemical stability — make them suitable candidates for new stationary phases, pseudostationary phases, and also for sorbents in solid-phase extraction (SPE) and solid-phase microextraction (SPME). This article outlines the latest applications for CNTs in chromatography and sample preparation.

María Asensio-Ramos, Antonio V. Herrera-Herrera, Miguel Ángel Rodríguez-Delgado, Salvatore Fanali, and Javier Hernández-Borges

Carbon nanotubes (CNTs) were officially discovered in 1991 by Sumio Iijima when an arc discharge method, previously used for fullerene synthesis, formed needle-like structures on the negative electrode (1). Microscopy studies revealed concentric tubes formed by two to 50 graphene sheets and these structures were named multi-walled carbon nanotubes (MWCNTs). A few years later, researchers discovered that on the addition of iron (Fe) or cobalt (Co) to one of the electrodes single graphite tubes known as single-walled carbon nanotubes (SWCNTs) were formed (2,3).

The controlled and specific synthesis of SWCNTs and MWCNTs in relatively high amounts is possible by techniques such as arc-discharge (4), laser ablation (5), or chemical vapor deposition (CVD) (6). These processes are, in general, difficult and expensive even before taking purification into account. Cost-effective methods to produce CNTs in larger volumes are still required.

However, the unique properties of CNTs make them potentially very useful in practice. The tensile strength and elastic modulus of CNTs makes them the strongest and hardest materials known because of the sp2 covalent bonds between carbon atoms. But these two properties are only part of their appeal. In general, they show other unique physical, chemical, thermal, and mechanical properties that make them useful for an extensive range of applications, primarily in electronics and electrochemistry. However, they are also used in other fields including gene therapy, drug delivery, neuroengineering, biosensor technology, and biomedical and tissue engineering. As a result, CNTs are probably one of the most intensively studied nanostructured materials (7).

CNTs are also playing a significant role in analytical chemistry (Figure 1). This short review attempts to summarize the most important applications relevant to chromatographers.

Unique Properties of CNTs

Both SWCNTs and MWCNTs have unique physical, chemical, thermal, and mechanical properties. The surface of CNTs can also be easily covalently or non-covalently modified to change their properties. This is useful because many of their desired properties can be preserved, while improving their solubility. Both pristine and modified CNTs have proven to be useful in analytical sciences (8–12) because of the excellent sorption capacity, and great thermal and chemical stability of CNTs. These properties make them potentially useful as stationary phases in gas chromatography (GC), liquid chromatography (LC) and capillary electrochromatography (CEC), as well as pseudo-stationary phases in capillary electrophoresis (CE) (8,9). Additionally, as a result of their sorption capacity — combined with their cave structure and ability to form a wide range of interactions with foreign molecules — they could also be useful stationary phases for sorption extraction techniques, such as solid-phase extraction (SPE) and solid-phase microextraction (SPME) (13,14). CNTs have also been proposed as substrates for matrix-assisted or surface-assisted laser desorption–ionization time-of-flight mass spectrometry (MALDI or SALDI-TOF-MS) (15), and also for the fabrication of polymeric membranes for filtration because of the presence of cores and their ability to let fluids move through them (11).

The electrical properties of CNTs, such as conductivity, dielectric constant, impedance, and refractive index, mean they are sensitive to interaction with analytes, or even with complex biological molecules (8). This is the foundation of their use as gas sensors (16) and biosensors (17). CNTs also have large active surface electrocatalytic properties and good electron transfer to nanoelectrodes.

In this respect, numerous applications describe their use as electrode materials or as modifiers of conventional working electrodes in analytical voltammetry (18). They have also found a place in anodic striping voltammetry because of the combination of electrical properties and the high sorption capacity (19), and as materials to construct and improve electrochemical detectors used in microchip CE (20).

It is important to emphasize that one of the main challenges of using CNTs in analytical chemistry is obtaining pure

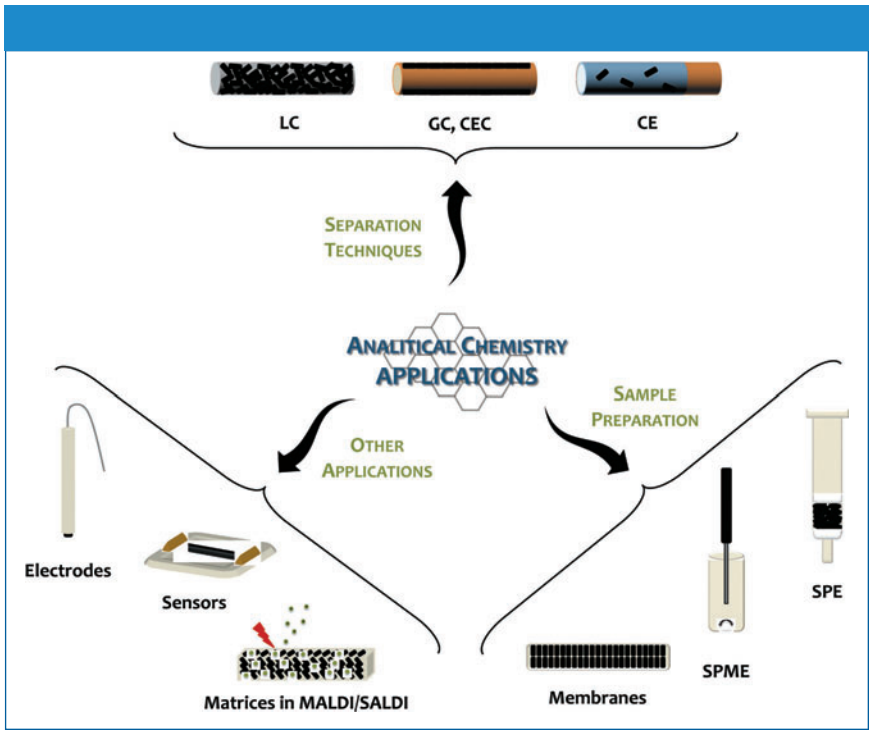

Figure 1: Principal applications of CNTs in analytical chemistry.

and well-characterized materials (21). However, commercially available CNTs comprise a distribution of nanotubes of different diameters and lengths depending on the manufacturer, which clearly affects their properties and behavior. For this reason, the selection of the type, dimensions, and producer of CNTs must be carefully chosen to ensure the successful transfer of methods developed between laboratories.

CNTs in Separation Techniques

Chromatographic and Electrochromatographic Applications: As a result of their intrinsic properties, excellent sorbent capacity and thermal and chemical stability, CNTs have been proposed as stationary phases for GC. Non-functionalized pure CNTs are stable up to 1200 °C under inert atmospheres, which prevents column bleeding and enables operation at higher temperatures than conventional columns (22). To produce these GC columns, a thin layer of CNTs is deposited on their surface by CVD (9) producing a homogeneous surface with a small number of polar groups that allows a better peak shape. The possibility of functionalizing the CNTs surface inside the column to improve selectivity has recently been explored; however, it should be noted that thermal stability must be carefully considered because impurities and functionalization directly affect the column reliability (23). Specifically, contaminating high amounts of heavy metals coming from the CNTs synthesis can affect their retention performance. However, the number of applications in this field is still low, and concerns mainly the separation of standard mixtures of volatile compounds such as alkanes, aromatic compounds, esters, and ketones.

The use of CNTs as stationary phases in LC has been explored even less (9,24). They have mainly been used in combination with a second packing material (normally silica) or incorporated in a porous polymeric monolith (11). In nearly all of these works, large columns of 4.6 mm of internal diameter have been used. Figure 2 shows the chromatograms of 11 acidic, neutral and alkaline organic compounds on PS-DVB-CNT columns containing 0%, 1%, and 5% MWCNTs. It should be noted that the resolution and plate number both reduced with superabundant MWCNTs in this specific case (25). Although the applications in this field have increased recently, only test mixtures of analytes have been used in the majority of these works; complex methodologies for real sample analysis have not been developed.

CNTs can be covalently or noncovalently immobilized onto the walls of silica capillaries to perform open-tubular CEC (OT-CEC) to determine different compounds (11). In one example, CNTs have been incorporated in porous polymer monolithic capillary columns to enhance separation of small molecules (26). To the best of our knowledge, CEC with CNT-packed capillaries has not been developed until now. It is also important to mention that there have been applications with CNTs in chips to perform chip-CEC for the determination of alkanes, thioamides, DNA fragments, and colorings (11).

In general, few works have been reported in the chromatographic and electrochromatographic fields so far, but the number of papers published in the future is likely to increase because of the interesting results that CNTs have produced.

Electrophoretic Applications: The use of CNTs in CE lies in their addition to the background electrolytes (BGEs) as pseudostationary phases for the development of electrokinetic chromatography (EKC) (22). However, because raw CNTs are not soluble in aqueous buffers or common solvents, they are usually covalently or non-covalently functionalized to form stable suspensions. In this regard, both MWCNTs and SWCNTs have been oxidized, mixed with surfactants, ionic liquids (ILs), or even dispersed in a microemulsion (aqueous solutions containing dispersed nanometer-size droplets of an immiscible liquid which are surrounded with a surfactant to reduce the surface tension between the two liquid layers) to analyze, for example, drugs in urine, vitamins in pharmaceutical formulations, antioxidants in different matrices, and nucleotides in an extract of chicken (11).

Although several strategies have been adopted to improve solubilization of CNTs in the BGE, it is worth mentioning that it is difficult to obtain accurate and reproducible concentration of the CNTs in the BGE.

CNTs in Sample Preparation

Solid-Phase Extraction: From a detailed review of the current literature one can

deduce that CNTs present an adequate sorption capacity for the extraction of both organic and inorganic compounds. In addition, the change in selectivity introduced by the covalent or non-covalent functionalization of their surface has favored their extensive use in this field (11,13,14,27).

On the one hand, the interaction of CNTs with metal ions is believed to occur because of the presence of functional groups in the surface of the material (28) and, as a whole, the metal-removal capability of CNTs is enhanced by the presence of active sites on their surface, the inner cavities and internanotube space. Additionally, the effect of pH is crucial and should be carefully studied. The existence of a pH value called "point of zero charge" (29) or "isoelectric point" (at which the electrical charge density on the CNTs surface is zero) causes the surface of CNTs to become negatively charged at a pH higher than that. This improves the adsorption of cationic species. On the contrary, when the pH is lower than this value, protons compete with metal cations for the same sites on the surface of CNTs. Precisely for this reason solutions containing acidic additives are frequently used to promote the elution of metals.

A number of approaches for metal ion extraction have been focused on the use of oxidized CNTs (o-MWCNTs or o-SWCNTs), obtained by submitting CNTs to a strong acid media at high temperatures. These conditions introduce –COOH, –OH, and –CO– groups, after which different substitution reactions could be performed. In this way, organic species or even biomolecules have also been immobilized on their surface to extend their application (14,27). Complexation of metal ions may not be necessary when using modified CNTs, contrary to what is needed when CNTs are not modified (as it usually occurs with other sorbent materials). In this field, the vast majority of works have been developed to extract inorganic analytes from aqueous samples, and only a few reports have dealt with solid or semisolid matrices (11,13,27).

The strong sorptive interaction of organic analytes has been attributed to π-π electron donor-acceptor relations between the aromatic system of organic molecules (electron acceptors) and the highly-polarizable graphene sheets of CNTs (electron donors) (8). For this reason, a number of authors have worked with non-modified CNTs in this respect, mainly to extract pesticides (13,30), but also other substances such as PAHs, parabens, antioxidants, pharmaceuticals, phthalate esters, phenolic, and biological compounds (11,13).

Conversely, the retention of polar organic analytes has been described to be more efficient with functionalized or modified CNTs. This is because the interaction between functional groups or immobilized organic molecules on the surface of CNTs is more selective. In this respect, o-CNTs have been successfully assayed, together with magnetic CNTs (m-CNTs) (31,32), constituted by the assembly of magnetic nanoparticles onto CNTs via chemical/physical modifications. Figure 3 shows the scanning electron microscopy (SEM) images of Fe/MWCNTs composites with different initial mass ratio of ferrocene to CNTs (33). Magnetic CNTs have facilitated the manipulation of CNTs in dSPE as they can be handled with an external magnetic field provided by a strong magnet.

Organic molecule modified-CNTs have been described for certain applications, and the introduction of molecularly imprinted polymers (MIPs) onto the surface of CNTs has also been exploited as one of the most selective ways to perform SPE, although multi-residue analysis cannot be undertaken often because of the high specificity of the template molecule. As occurred with inorganic analytes, CNTs have been mainly applied to extract organic compounds from different types of water, although different complex matrices (milk, oil, honey, eggs, fish, meat, cosmetics, and soils) have also been analyzed (11,13,27).

CNTs with different dimensions, number of walls, or type of functionalization have been compared. The performance of CNTs in relation to other types of stationary phases, such as C18, activated carbon, graphitized carbon black (GCB), and polymeric sorbents has also been studied. In most cases, CNTs exhibited higher sorption capability or, at the very least, similar effectiveness. With regards to the amount of CNTs required for extraction, it is very frequent to use between 30 mg and 100 mg, even for the extraction of high volumes of liquid samples or extracts (11).

Finally, and like other SPE sorbents, CNTs have been a part of studies regarding automated and miniaturized procedures. Automation also implies a certain degree of miniaturization because SPE mini-columns are used. However, in the case of CNTs and as a result of their dimension and structure, they tend to create flow resistance when using them as mini-column packing materials, with a risk of canalization. For this reason, the use of alternative μ-SPE systems by packing CNTs in the inside of porous materials has offered a good alternative for μ-SPE using mini-columns (11).

Solid-Phase Microextraction: The most challenging task in CNTs-SPME relies on finding a suitable, replicable, and durable coating procedure. Different methods have been settled to deposit CNTs in SPME fibers including sol-gel technology, chemical bonding, electrochemical polymerization, electrophoretic deposition, physical agglutinate by an organic binder, atom transfer radical polymerization, and magnetron sputtering (34,35). Traditionally, fused silica has been used as an appropriate fiber material because of the presence of silanol groups on the surface. However, the fragile fused-silica fibers are being replaced by metal fibers, like stainless steel wires, to solve this important problem.

In general, sol-gel technology has been most widely used but its inadequate reproducibility has made way for other methods, such as simpler chemical bonding methods (35). Also, electrochemical polymerization could be an alternative, but the lack of bonding between the coating and the substrate generates fibers with low thermal stability and swelling in organic solvents. Likewise, electrophoretic deposition has emerged as an alternative to prepare firmer and more stable CNT-SPME fibers. However, until now, a limited number of researchers have used these methods to coat the SPME fibers with CNTs (11,13,35). Physical agglutination with adhesives also provides fibers with low stability and resistance, with the added inconvenience that glues may block the

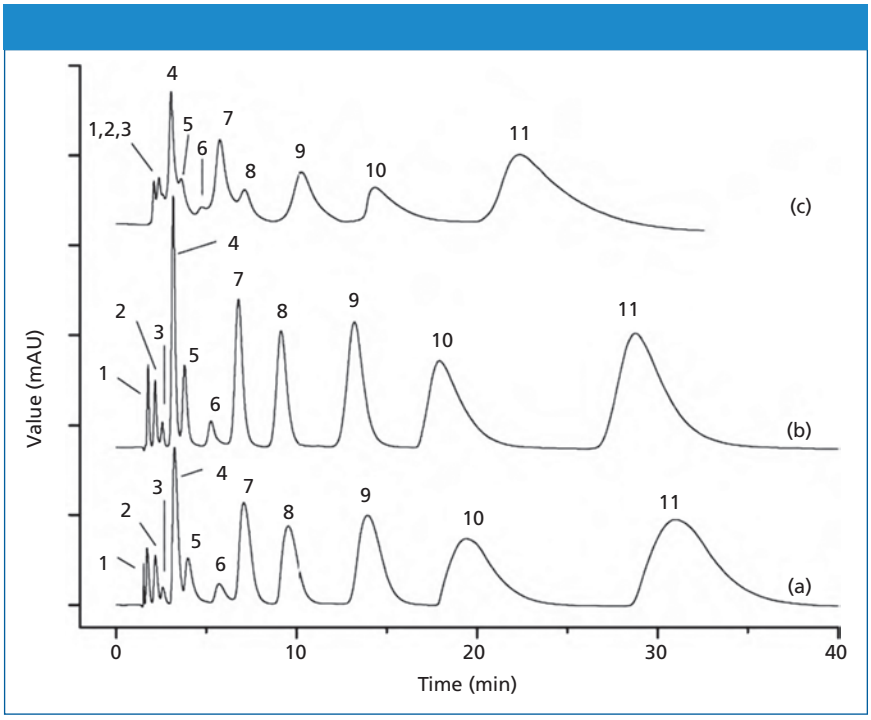

Figure 2: Separation of 11 organic compounds on (a) PS-DVB column, (b) PS-DVB-CNT columns (1% MWCNTs), and (c) PS-DVB-CNT column (5% MWCNTs). Column: PS-DVB and PS-DVB-CNT particles packed in a 150 mm × 4.6 mm stainless steel column. Mobile phase: methanol/water (90:10, v/v). Detection: UV absorbance at 254 nm. Flow rate: 1.0 mL/min. Peak identification: 1 = resorcinol, 2 = sulfadimidine, 3 = benzylalcohol, 4 = aniline, 5 = p-toluidine, 6 = 2-naphthol, 7 = p-methoxybenzaldehyde, 8 = anisole, 9 = *N,N*-dimethylaniline, 10 = 1,3,5-trimethylbenzene, 11 = 2-methoxynaphthalene. Adapted from reference 25 with permission from Elsevier.

coating pores or even change extraction selectivity.

As in SPE, the selectivity of the CNTs can be modified by introducing functional groups on their surface for the determination of polar compounds. For this reason, both modified and pristine CNTs (MWCNTs and SWCNTs) have been used as SPME coatings for the extraction of organic analytes like multi-class pesticides, phenols, and drugs among others (11, 35), and to a lesser extent for the extraction of inorganic ion traces (11).

Normally, homemade CNTs-fibers have been compared with commercially available fibers to evaluate their performance in terms of extraction efficiency and durability. In most of the papers, CNTs fibers showed higher sensitivity and selectivity and higher or similar extraction efficiency, as well as better thermal and physical resistance.

Membranes: Traditional polymeric membranes used for water purification and gas separation experience different problems: low selectivity, permeability, and susceptibility to obstruction or fouling. CNTs have been used to solve some of these drawbacks and most manuscripts have focused on the use of different types of membranes with CNTs embedded in a polymer matrix. Although these types of membranes offer high stability and efficiency, low cost, and ease of operation, their fabrication is still under development to prevent aggregation. However, some of them have already been used for different applications with success (11).

Other Applications

Electrodes: There are a large number of applications in the literature based on applications of CNTs as electrode materials or modifiers of conventional working electrodes (8,18,36). Their use is justified by their important advantages in electrochemical measurements such as the large active surface at electrodes of small dimensions, the enhanced electron transfer or the often indicated electrocatalytic properties. Analytical methods based on voltammetric stripping techniques have also benefited from the unique properties of these electrodes such as the stronger adsorption of many organic compounds, the less extreme potential of the resulting stripping responses, and the enhanced electroanalytical signals.

Electrochemical Detectors: The excellent electroanalytical properties of CNTs-modified electrodes have favored their use as electrochemical detection systems coupled to separation techniques because they improve the determination of certain compounds (37). In addition, nano-electrodes and nanoelectrode arrays made-up from CNTs can be integrated with microelectronics and microfluidic chips, a fact that extends their application in this area.

Gas Sensors and Biosensors: The use of CNTs in gas sensors is based on changes in the electrical properties (conductivity, dielectric constant, impedance, and refractive index) of these materials induced by charge transfer with gas molecules (8,38). In this way, changes in the resistance of the CNT layer (and thus in the impedance) have been exploited for detection of polar (NH_3, CO, O_3) and nonpolar (He, Ar, N_2, O_2, CO_2) gases (8). The sorption properties of CNTs have been utilized in piezoelectric detection of volatile analytes like alcohols and inorganic gases (He, Ar, O_2, N_2) and in surface acoustic wave sensors to detect volatile organic compounds (8,38). Also, thermoelectric properties of SWCNTs have been used for the analysis of gases in contact with them (39). Pristine as well as polymer-modified CNTs have been used to construct gas sensors, which takes several hours to release the analyte at room temperature before they can be reused (38).

CNTs have also been used to construct electrochemical biosensors to detect enzymes, genes, immunological proteins, neurotransmitters, and other redox proteins (37,40,41) as a result of their ability to promote electron transfer in electrochemical reactions. The most favorable procedure is the direct attachment of specific proteins or clinically important biomolecules to CNTs. Different types of electrochemical methods have been used in these sensors, including direct electro-

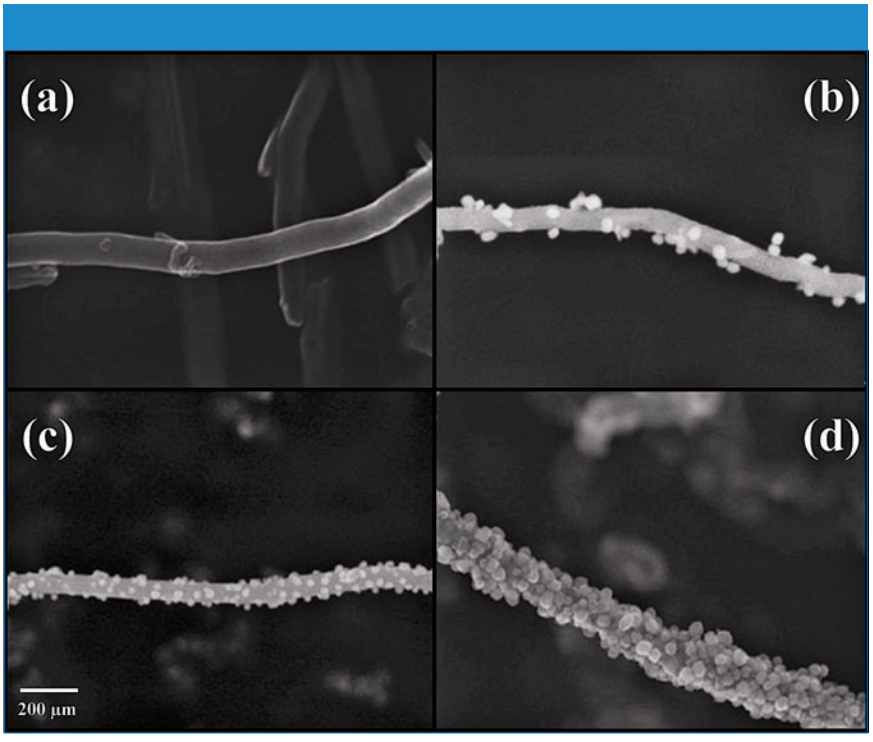

Figure 3: SEM images of (a) pristine MWCNTs and Fe/MWCNTs composites with an initial mass ratio of ferrocene to CNTs of (b) 1:1, (c) 2:1, and (d) 3:1. Adapted from reference (33) with permission from Elsevier.

chemical detection with amperometry or voltammetry, indirect detection of an oxidation product using enzyme sensors, and detection of conductivity changes using CNT-field effect transistors. The electron transference in the detection process can be directly made in the CNTs, in CNTs-polymer composites, in CNTs-metal nanoparticles, and in other CNTs composites (including biological composites).

Matrices in Laser Desorption–Ionization: The use of CNTs as matrices in laser desorption–ionization overcomes some of the disadvantages that exist when molecules with masses lower than 500 Da are analysed by these methods. Most of the organic matrices are decomposed in low mass interferences which generate a high matrix background that hinders mass spectra interpretation (42). The large surface area of CNTs allows the analytes to be dispersed sufficiently, preventing sample aggregation as well as strong UV laser absorption. Nevertheless, contamination of the source by CNTs flying off from the target has been described and therefore some caution must be taken. To avoid this, an adhesion agent may be added to keep the particles attached to the stainless steel plate. In the few existing applications in this field, different molecules have been analyzed, including peptides, carbohydrates, amino acids, pyrenes, low fatty chains, and other low-mass biomolecules (11).

Conclusions

The combination of structures, dimensions, and topologies make CNTs interesting alternative materials, and so research for their applications in separation science is set to increase.

CNTs as stationary phases in GC and LC and as pseudostationary phases in CE are gaining more attention; however, they have modest potential at the moment. Conversely, their growth in sample preparation applications, especially in SPE, has increased substantially, with a huge number of works published in this area.

The most important drawback is that CNTs may contain some impurities from the synthesis procedure that interfere with the ulterior analysis, but this is something that can be easily solved by acid treatment or solvent wash.

The possibility of simple functionalization, binding of complex foreign molecules and solubilization makes CNTs very inspiring and powerful materials. This greatly expands their application in analytical chemistry and further research in this respect is expected to increase.

Although a wide variety of highly pure CNTs are already commercially available they are relatively expensive. This is probably because of their low demand and the low yields obtained in the synthesis steps. However, a reduction in prices is expected when these materials become more commonly used, particularly in sample preparation. CNTs have a rich and unique history with a lot of potential for the future.

References

(1) S. Iijima, *Nature* **354**(6348), 56–58 (1991).

(2) S. Iijima and T. Ichihashi, *Nature* **363**(6430), 603–605 (1993).

(3) D.S. Bethune, C.H. Klang, M.S. de Vries, G. Gorman, R. Savoy, J. Vasquez, and R. Beyers, *Nature* **363**(6430), 605–607 (1993).

(4) C. Journet, W.K. Matser, P. Bernier, L. Laiseau, S. Lefrant, P. Deniard, R. Lee, and J.E. Fischer, *Nature* **388**(6644), 756–758 (1997).

(5) A. Thess, R. Lee, P. Nikolaev, H. Dai, P. Petit, J. Robert, C. Xu, Y.H. Lee, S.G. Kim, A.G. Rinzler, D.T. Colbert, G.E. Scuseria, D. Tománek, J.E. Fischer, and R.E. Smalley, *Science* **273**(5274), 483–487 (1996).

(6) E. Flahaut, C. Laurent, and A. Peigney, *Carbon* **43**(2), 375–383 (2005).

(7) M. Meyyappan, in *Carbon Nanotubes-Science and Applications*, M.J. O'Connell, Ed. (Taylor & Francis, Boca Raton, 2004).

(8) M. Trojanowicz, *TrAC-Trends Anal. Chem.* **25**(5), 480–489 (2006).

(9) M. Valcárcel, S. Cárdenas, B.M. Simonet, Y. Moliner-Martínez, and R. Lucena, *TrAC-Trends Anal. Chem.* **27**(1), 34–43 (2008).

(10) K. Scida, P.W. Stege, G. Haby, G.A. Messina, and C.D. García, *Anal. Chim. Acta* **691**(1–2), 6–17 (2011).

(11) A.V. Herrera-Herrera, M.A. González-Curbelo, J. Hernández-Borges, and M.A. Rodríguez-Delgado, *Anal. Chim. Acta* **734**, 1–30 (2012).

(12) B. Pérez-López and A. Merkoci, *Microchim. Acta* **179**(1–2), 1–16 (2012).

(13) L.M. Ravelo-Pérez, A.V. Herrera-Herrera, J. Hernández-Borges, and M.A.

Rodríguez-Delgado, *J. Chromatogr.* A **1217**(16), 2618–2641 (2010).
(14) C. Herrero Latorre, J. Álvarez Méndez, J. Barciela García, S. García Martín, and R.M. Peña Crecente, *Anal. Chim. Acta* **749**, 16–35 (2012).
(15) M. Najam-ul-Haq, M. Rainer, Z. Szabó, R. Vallant, C.W. Huck, and G.K. Bonn, *J. Biochem. Biophys. Methods* **70**(2), 319–328 (2007).
(16) C. Li, E.T. Thostenson, and T.-S. Chou, *Compos. Sci. Technol.* **68**(6), 1227–1249 (2008).
(17) G.A. Rivas, M.D. Rubianes, M.C. Rodríguez, N.F. Ferreyra, G.L. Luque, M.L. Pedano, S.A. Miscoria, and C. Parrado, *Talanta* **74**(3), 291–307 (2007).
(18) J. Li, J.E. Koehne, A.M. Cassell, H. Chen, H.T. Ng, Q. Ye, W. Fan, J. Han, and M. Meyyppan, *Electroanalysis* **17**(1), 15–27 (2005).
(19) L. Xiao, G.G. Wildgoose, and R.G. Compton, *Anal. Chim. Acta* **620**(1–2), 44–49 (2008).
(20) G. Chen, *Talanta* **74**(3), 326–332 (2007).
(21) P.-X. Hou, C. Liu, and H.-M. Cheng, *Carbon* **46**(15), 2003–2025 (2008).
(22) M. Valcárcel, B.M. Simonet, S. Cárdenas, and B. Suárez, *Anal. Bioanal. Chem.* **382**(8), 1783–1790 (2005).
(23) A. Speltini, D. Merli, E. Quartarone, and A. Profumo, *J. Chromatogr. A*, **1217**(17), 2918–2924 (2010).
(24) A.-H. Duan, S.-M. Xie, and L.-M Yuan, *TrAC-Trends Anal. Chem.* **30**(3), 484–491 (2011).
(25) Y. Zhong, W. Zhou, P. Zhang, and Y. Zhu, *Talanta* **82**(4), 1439–1447 (2010).
(26) S.D. Chambers, F. Svec, and J.M. Frèchet, *J. Chromatogr. A* **1218**(18), 2546–2552 (2011).
(27) R. Sitko, B. Zawiska, and E. Malicka, *TrAC-Trends Anal. Chem.* **37**, 22–31 (2012).
(28) K. Pyrzynska, *TrAC-Trends Anal. Chem.* **29**(7), 718–727 (2010).
(29) H.P. Boem, *Carbon* **40**(2), 145–149 (2002).
(30) K. Pyrzynska, *Chemosphere* **83**(11), 1407–1413 (2011).
(31) L. Jiang and L. Gao, *Chem. Mater.* **15**(14), 2848–2853 (2003).
(32) Y. Deng, C. Deng, D. Yang, C. Wang, S. Fu, and X. Zhang, *Chem. Commun.* (44), 5548–5550 (2005).
(33) F. Zhao, H. Duan, W. Wang, and J. Wang, *Physica B* **407**(13), 2495–2499 (2012).
(34) V.F. Samanidou and E.G. Karageorgou, *Curr. Org. Chem.* **16**(14), 1645–1669 (2012).
(35) A. Mehdinia and M.O. Aziz-Zanjani, *TrAC-Trends Anal. Chem.* **42**, 205–215 (2013).
(36) Q. Zhao, Z. Gao, and Q. Zhuang, *Electroanalysis* **14**(23), 1609–1613 (2002).
(37) L. Agüí, P. Yáñez-Sedeño, and J.M. Pingarrón, *Anal. Chim. Acta* **622**(1–2), 11–47 (2008).
(38) L. Dai, P. Soundarrajan, and T. Kim, *Pure Appl. Chem.* **74**(9), 1753–1772 (2002).
(39) G.U. Sumanasekera, B.K. Pradham, C.K.W. Adu, H.E. Romero, H.C. Foley, and P.C. Eklund, *Mol. Cryst. Liq. Cryst.* **387**(1), 31–37 (2002).
(40) C.B. Jacobs, M.J. Peairs, and B.J. Venton, *Anal. Chim. Acta* **662**(2), 105–127 (2010).
(41) S.K. Vashist, D. Zheng, K. Al-Rubeaan, J.H.T. Luong, and F.-S. Sheu, *Biotechnol. Adv.* **29**(2), 169–188 (2011).
(42) A.K. Buryak and T.M. Serdyuk, *Prot. Met. Phys. Chem. Surf.* **47**(7), 911–920 (2011)

María Asensio-Ramos obtained her BS degree in chemistry from the University of La Laguna (ULL) in Tenerife (Canary Islands, Spain) in 2007 and her PhD in chemistry in 2012, having performed a pre-doc stay at the Institute of Chemical Methodologies of the Italian National Research Council (CNR) in Monterotondo (Rome, Italy). She currently has a grant from the General Research Support Service of the ULL (SEGAI) and also collaborates with the Department of Analytical Chemistry, Nutrition and Food Science of the University of La Laguna (ULL) in Tenerife (Canary Islands, Spain). Her research focuses on the development of new methods for the extraction and preconcentration of organic contaminants in environmental and food samples by chromatographic and electromigration techniques, also using CNTs.

Antonio V. Herrera-Herrera obtained his BS degree in chemistry from the University of La Laguna (ULL) in Tenerife (Canary Islands, Spain) in 2007 and recently completed his PhD in chemistry at the same university, having performed a pre-doctoral stay at the Institute of Food Science Research (CIAL) which belongs to the National Research Council of Spain (CSIC) and to the Autonomous University of Madrid (UAM). Currently, he has a grant from the General Research Support Service of the ULL (SEGAI) and also collaborates with the Department of Analytical Chemistry, Nutrition and Food Science of the University of La Laguna (ULL) in Tenerife (Canary Islands, Spain). His research focuses on the development of new methods for the extraction and preconcentration of organic contaminants in environmental and food samples by chromatographic and electromigration techniques, using CNTs as extractant sorbents.

Miguel Ángel Rodríguez-Delgado is full professor of analytical chemistry at the Department of Analytical Chemistry, Nutrition and Food Science of the University of La Laguna (ULL) in Tenerife (Canary Islands, Spain). In 1991 he became associate professor, he received his PhD in chemistry in 1994 and in 1997 he became full professor. His research activities involve the advancement of new methods for the analysis of organic pollutants, as well as food contaminants and residues in environmental and food matrices, including the use of CNTs as stationary phases for SPE applications.

Salvatore Fanali is a senior researcher (Research Director) at Institute of Chemical Methodologies, Italian National Research Council in Monterotondo (Rome, Italy). His research activity is focused mainly on the development of new miniaturized instrumentation and methods including CE, CEC, capillary LC and nano-LC — all hyphenated with MS. The techniques are currently applied to food, environmental, drug and forensic analysis. He also studies preconcentration methods.

Javier Hernández-Borges is associate researcher (Ramón y Cajal Program) at the Department of Analytical Chemistry, Nutrition and Food Science of the University of La Laguna (ULL) in Tenerife (Canary Islands, Spain). In 2005 he received his PhD degree in chemistry from the University of La Laguna, performing several pre-doctoral and a post-doc stay at the Institute of Chemical Methodologies of the Italian National Research Council (CNR) in Monterotondo (Rome, Italy). His research currently focuses on the development of new methods for the extraction and preconcentration of pesticides, antibiotics, and estrogens in environmental and food samples by chromatographic and electromigration techniques, also using CNTs. Direct correspondence to: jhborges@ull.edu.es ■

Application of Paper Strip Extraction in Combination with LC–MS-MS in Pharmacokinetics

Recent advances in sampling techniques in the pharmaceutical industry sparked significant interest in applying improvements to extraction methods for greater analyte detection and quantitation. In particular, the dried blood spot (DBS) sampling technique has numerous advantages compared to traditional methods such as liquid–liquid extraction, including the use of small sample volumes, less sample processing, and less exposure to toxic solvents (ether, methyl tert-butyl ether [MTBE], and dichloromethane). In this article, we discuss the adaptation of DBS technology to develop and validate a novel paper strip extraction method for the analysis of natural product metabolites in biological samples obtained from a human pharmacokinetic study of xanthohumol, a hop prenylflavonoid.

LeeCole L. Legette, Ralph L. Reed, Lia Murty, Claudia S. Maier, and Jan F. Stevens

Globally, chronic diseases serve as the leading cause of death (1,2) and are projected to be responsible for 64 million deaths annually by 2015 (1). The economic and social impact of chronic diseases necessitated continuous advances in analytical techniques for the development and discovery of therapeutic agents. Improvements in mass spectrometry (MS) technology have allowed for the creation of high-throughput methods, which are used in quantitative analysis of drugs and metabolites in biological samples. The complexity of biological samples (that is, plasma, urine, feces, and so on) influences the sensitivity and selectivity of MS methods and emphasizes the importance of sample preparation. Proteins, salts, and organic compounds present in biological samples may interfere with the detection of the analytes of interest, particularly if they are present in trace amounts, thus requiring protocols for extraction, isolation, or concentration of analytes from samples, which may affect accuracy and reproducibility of analyte measurements (3–9).

Common sample preparation methods include liquid–liquid extraction (LLE) and solid-phase extraction (SPE). Traditionally, LLE has been the prominent extraction method for the analysis of natural products (10) and one of its main strengths is providing aqueous and organic fractions during analysis. However, two major limitations of LLE (sample preparation time and toxic solvent use) (10) have led to the emergence of SPE as a preferred extraction method. SPE lowers analysis costs, organic solvent use, and time compared to LLE (10). SPE involves the adsorption of analytes on solid material before elution with the solvent and has been used in clinical toxicological analysis of drugs (11). Disadvantages of SPE methodology include sample volume and the potential need for optimization of SPE methods including adsorptive material and elution solvent for analytes. Challenges with SPE methods prompted a search for alternative sample preparation methods, specifically dried blood spot (DBS) sampling. Interest in DBS sampling has grown significantly, particularly within the pharmaceutical industry because of the lower costs associated with the technique. The DBS technique consists of collecting and drying a biological sample on a small filter paper disk and processing for subsequent liquid chromatography–tandem mass spectrometry (LC–MS-MS) analysis. With the use of filter paper, DBS uses the adsorptive properties of cellulose for analyte extraction, which may lead to lower costs compared to the adsorptive material of SPE (for example, C18). The cellulose fibers in the filter paper aid in the removal of matrix components that interfere with analyte detection (that is, protein precipitation from plasma samples). Thomas and colleagues (12) illustrated the use of DBS in the detection of various drugs and their phase I and II metabolites. DBS has numerous advantages including minimization of analyte loss, the use of small sample volumes, fewer sample processing steps, low matrix effects, and less exposure to toxic organic solvents compared to traditional methods such as LLE (13).

All of the current sample extraction methods (DBS, SPE, and LLE) have advantages and limitations. The aim of this study is to combine aspects of DBS, SPE, and LLE methods to develop and validate a novel paper strip extraction (PSE) method that maximizes the strength of each while eliminating the weaknesses. The PSE method uses an LC–MS-MS compatible elution solvent for analyte extraction. PSE also incorporates filter paper as its adsorption material, similar to DBS, but enlarges size and alters shape to account for larger sample size and eliminates one of the drawbacks of DBS — the need for high analyte concentration because of small samples, which dictates a small concentration range for analyte detection.

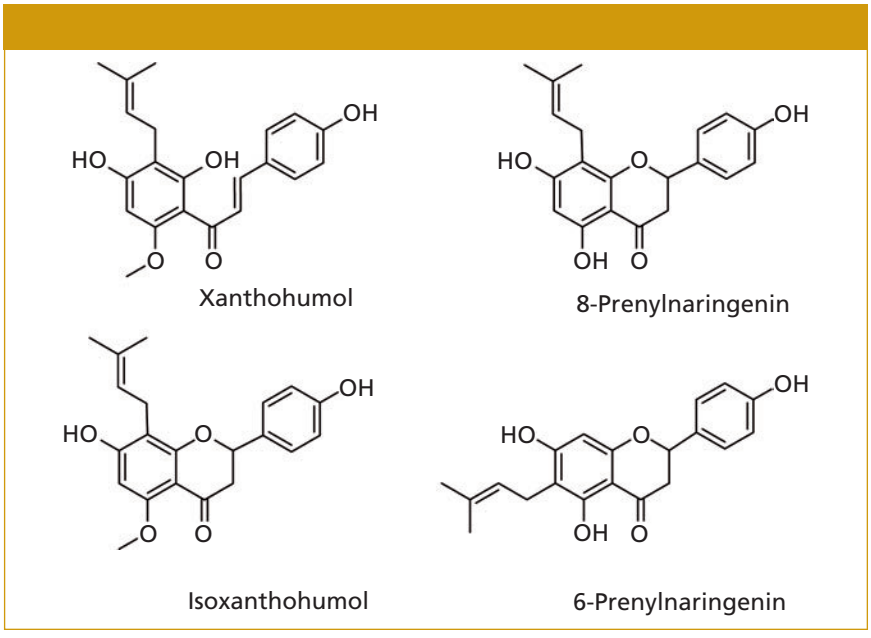

Figure 1: Structures of analytes of interest: natural product metabolites of xanthohumol, a hop prenylflavonoid with antiobesity activity.

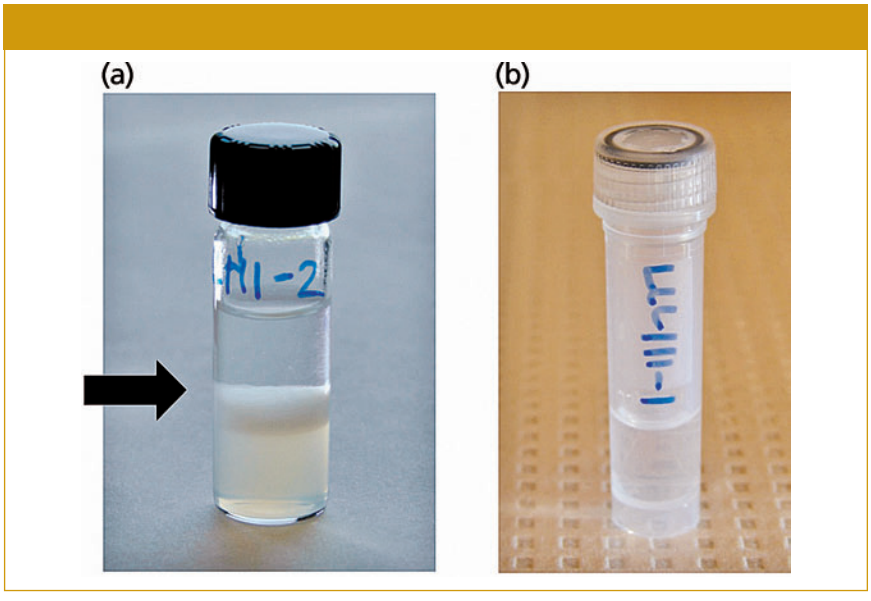

Figure 2: Representative images of human plasma samples following (a) liquid–liquid and (b) paper strip extraction before sample removal for LC–MS-MS analysis. The black arrow in (a) denotes the emulsion interface between the aqueous and organic phases.

We evaluated the PSE method in the analysis of natural product metabolites (Figure 1) in biological samples obtained from a human pharmacokinetic study of xanthohumol, a hop prenylflavonoid.

Experimental

Sample Preparation

A pharmacokinetic (PK) study of a natural product, xanthohumol (XN), a hop prenylflavonoid with antiobesity activity (14), provided all human plasma and urine samples utilized in the PSE method development. Details of the PK study are fully described elsewhere (15). Before extraction, samples underwent enzymatic hydrolysis for conversion of glucuronide conjugates to their corresponding aglycones. Incubation mixtures consisted of 100 µL of biological sample; 380 µL of 0.1 M sodium acetate buffer (pH 4.7); 10 µL of an internal standard, 4,2′-dihydroxychalcone; and 100 µL of *Helix pomatia* sulfatase–glucuronidase for a total volume of 600 µL. We incubated samples for 2 h at 37 °C in 2-mL screw-cap tubes before proceeding with either LLE or PSE.

Liquid–Liquid Extraction

After incubation, we extracted samples with diethyl ether (3 × 1 mL) before drying under nitrogen gas and reconstitution in methanol.

Paper Strip Extraction

After incubation, we vortexed (10 s) and centrifuged (2 min, 13,000 rpm) the samples. We placed pointed paper strips (Whatman #1 filter paper, 8 × 45 mm) in the sample tubes with the tip immersed in the sample solution. Samples were dried overnight onto paper strips in a vacuum dessicator over Drierite (W.A. Hammond Drierite Co.). Dry paper strips were extracted with acidified methanol (0.1% formic acid, 0.5 mL). After the addition of the extraction solvent, samples were vortexed (30 s) and were shaken (30 min) before removal of paper strips. After centrifugation (2 min, 13,000 rpm), we conducted LC–MS-MS analysis for XN and its metabolites (isoxanthohumol [IX], 8-prenylnaringenin, [8PN], and 6-prenylnaringenin [6PN]).

MS Conditions

We described LC–MS-MS conditions for identification and quantitation of XN and its metabolites in earlier work (16).

Comparison of Extraction Methods

We compared LLE and PSE for accuracy, precision, and recovery of XN and its metabolites (IX, 8PN, 6PN).

Calibration Curves

We prepared primary standard stock solutions of XN as well as a metabolite mix (IX, 8PN, 6PN) in methanol. From stock solutions, we aliquoted seven concentrations of XN as well as its metabolites and used the solutions

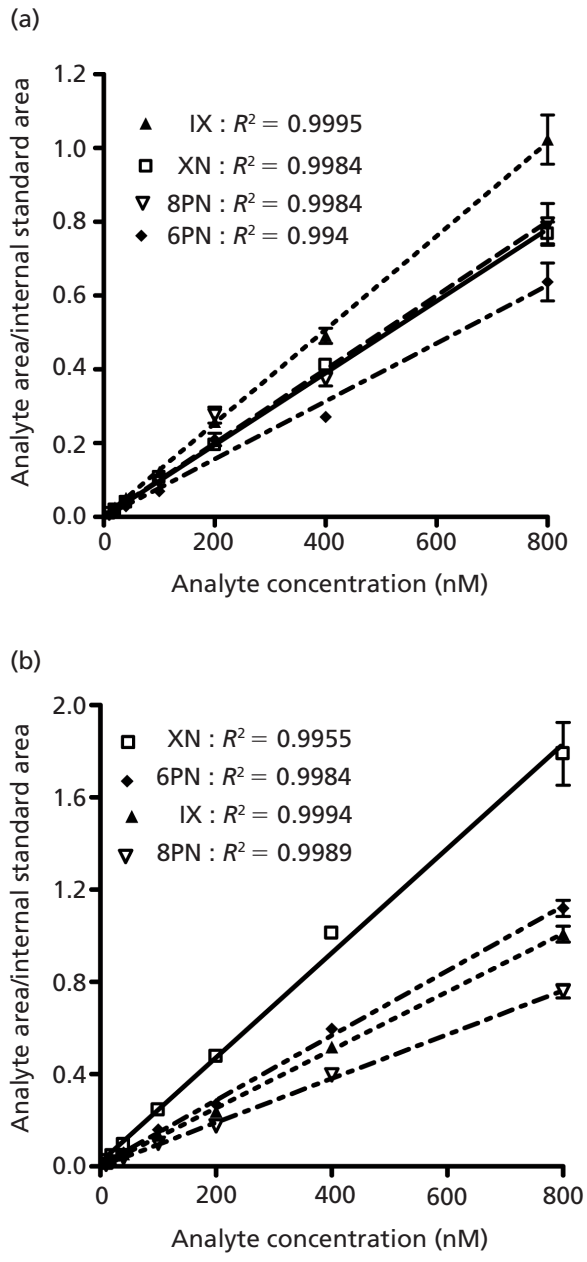

Figure 3: (a) Human plasma and (b) urine matrix-based calibration curves produced using paper strip extraction before LC–MS-MS analysis of xanthohumol (XN) and its metabolites (isoxanthohumol [IX], 8-prenylnaringenin [8PN], and 6-prenylnaringenin [6PN]). Each concentration level was analyzed in triplicate.

to construct matrix-based standard curves to analyze human plasma and urine samples.

Accuracy

We spiked blank human plasma samples with three different concentrations (n = 6 per concentration level) of XN, IX, 8PN, and 6PN to evaluate the accuracy associated with PSE.

Precision

We analyzed samples from three subjects in the XN PK study in replicates of six to determine precision of PSE. Subjects 1001, 1003, and 1005 received 20, 60, and 180 mg XN, respectively.

Recovery

We performed recovery experiments in replicates of five by comparing analytical results (peak area ratios of analyte to internal standard) for extracted samples (that is, extracts of blank plasma samples spiked with known amounts of analytes) at three concentrations with unextracted samples that represent 100% recovery.

Results and Discussion

General Observations

Based on previous work with LLE in XN analysis (16,17) and current PSE experimental findings, we noted similar accuracy and precision for both PSE and LLE, but better analyte recovery with PSE compared to LLE from urine samples. We also observed that there is less chance of sample contamination and analyte losses with PSE versus LLE because of the complex interface that occurs in LLE, which makes phase extraction intricate and time-consuming (Figure 2). We processed samples manually at a rate of 4 min/sample with LLE compared to 1 min/sample with PSE. PSE also requires less organic solvent; previous works by us (16) as well as others (18) demonstrate that traditional LLE methods for XN analysis use 3–4 mL of solvent compared to 0.5 mL solvent for PSE.

Calibration Curves

Calibration curves included seven different analyte concentrations (10, 20, 40, 100, 200, 400, and 800 nM), with the lower limit of quantitation (LLOQ) and upper limits of quantitation (ULOQ) defined as the lowest and highest standard of the calibration curve, respectively. We evaluated matrix-based calibration standards and validation quality control (QC) samples using the following acceptance criteria: LLOQ is within 80–120% accuracy compared to nominal concentration; standards other than LLOQ are within 85–115% accuracy compared to nominal concentration; and at least five out of seven nonzero standards meet the above criteria, including the LLOQ and ULOQ. Human plasma and urine matrix-based calibration curves for XN, IX, 8PN, and 6PN met all of the criteria. We found that a linear-based regression model described the relationship between analyte concentration and response best (Figure 3).

Table I: Determination of accuracy of the paper strip method for xanthohumol (XN) and its metabolites (isoxanthohumol [IX]; 8-prenylnaringenin [8PN]; and 6-prenylnaringenin [6PN]) at low, medium, and high concentrations using human plasma and urine as biological matrices (n = 6 per concentration level)*

		Standards					
		Human Plasma			Human Urine		
Analytes		Low QC 15 nM	Medium QC 75 nM	High QC 300 nM	Low QC 15 nM	Medium QC 75 nM	High QC 300 nM
XN	Calc. conc. (nM)	12 ± 2	63 ± 6	302 ± 35	14 ± 2	78 ± 7	334 ± 18
	% Accuracy	80 ± 10	85 ± 9	101 ± 12	94 ± 15	103 ± 10	111 ± 5
	% RSD	13	10	12	15	10	5
IX	Calc. conc. (nM)	14 ± 2	72 ± 8	266 ± 27	15 ± 1	73 ± 4	269 ± 17
	% Accuracy	96 ± 10	96 ± 11	89 ± 9	99 ± 8	97 ± 5	90 ± 6
	% RSD	11	12	10	8	6	6
8PN	Calc. conc. (nM)	18 ± 1	75 ± 5	278 ± 31	15 ± 1	75 ± 3	272 ± 23
	% Accuracy	122 ± 8	100 ± 7	93 ± 10	102 ± 7	99 ± 4	91 ± 8
	% RSD	7	7	11	7	4	9
6PN	Calc. conc. (nM)	14 ± 1	73 ± 11	299 ± 36	16 ± 1	76 ± 2	271 ± 20
	% Accuracy	95 ± 7	97 ± 14	100 ± 12	109 ± 10	101 ± 2	90 ± 7
	% RSD	7	14	12	9	2	7

*Values are mean ± standard deviation

Table II: Determination of precision of the paper strip method for xanthohumol (XN) and its metabolites (isoxanthohumol [IX]; 8-prenylnaringenin [8PN]; and 6-prenylnaringenin [6PN]) at low, medium, and high concentrations using plasma and urine samples from subjects receiving various doses of XN in a pharmacokinetic study (n = 6 per concentration level). Subjects 1000, 1003, and 1005 received a single oral dose of 20, 60, or 180 mg xanthohumol, respectively.*

		Standards					
		Human Plasma			Human Urine		
Analytes		Subject 1000	Subject 1003	Subject 1005	Subject 1000	Subject 1003	Subject 1005
XN	Calc. conc. (nM)	61 ± 5	132 ± 15	6 ± 0	52 ± 3	54 ± 6	98 ± 11
	% RSD	9	12	8	5	11	11
IX	Calc. conc. (nM)	ND	ND	ND	116 ± 5	110 ± 4	365 ± 31
	% Accuracy	ND	ND	ND	4	4	8
8PN	Calc. conc. (nM)	ND	ND	ND	ND	33±2	ND
	% RSD	ND	ND	ND	ND	6	ND
6PN	Calc. conc. (nM)	ND	ND	ND	ND	ND	ND
	% RSD	ND	ND	ND	ND	ND	ND

*Values are mean ± standard deviation. ND = not detectable

Accuracy

We assessed accuracy of the PSE method by replicate analysis (n = 6) of plasma and urine samples containing known amounts of the analyte at three concentration levels: a low QC, 15 nM; a mid-range QC, 75 nM; and a high QC, 300 nM. The deviation of the mean from the true value served as the measure of accuracy. PSE met the Food and Drug Administration (FDA) method validation requirements (19) for accuracy (85–115%, except at concentrations at or near the LLOQ, which were still within 80–120%) at all three concentration levels for both plasma and urine (Table I). Accuracy data for PSE corresponds to findings from LLE (18).

Precision

Precision experiments used plasma and urine samples from XN PK study participants who received three different doses of XN (20, 60, or 180 mg XN). PSE met FDA method validation requirements (19) for precision (RSD ≤15% except at concentrations at or near the LLOQ, where RSD was ≤20%) for both plasma and urine (Table II) for XN and IX. The metabolites 8PN and 6PN were not detected in the human plasma or urine samples of dosed subjects.

Recovery

We executed recovery experiments by comparing the analytical results for extracted samples (that is, extracts of blank plasma and urine samples spiked with known amounts of analytes) at three concentrations (low, medium, and high) with unextracted standards that represent 100% recovery in replicates of five. The recovery

Table III: Determination of analyte recovery of xanthohumol (XN) and its metabolites (isoxanthohumol [IX]; 8-prenylnaringenin [8PN]; and 6-prenylnaringenin [6PN]) at low, medium, and high concentrations using paper strip extraction with human plasma and urine as biological matrices (*n* = 5 per concentration level)*

			Standards				
			Human Plasma		Human Urine		
Analytes		Low Conc. 5 nM	Medium Conc. 50 nM	High Conc. 400 nM	Low Conc. 5 nM	Medium Conc. 50 nM	High Conc. 400 nM
XN	%Recovery	76 ± 8	66 ± 8	67 ± 2	65 ± 5	87 ± 10	101 ± 10
	% RSD	10	13	3	7	11	10
IX	%Recovery	105 ± 11	89 ± 6	88 ± 7	117 ± 9	109 ± 8	108 ± 4
	% RSD	10	7	8	7	7	4
8PN	%Recovery	95 ± 7	87 ± 10	85 ± 8	111 ± 8	100 ± 6	105 ± 4
	% RSD	8	12	9	7	6	4
6PN	%Recovery	81 ± 5	74 ± 5	68 ± 5	109 ± 4	108 ± 10	110 ± 3
	% RSD	6	7	7	3	9	2

*Values are mean ± standard deviation

of IX, 8PN, 6PN, and XN ranged from 65–117% at various plasma and urine concentration levels (Table III). All concentration levels had an RSD ≤15%, which met the FDA method validation requirements (19). We also observed better recovery of XN from urine samples with PSE (65–101%) compared to LLE (60–80%).

Conclusion

Rising incidences of chronic diseases worldwide have spurred great interest in advancing analytical techniques for effective analysis of therapeutic drugs. Advances in analytical MS instrumentation have allowed for high throughput methods that are also very sensitive and specific; however MS analysis may be significantly influenced by sample preparation methods. In creating a novel PSE method, we combined the individual strengths of common methods including DBS, SPE, and LLE while removing the drawbacks. The PSE method was evaluated using plasma and urine samples from a human XN PK study and resulted in 80–122% accuracy over a large range of concentrations, ≤15% RSD for precision, and losses of ≤35% for XN and its metabolites. In terms of accuracy, precision, and recovery, PSE performs similarly to or better than LLE while offering several benefits including less solvent use, reduced exposure to toxic solvents, higher sample throughput, and lower labor costs.

References

(1) K. Strong, C. Mathers, J. Epping-Jordan, and R. Beaglehole, *Int. J. Epidemiol.* **35**(2), 492–494 (2006).

(2) D. Yach, C. Hawkes, C.L. Gould, and K.J. Hofman, *JAMA* **291**(21), 2616–2622 (2004).

(3) H. Gika and G. Theodoridis, *Bioanalysis* **3**(14), 1647–1661 (2011).

(4) T. Hyotylainen, *Anal. Bioanal. Chem.* **394**(3), 743–758 (2009).

(5) H. Kataoka, *Anal. Sci.* **27**(9), 893–905 (2011).

(6) W.M. Mullett, *J. Biochem. Biophys. Methods* **70**(2), 263–273 (2007).

(7) C. Nerin, J. Salafranca, M. Aznar, and R. Batlle, *Anal. Bioanal. Chem.* **393**(3), 809–833 (2009).

(8) L. Novakova and H. Vlckova, *Anal. Chim Acta* **656**(1–2), 8–35 (2009).

(9) Y. Saito, M. Kawazoe, M. Imaizumi, Y. Morishima, Y. Nakao, K. Hatano, M. Hayashida, and K. Jinno, *Anal. Sci.* **18**(1), 7–17 (2002).

(10) C. Mahugo Santana, Z. Sosa Ferrera, M. Esther Torres Padron, and J. Juan Santana Rodriguez, *Molecules* **14**(1), 298–320 (2009).

(11) F. Degel, *Clin. Biochem.* **29**(6), 529–540 (1996).

(12) A. Thomas, J. Deglon, T. Steimer, P. Mangin, Y. Daali, and C. Staub, *J. Sep. Sci.* **33**(6–7), 873–879 (2010).

(13) J. Deglon, A. Thomas, P. Mangin, and C. Staub, *Anal. Bioanal. Chem.* **402**(8), 2485–2498 (2012).

(14) J.S. Kirkwood, L.L. Legette, C.L. Miranda, Y. Jiang, and J.F. Stevens, *J. Biol. Chem.* **288**(26), 19000–19013 (2013).

(15) L. Legette, C. Karnpracha, R.L. Reed, J. Choi, G. Bobe, J.M. Christensen, R. Rodriguez-Proteau, J.Q. Purnell, and J.F. Stevens, *Mol. Nutr. Food Res.* in press, http://www.ncbi.nlm.nih.gov/pubmed/24038952 (2013).

(16) L. Legette, L. Ma, R.L. Reed, C.L. Miranda, J.M. Christensen, R. Rodriguez-Proteau, and J.F. Stevens, *Mol. Nutr. Food Res.* **56**(3), 466–474 (2012).

(17) L.L. Legette, A.Y. Luna, R.L. Reed, C.L. Miranda, G. Bobe, R.R. Proteau, and J.F. Stevens, *Phytochemistry* **91,** 236–241 (2013).

(18) Y. Yuan, X. Qiu, D. Nikolic, J.H. Dahl, and R.B. van Breemen, *J. AOAC Int.* **95**(6), 1744–1749 (2012).

(19) US Food and Drug Administration, Guidance for Industry: Bioanalytical Method Validation, (FDA, Rockville, Maryland, 2001).

LeeCole L. Legette, Ralph L. Reed, and Jan F. Stevens are with the Linus Pauling Institute and the College of Pharmacy at Oregon State University in Corvallis, Oregon. **Lia Murty** is with the College of Pharmacy at Oregon State University. **Claudia S. Maier** is with the Department of Chemistry at Oregon State University. Direct correspondence to: fred.stevens@oregonstate.edu ■

Comprehensive Analysis of Human Plasma Using Gas Chromatography–High Resolution Time-of-Flight Mass Spectrometry: A Workflow to Leverage Electron and Chemical Ionization

Gas chromatography with electron ionization and mass spectrometry (GC–EI-MS) detection is a workhorse among analytical techniques in metabolomics. A major challenge in the utilization of GC–EI-MS in metabolomics is the identification of unknowns. The recent availability of high resolution, accurate mass, time-of-flight mass spectrometry (TOF-MS) systems provides great potential for identifying unknowns by reducing uncertainty in possible formulas and enhancing detection continuity between sample sets. A workflow using GC–EI-MS spectra for library identification, with molecular formula information for unknowns provided by chemical ionization-mass spectrometry (CI-MS) and accurate mass analysis was used for the analysis of blood plasma.

David E. Alonso, Joe Binkley, John Heim, and Jeff Patrick

Metabolomics provides a foundation for quantitative, comparative biology and is indispensable for the comprehensive characterization of molecules and differential analysis of populations. It entails instrumental detection, characterization, and quantification of small molecules (molecular weight < 1500 Da) produced, or transformed in the cells of living organisms (1,2). Although no single instrument is capable of fully profiling the metabolome, the unique capabilities of time-of-flight mass spectrometry (TOF-MS) make it an ideal tool for metabolomic studies. Gas chromatography–time-of-fight-mass spectrometry (GC–TOF-MS) is a powerful approach for unbiased metabolic profiling and quantitation of a diverse array of metabolites (3,4). High-resolution TOF-MS provides additional benefits such as mass accuracies below 1 ppm for robust formula determinations and resolving power in excess of 50,000 for resolution of isobars and minimization of background interferences. A workflow that combines accurate mass electron ionization (EI) and chemical ionization (CI) high-resolution TOF-MS for confident characterization of different compound classes was used for the analysis of human blood plasma. It includes recommendations for sample preparation, analytical conditions, and data analysis.

General Workflow

The majority of metabolites in blood plasma are labile and exhibit low volatility making their analysis by GC difficult. This is addressed by using a two step derivatization procedure involving the treatment of samples with O-methylhydroxylamine hydrochloride in pyridine (MEOX) followed by silylation with *N*-methyl-*N*-trifluoroacetamide/1% trimethylchlorosilane (MSTFA) (5). This two-step procedure minimizes the number of possible forms of reducing sugars as shown for glucose in Figure 1. Treatment of glucose with MSTFA (Figure 1b) results in four different forms (α- and β-furanose and pyranose trimethylsilyl derivatives), while the two-step procedure typically produces two geometric isomers of the open chain structure of the monosaccharide (Figure 1a). Note that one isomer is produced preferentially in this two-step derivatization of glucose. This not only simplifies the analysis of blood samples, but also increases the likelihood of compound detection.

GC–MS compound characterization in metabolomics relies primarily on retention time and spectral similarity. A higher confidence for feature identification can be achieved through the addition of accurate mass formula determinations for molecular ions, quasimolecular ions,

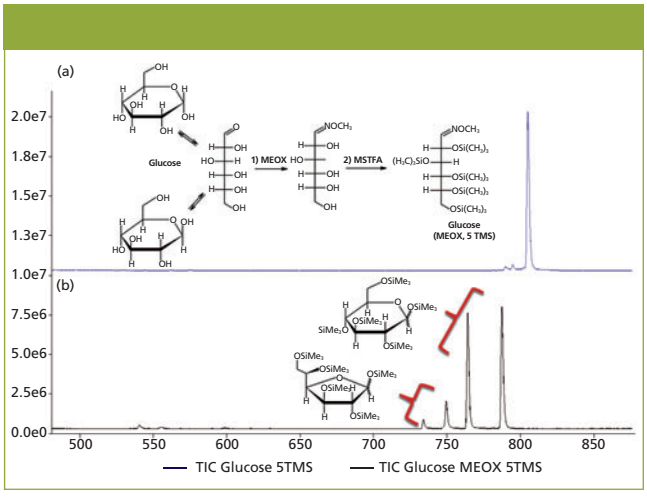

Figure 1: (a) Extracted ion chromatogram showing one major product for the two-step derivatization of glucose. (b) Products for the one-step MSTFA derivatization of glucose.

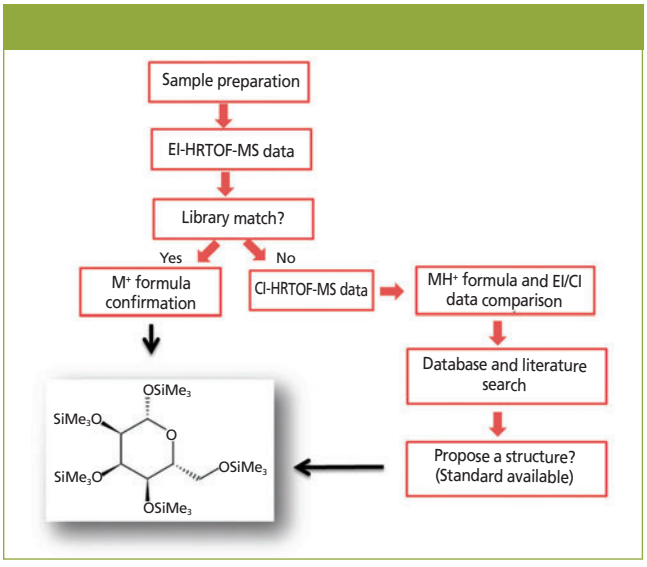

Figure 2: General workflow.

Table III: Representative compounds in NIST human plasma

Peak	Name	Formula	R.T. (s)	Area	Similarity
1	Phosphate (3 TMS)	$C_9H_{27}O_4PSi_3$	533	10740930	857
2	Threonine (3 TMS)	$C_{13}H_{33}NO_3Si_3$	583	1694554	894
3	5-Oxo-proline (2 TMS)	$C_{11}H_{23}NO_3Si_2$	639	8477106	912
4	Creatinine (3 TMS)	$C_{13}H_{31}N_3OSi_3$	652	2302177	866
5	Citric acid (4 TMS)	$C_{18}H_{40}O_7Si_4$	739	824486	851
6	Maltose (MEOX, 8 TMS)?	$C_{37}H_{89}NO_{11}Si_8$?	805	20744340	829
7	Inositol (6 TMS)	$C_{24}H_{60}O_6Si_6$	823	1093541	895
8	Arachidonic acid (TMS)	$C_{23}H_{40}O_2Si$	898	597056	848
9	α-Tocopherol (TMS)	$C_{32}H_{58}O_2Si$	1148	266286	849
10	Cholesterol (TMS)	$C_{30}H_{54}OSi$	1164	11656743	915

Table IV: Mass accuracy values for representative compounds in NIST human plasma

Peak	Name	Species	Observed Ion *m/z*	Expected Ion *m/z*	Mass Accuracy (ppm)
1	Phosphate (3 TMS)	$M^{+\cdot}$	314.09463	314.09463	–1.00
2	Threonine (3 TMS)	$[M–C_5H_{13}OSi]^{+\cdot}$	218.10271	218.10256	–0.70
3	5-Oxo-proline (2 TMS)	$M^{+\cdot}$	273.12080	273.12110	–1.10
4	Creatinine (3 TMS)	$M^{+\cdot}$	329.17665	329.17694	–0.90
5	Citric acid (4 TMS)	$[M–CH_3]^+$	465.16109	465.16064	–1.00
6	Maltose (MEOX, 8TMS)?	$C_{15}H_{33}O_4Si_3$?	361.16783	361.16812	–0.80
7	Inositol (6 TMS)	$[M–C_{12}H_{31}O_3Si_3]^{+\cdot}$	305.14190	305.14186	–0.10
8	Arachidonic acid (TMS)	$M^{+\cdot}$	376.27935	376.2921	0.40
9	α-Tocopherol (TMS)	$M^{+\cdot}$	502.41990	502.42006	–0.30
10	Cholesterol (TMS)	$M^{+\cdot}$	458.39384	458.39359	–0.60

and fragments. Key to the success of analyte identification was a workflow that included both EI and CI high-resolution TOF-MS data acquisition (Figure 2) (6). CI high-resolution TOF-MS data were critical in characterizing compounds that produced poor spectral matches in relation to commercially available libraries or did not exhibit molecular ions in their EI high-resolution TOF-MS mass spectra.

Sample Preparation

Blood plasma (100 µL) was transferred to a 2-mL microtube and treated with 400 µL of methanol to precipitate proteins. The heterogeneous mixture was vortexed for 30 s at 2500 rpm and centrifuged for 15 min at 15,000 rpm. The supernatant was removed and transferred to a GC vial (400 µL insert). The mixture was dried with a SpeedVac for 2 h and lyophilized overnight at -50 °C to remove residual water. The dry sample was treated with 25 µL of MEOX reagent (20 mg/mL in pyridine) and shaken at 80 °C for 15 min. It was then treated with 75 µL of MSTFA and shaken at 80 °C for 15 min. The product mixture was allowed to cool to room temperature, vortexed for 30 s and analyzed by EI and CI high-resolution TOF-MS.

Data Acquisition (Instrument Settings)

See Tables I and II in the on-line version of this article for the GC and MS instrument settings.

Table V: Library hits for compound 6			
Hit	Name	Formula	Similarity
1	Maltose, octakis (trimethlysilyl) ether, methyloxime (isomer 2)	$C_{37}H_{89}NO_{11}Si_8$	829
2	3-α-Mannobiose, octakis (trimethlysilyl) ether (isomer 2)	$C_{36}H_{86}O_{11}Si_8$	820
3	D-(+)-Cellobiose, octakis (trimethlysilyl) ether, methyloxime (isomer 2)	$C_{37}H_{89}NO_{11}Si_8$	818
4	D-Lactose, octakis (trimethlysilyl) ether, methyloxime (isomer 2)	$C_{37}H_{89}NO_{11}Si_8$	818
5	3-α-Mannobiose, octakis (trimethlysilyl) ether (isomer 1)	$C_{36}H_{86}O_{11}Si_8$	813
6	D-(+)-Cellobiose, octakis (trimethlysilyl) ether, methyloxime (isomer 1)	$C_{37}H_{89}NO_{11}Si_8$	813
7	α-Gentiobiose, octakis (trimethlysilyl) ether, methyloxime (isomer 2)	$C_{37}H_{89}NO_{11}Si_8$	811
8	2-α-Mannobiose, octakis (trimethlysilyl) ether (isomer 1)	$C_{36}H_{86}O_{11}Si_8$	809
9	Lactulose, octakis (trimethlysilyl) ether, methyloxime (isomer 1)	$C_{37}H_{89}NO_{11}Si_8$	808
10	Maltose, octakis (trimethlysilyl) ether, methyloxime (isomer 1)	$C_{37}H_{89}NO_{11}Si_8$	803

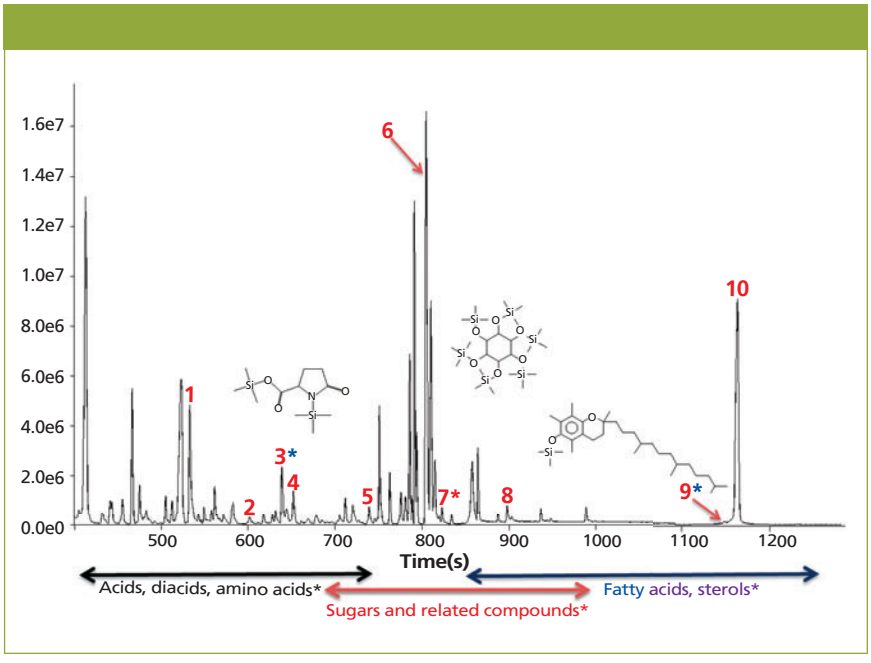

Figure 3: EI high-resolution TOF-MS, AIC of NIST human plasma.

Results

An analytical ion chromatogram (AIC) for National Institute of Standards and Technology (NIST) human plasma is displayed in Figure 3, and can be divided into three general areas based on compound classes: acids, diacids, amino acids; sugars and related compounds; and fatty acids and sterols. Chromatographic peaks corresponding to derivatives of 5-oxo-proline, inositol, and α-tocopherol are marked with asterisks (*).

Quality EI high-resolution TOF-MS data indicated traditional fragmentation and facilitated searches against nominal mass libraries as evident by similarity values for representative compounds in human plasma (Table III). Similarity values for nine of the compounds ranged from 848 to 915 out of a possible score of 1000.

An increased level of confidence for compound identification was achieved through accurate mass molecular and fragment ion formula determinations. For example, the peak true (deconvoluted) mass spectrum, NIST library match, and molecular ion mass accuracy values for a creatinine derivative (3 TMS) in human plasma are shown in Figure 4 in the on-line version.

Mass accuracy values for creatinine ions at m/z = 329.17665 $[M]^+$ and m/z = 314.15323 $[M\text{-}CH_3]^+$ were -0.90 and -0.76 ppm, respectively. Additional molecular and fragment ion mass accuracy values for the other representative compounds in NIST human plasma are listed in Table IV. Values ranged from -1.10 to 0.40 ppm (mean |ppm| = 0.69).

Combining EI and CI high-resolution TOF-MS accurate mass data is particularly useful for compounds without molecular ions in their EI high-resolution TOF-MS spectra. This is illustrated in the EI high-resolution TOF-MS data for inositol where the molecular ion is absent; however, a strong protonated molecular ion $[M+H]^+$ is visible in its CI high-resolution TOF-MS spectrum at m/z = 613.30730 (Figure 5).

Leveraging accurate mass data was critical for the characterization of compound 6 (Tables III and IV) because spectral similarity searches were inconclusive. It was misidentified as the MEOX/TMS derivative of maltose (similarity = 829/1000). Furthermore, the first 10 library hits (similarity >800) were derivatized disaccharides (Table V). This was not surprising since sugars are difficult to characterize because of their thermal instability and similar EI-MS fragmentation patterns.

Acquisition of CI high-resolution TOF-MS data for compound 6

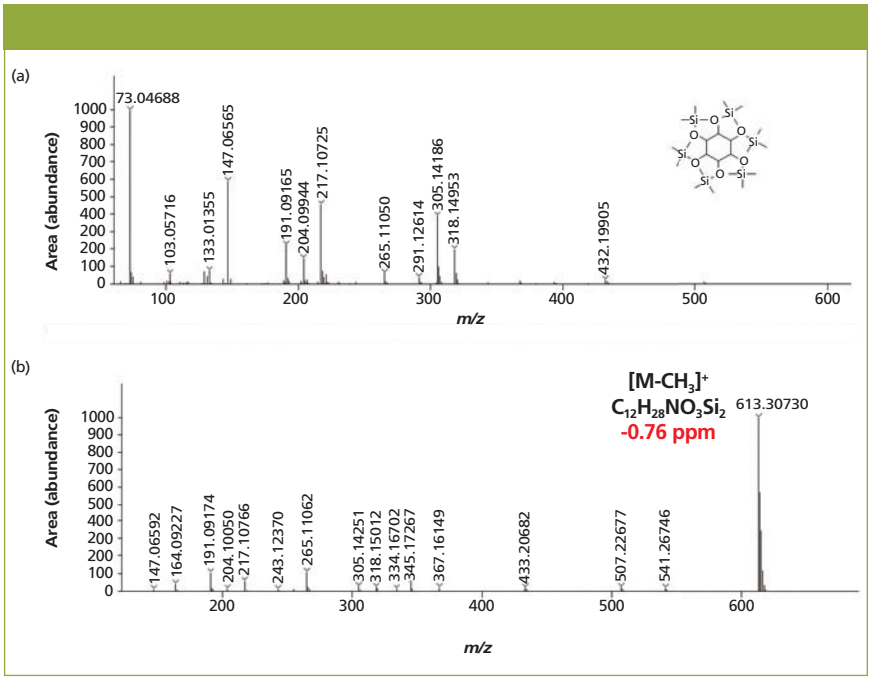

Figure 5: (a) EI and (b) CI high-resolution TOF-MS spectra for inositol.

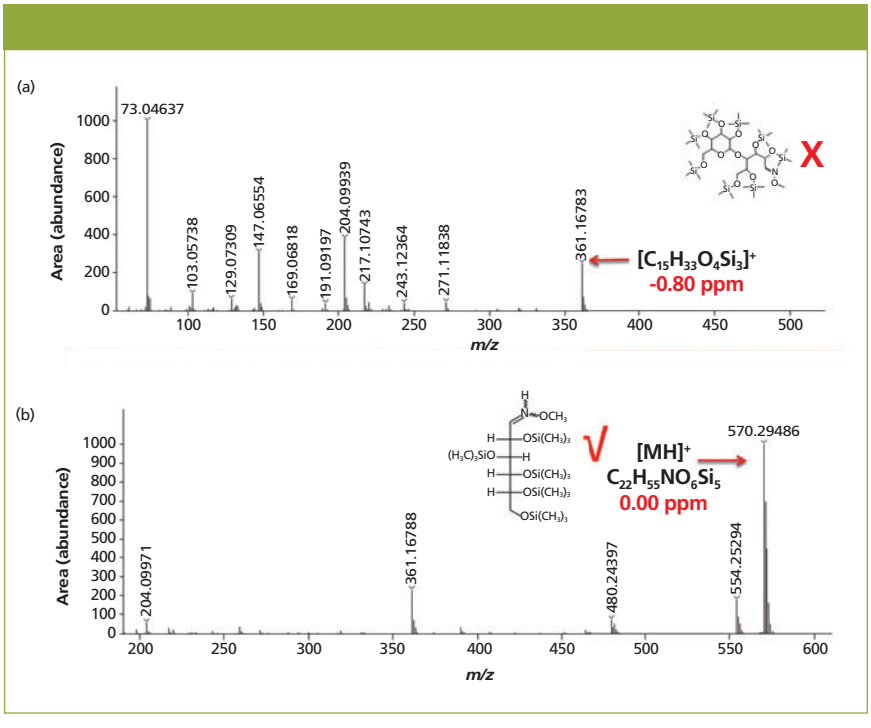

Figure 6: (a) EI and (b) CI high-resolution TOF-MS data for compound 6 in human plasma.

(Figure 6) resulted in a protonated molecular ion at m/z = 570.29486 ($C_{22}H_{55}NO_6Si_5$, MA = 0.00 ppm). Compound 6 was determined unequivocally to be glucose (MEOX, 5 TMS) after comparison to data obtained from a derivatized authentic standard.

Conclusion

The methodology presented in this study provides a workflow for rapid and reliable profiling of human plasma. While high quality spectral data and excellent mass accuracy values resulted in confident identification of most compounds using EI, the addition of CI high-resolution TOF-MS data was essential for characterization of labile blood plasma compounds with absent or low-abundance molecular ions.

On-Line Edition

The on-line version of this article includes Figure 4 as well as Tables I and II. To see the full version please visit: spectroscopyonline.com/AlonsoCTMS1013.

References

(1) T. Kind, G. Wohlgemuth, D.Y. Lee, M. Palazoglu, S. Shahbaz, and O. Fiehn, *Anal. Chem.* **81,** 10038–10048 (2009).

(2) A. Jiye, J. Trygg, J. Gullberg, A.I. Johansson, P. Johnsson, H. Antti, S.L. Marklund, and T. Moritz, *Anal. Chem.* **77,** 8086–8094 (2005).

(3) B. Ma, Q. Zhang, G.-J. Wang, J.-Y. A, D. Wu, Y. Liu, B. Cao, L.-S. Liu, Y.-Y. Hu, Y.-I. Wang, and Y.-Y. Zhen, *Acta Pharmacol. Sin.* **32,** 270–278 (2011).

(4) J.W. Allwood, A. Erban, S. de Koning, W.B. Dunn, A. Luedemann, A. Lommen, L. Kay, R. Loscher, J. Kopka, and R. Goodacre, *Metabolomics* **5,** 479–496 (2009).

(5) W.B. Dunn, D. Broadhurst, P. Begley, E. Zelena, S. Francis-McIntrye, N. Anderson, M. Brown, J.D. Knowles, A. Halsall, J.N. Haselden, A.W. Nicholls, J.D. Wilson, D.B. Kell, and R. Goodacre, *The Human Serum Metabolome (HUSERMET) Consortium Nature Protocols* **6**(7), 1060–1083 (2011).

(6) S. Abate, Y.G. Ahn, T. Kind, T.R.I. Cataldi, and O. Fiehn, *Rapid Commun. Mass Spectrom.* **24,** 1172–1180 (2010).

David E Alonso, Joe Binkley, John Heim, and Jeff Patrick are with LECO Corporation.

Direct correspondence to:
david_alonso@leco.com ■

Optimizing LC–MS and LC–MS-MS Methods

Many parameters within liquid chromatography–mass spectrometry (LC–MS) methods are "locked and left" — that is, they are optimized using a few methods when new, then only changed if absolutely necessary because of poor analytical performance. This is fine when methods are performing as they should be and producing data which is fit for purpose, but the following question should also be asked: Do you know when your data aren't as good as they could be? Here we consider some parameters in LC–MS that can be optimized to improve sensitivity and reproducibility in LC–MS.

The most significant choice in many LC–MS methods is the mode of ionization. The generally accepted rule is that electrospray ionization (ESI) works best for higher-molecular-weight compounds that are more polar or ionizable, and atmospheric pressure chemical ionization (APCI) is best for lower-molecular-weight, less-polar compounds. Atmospheric pressure photoionization (APPI) was originally designed to work with less-polar analytes, however the careful choice of dopant or the use of direct ionization sources can significantly extend the capability of APPI techniques. In all atmospheric pressure ionization source types there are a multitude of interrelated factors that affect the degree of analyte ionization, including analyte pK_a value, electronegativity, relative proton affinity, ionization energy, and volatility. "New" analytes should be screened using all available techniques to optimize instrument response. Furthermore, although the "polarity" of the interface may seem obvious when screening lower-molecular-weight acids or bases, one can often be surprised at which polarity mode gives the optimum signal with more-complex molecules. Be sure to screen analytes in both polarity modes to ensure optimum response, especially when the analyte is not ionizable, and avoid "guessing" which mode might be best.

The capillary (sprayer) voltage can have a major effect on efficiency of ionization, and it will change with the analyte type, eluent system, and flow rate. This parameter is perhaps the most overlooked variable in terms of improving instrument response and one should consider optimizing to improve not only sensitivity but also reproducibility. At a higher applied potential, one should be cautious to assess quantitative reproducibility because there are various nonideal spray modes that will give rise to a signal but will result in variable ionization efficiency.

The efficiency of ion sampling from within the electrospray will vary widely with analyte type, applied voltage, solvent system, drying gas parameters, and eluent flow rate. The position of the sprayer relative to the sampling orifice (both axially and laterally) should be optimized when the highest sensitivity is required.

Nebulizing gas flow rate and heating requirements will change with the nature and flow rate of the eluent, and, in general, smaller droplets are preferred within ESI experiments to improve the efficiency of the droplet charging process. When changing eluent systems (especially the amount or nature of the organic component) or flow rate, consider optimizing the nebulizing gas settings. Similarly, drying gas requirements will change with the changing nature of the eluent system (including during gradient analyses where the range of organic composition alters greatly [large $\Delta\Phi$]) and should be optimized especially when eluent systems are highly aqueous. Electrospray efficiency is often improved by adding "dopants" such as isopropanol to allow a reduction in droplet surface tension; however, note that the sprayer position, nebulizing gas, and drying gas settings may need to be altered for optimum signal response.

In ESI, analytes may be charged through processes such as charge transfer or triboelectric charging at the capillary tip. Although this may produce a satisfactory response, one should consider adjusting the eluent system to give the ionized form of the analyte in solution (eluent pH higher than analyte pK_a for acids and lower for bases). This can result in orders of magnitude improvement in instrument sensitivity; however, it may also require an adjustment in high performance liquid chromatography (HPLC) operating conditions to properly retain the ionized analyte or reoptimize the separation selectivity. The use of ion-pairing reagents such as trifluoroacetic acid should be avoided and volatile buffers chosen so that the buffer pK_a is within ±1 pH unit of the eluent system pH.

Ion suppression or enhancement effects occur when there are species that strongly compete with, or are suppressed by, the presence of your analyte. When quantitative sensitivity is poor or the analyte signal is highly irreproducible, one should investigate the effects of the eluent system and matrix on the instrument response. These effects can often be overcome by altering the eluent system to reduce the ionic strength or change the buffer type, or by more studious sample preparation, designed to isolate the analyte from the interfering matrix component.

The vast majority of LC–MS instruments are capable of analyte declustering, especially with respect to water molecule clusters. The application of an accelerating voltage in the first stage of the mass spectrometer to cause low energy collisions with background molecules can often lead to an improvement in instrument sensitivity, primarily due to a reduction in noise around the analyte signal.

When performing MS-MS analysis, it is important when seeking optimum sensitivity and quantitative accuracy to optimize the collision energy as well as the "dwell" time between measuring ion transitions to avoid "cross-talk" effects that can significantly affect quantitative measurements.

More Online:

Get the full tutorial at
www.CHROMacademy.com/Essentials
(free until February 20).

THE APPLICATION NOTEBOOK

Call for Application Notes

LCGC is planning to publish the next issue of *The Application Notebook* special supplement in June. The publication will include vendor application notes that describe techniques and applications of all forms of chromatography and capillary electrophoresis that are of immediate interest to users in industry, academia, and government. If your company is interested in participating in these special supplements, contact:

Michael J. Tessalone, Group Publisher, (732) 346-3016
Edward Fantuzzi, Associate Publisher, (732) 346-3015
Stephanie Shaffer, East Coast Sales Manager, (774) 249-1890

Application Note Preparation

It is important that each company's material fit within the allotted space. The editors cannot be responsible for substantial editing or handling of application notes that deviate from the following guidelines:

Each application note page should be no more than 500 words in length and should follow the following format.

Format

- **Title:** short, specific, and clear
- **Abstract:** brief, one- or two-sentence abstract
- **Introduction**
- **Experimental Conditions**
- **Results**
- **Conclusions**
- **References**
- **Two graphic elements:** one is the company logo; the other may be a sample chromatogram, figure, or table
- **The company's full mailing address, telephone number, fax number, and Internet address**

All text will be published in accordance with *LCGC*'s style to maintain uniformity throughout the issue. It also will be checked for grammatical accuracy, although the content will not be edited. Text should be sent in electronic format, preferably using Microsoft Word.

Figures

Refer to photographs, line drawings, and graphs in the text using arabic numerals in consecutive order (Figure 1, etc.). Company logos, line drawings, graphs, and charts must be professionally rendered and submitted as .TIF or .EPS files with a minimum resolution of 300 dpi. Lines of chromatograms must be heavy enough to remain legible after reduction. Provide peak labels and identification. Provide figure captions as part of the text, each identified by its proper number and title. If you wish to submit a figure or chromatogram, please follow the format of the sample provided below.

Tables

Each table should be typed as part of the main text document. Refer to tables in the text by Roman numerals in consecutive order (Table I, etc.). Every table and each column within the table must have an appropriate heading. Table number and title must be placed in a continuous heading above the data presented. If you wish to submit a table, please follow the format of the sample provided below.

References

Literature citations must be indicated by arabic numerals in parentheses. List cited references at the end in the order of their appearance. Use the following format for references:

(1) T.L. Einmann and C. Champaign, *Science* **387**, 922–930 (1981).

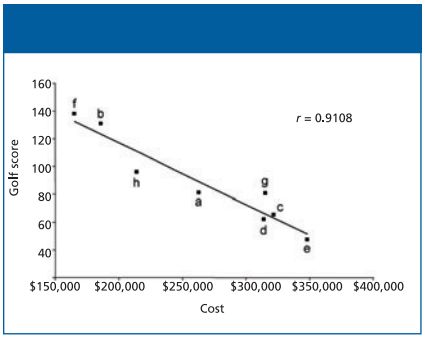

Figure 1: Chromatograms obtained using the conditions under which the ion suppression problem was originally discovered. The ion suppression trace is shown on the bottom. Column: 75 mm × 4.6 mm ODS-3; mobile-phase A: 0.05% heptafluorobutyric acid in water; mobile-phase B: 0.05% heptafluorobutyric acid in acetonitrile; gradient: 5–30% B in 4 min. Peaks: 1 = metabolite, 2 = internal standard, 3 = parent drug.

Table I: Factor levels used in the designs

Factor	Nominal value	Lower level (−1)	Upper level (+1)
Gradient profile	1	0	2
Column temperature (°C)	40	38	42
Buffer concentration	40	36	44
Mobile-phase buffer pH	5	4.8	5.2
Detection wavelength (nm)	446	441	451
Triethylamine (%)	0.23	0.21	0.25
Dimethylformamide	10	9.5	10.5

The deadline for submitting application notes for the June issue of *The Application Notebook* is:

April 16, 2014

This opportunity is limited to advertisers in *LCGC North America*.
For more information, contact:
Mike Tessalone at (732) 346-3016, Ed Fantuzzi at (732) 346-3015, or Stephanie Shaffer at (774) 249-1890.

DiamondAnalytics

Expanding the range of analytical capabilities

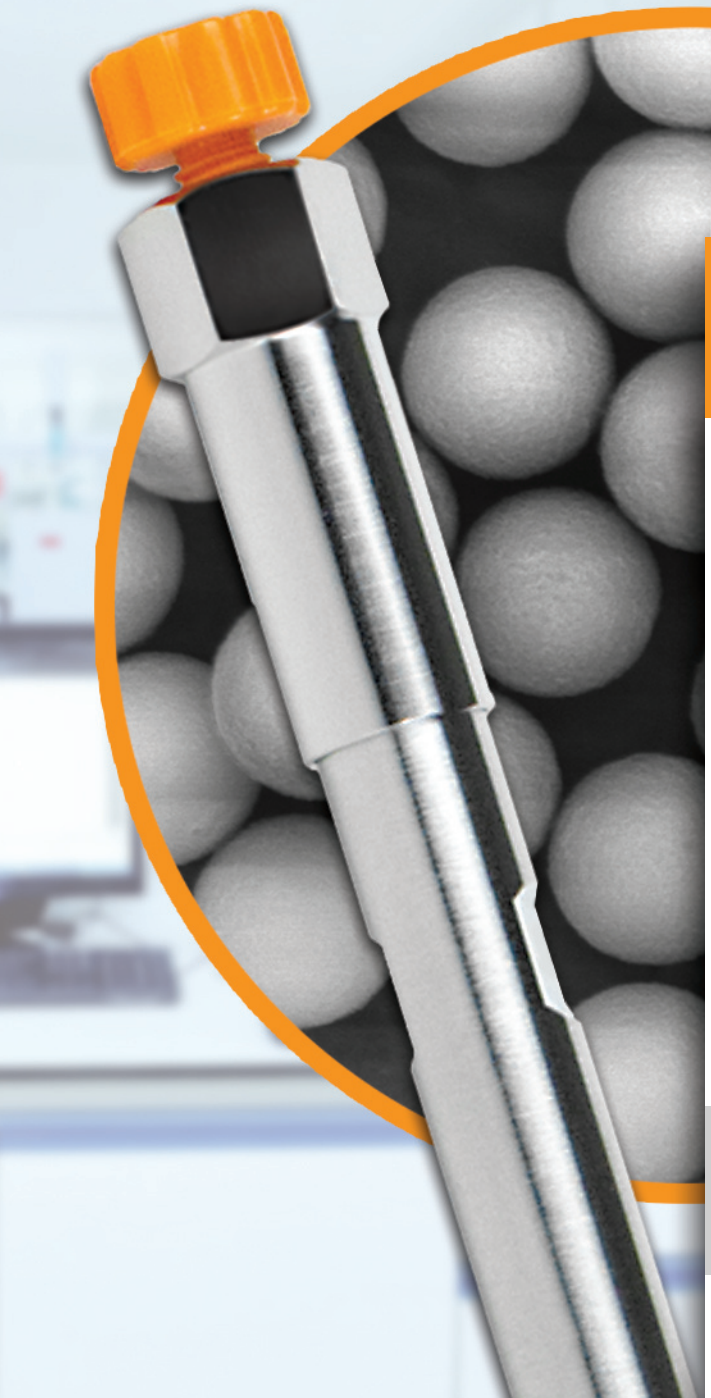

1st Carbon Core Shell Particle

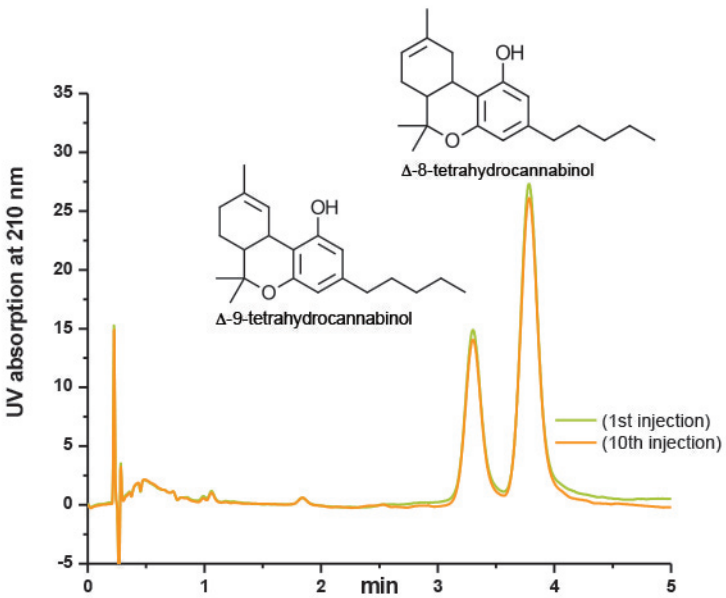

Column: Flare 4.6 x 33 mm C18 mixed mode
Temp: 45 °C
Mobile phase: 410 ml water + 440 ml methanol + 150 ml MTBE
Flow rate: 1ml/min
Injection: 0.5µl, Detection: UV at 210 nm

Learn more at:
diamond-analytics.com